

Document Room, DOCUMENT ROOM 36-412  
Research Laboratory of Electronics  
Massachusetts Institute of Technology

#3

# A STUDY OF THE PERSISTENCE CHARACTERISTICS OF VARIOUS CATHODE RAY TUBE PHOSPHORS

W. T. DYALL

LOAN COPY only

TECHNICAL REPORT NO. 56

JANUARY 16, 1948

RESEARCH LABORATORY OF ELECTRONICS  
MASSACHUSETTS INSTITUTE OF TECHNOLOGY



Bookcase

MASSACHUSETTS INSTITUTE OF TECHNOLOGY  
Research Laboratory of Electronics

Technical Report No. 56

January 16, 1948

A STUDY OF THE PERSISTENCE CHARACTERISTICS  
OF VARIOUS CATHODE RAY TUBE PHOSPHORS \*

W. T. Dyall

Abstract

Persistence characteristics, as well as measurements of flash, buildup, and fluorescence are presented in this report for five types of cathode ray tube screens, viz., sulphide (Ag), zinc-cadmium sulphide (Ag), P4, P14, and P7. These measurements cover a range of light values of nearly ten million to one. Plots of the characteristics and a complete discussion of them are given. The final section summarizes general conclusions regarding these characteristics.

---

\* This report is a slight modification of a thesis with the same title submitted by the author in partial fulfillment of the requirements for the degree of Master of Science in Physics at the Massachusetts Institute of Technology, 1948.

1  
2  
3  
4  
5  
6  
7  
8  
9  
10  
11  
12  
13  
14  
15  
16  
17  
18  
19  
20  
21  
22  
23  
24  
25  
26  
27  
28  
29  
30  
31  
32  
33  
34  
35  
36  
37  
38  
39  
40  
41  
42  
43  
44  
45  
46  
47  
48  
49  
50  
51  
52  
53  
54  
55  
56  
57  
58  
59  
60  
61  
62  
63  
64  
65  
66  
67  
68  
69  
70  
71  
72  
73  
74  
75  
76  
77  
78  
79  
80  
81  
82  
83  
84  
85  
86  
87  
88  
89  
90  
91  
92  
93  
94  
95  
96  
97  
98  
99  
100

TABLE OF CONTENTS

	Page
I. Introduction	1
II. Considerations for the Establishment of Screen Specifications	4
III. Theoretical Considerations and General Information	8
1. Buildup and Decay of Screen Luminescence	8
2. Qualitative Mechanism of Phosphorescence	13
3. Brief Remarks on the Centibel Scale	16
IV. Description of Equipment	17
1. General	17
2. Screen Excitation and Light Measurement	19
3. Calibration of Light Measuring Circuits	21
4. Spectral Response	23
V. Methods of Measurement	25
1. Phosphorescence	25
2. Buildup	31
3. Integrated Flash and Fluorescence	32
VI. Analysis of Measurements by Screen Type	33
1. GE 4633, zinc-cadmium sulphide (Ag)	33
2. GE 4665, zinc-cadmium sulphide (Ag)	36
3. GE 4609, zinc sulphide (Ag)	38
4. RCA 5FP4 A 1	40
5. RCA 5FP14 A 6331	43
6. RCA 5FP14 C7570N 3940-18	46
7. GE 5FP14 C72745	49
8 and 9. RCA 5FP7 A, 1 and 2	52

	Page
VII. Analysis of Measurements by Comparisons among Tube Types	57
1. Phosphorescence	57
2. Buildup	63
3. Integrated Flash and Fluorescence	66
VIII. Summary of General Conclusions	69
1. Phosphorescence	69
2. Buildup	71
3. Integrated Flash and Fluorescence	72
Appendix. Plots	73
Bibliography	102

LIST OF FIGURES

	Page
1. The Rise and Fall of Screen Luminance under Pulse Excitation	8
2. Plots of $I = I_0 e^{-t/t_0}$ and $I = I_0 \left( \frac{a}{a + t^n} \right)$	11
3. Model Mechanism of Excitation of a Phosphor by Light	14
4. Simplified Block Diagram of Nottingham Cathode Ray Tube Test Equipment	18
5. Response Characteristics of 931 Photomultiplier with and without Filter and Photopic Eye	24
6. Backtrace Effect on Measured Decay Characteristic for Various Slit Positions	28
 <u>Decay after One Raster:</u>	
7. GE 4633, 4 kv	74
8. " , 6 kv	74
9. GE 4665, 4 kv	75
10. " , 6 kv	75
11. GE 4609, 4 kv	76
12. " , 6 kv	76
13. RCA 5FP4 A 1, 4 kv	77
14. " , 6 kv	77
15. RCA 5FP14 A 6331, 4 kv	78
16. " , 6 kv	78
17. RCA 5FP14 3940-18, 4 kv	79
18. " , 6 kv	79
19. GE 5FP14, 4 kv	80
20. " , 6 kv	80
21. RCA 5FP7 A 1, 4 kv	81
22. " , 6 kv	81
23. RCA 5FP7 A 2, 4 kv	82
24. " , 6 kv	82

Slope of Decay Curves:

25.	GE 4633, 4 kv	83
26.	" , 6 kv	83
27.	GE 4665, 4 kv and 6 kv	84
28.	GE 4609, 4 kv	85
29.	" , 6 kv	85
30.	RCA 5FP4 A 1, 4 kv	86
31.	" , 6 kv	86
32.	RCA 5FP14 A 6331, 4 kv and 6 kv	87
33.	RCA 5FP14 3940-18, 4 kv and 6 kv	87
34.	GE 5FP14, 4 kv and 6 kv	88
35.	RCA 5FP7 A 1, 4 kv and 6 kv	89
36.	RCA 5FP7 A 2, 4 kv and 6 kv	89

Buildup:

37.	RCA 5FP14 A 6331	90
38.	RCA 5FP14 3940-18	90
39.	GE 5FP14	91
40.	RCA 5FP7 A 1	92
41.	RCA 5FP7 A 2	92

cb<sub>1</sub>, cb<sub>5</sub>, cb<sub>10</sub> as Functions of Beam Current:

42.	RCA 5FP14 A 6331	93
43.	RCA 5FP14 3940-18	93
44.	GE 5FP14	94
45.	RCA 5FP7 A 1	95
46.	RCA 5FP7 A 2	95

Fluorescence and Integrated Flash:

47.	GE 4633	96
48.	GE 4665	96
49.	GE 4609	97
50.	RCA 5FP4 A 1	98
51.	RCA 5FP14 A 6331	99
52.	RCA 5FP14 3940-18	99
53.	GE 5FP14	100
54.	RCA 5FP7 A 1	101
55.	RCA 5FP7 A 2	101



LIST OF TABLES

	Page
1. Description of Tubes Measured	3
2. Nomenclature of RMA Registered Screen Types	7
3. Condensed Data on Decay and Slopes	58
4. Some Data on Slopes of Decay Characteristics	61
5. Average Slopes of Plots of "cb <sub>1</sub> , cb <sub>5</sub> , cb <sub>10</sub> as functions of beam current"	64
6. Flash and Fluorescence Characteristics	67
7. Dependence of Fluorescence and Flash on Anode Voltage	68



## I. INTRODUCTION

The research and study presented in this report is prompted by the need, enhanced by the rapid development of cathode ray tubes for radar and television, for more detailed information about the light emitting characteristics of CRT screens. Such detailed information is necessary in order to allow continued improvements in screen quality and to provide data for the specification of phosphor screens by the Radio Manufacturers' Association.

Measurements of flash, buildup, fluorescence, and decay, over a range of light values of nearly ten million to one, for nine tubes, viz. three with P4 component screens, one having a P4 screen, two having P7 screens, and three with P14 screens, are presented in this report. Physical properties of these screens are given in Table 1, p. 3. Plots of the characteristics determined from these measurements are presented for each screen for various excitation conditions, in the Appendix. In Section VI, a complete discussion of the characteristics of each tube is given, divided according to tube type, so that any one tube may be studied independently. Section VII discusses the tubes according to characteristics, giving similarities and differences among the tubes for each characteristic, and Section VIII gives a summary of general conclusions.

The equipment<sup>22-27</sup> used for these measurements was designed by Professor W. B. Nottingham and collaborators at the Radiation Laboratory in 1942. The apparatus was used to measure hundreds of tubes during the war.<sup>1-11</sup> Many basic screen properties were analyzed and

many improvements in screens were made possible. The original design of the apparatus was for the study of the P7 type, long persistence CRT screens, but it is of such flexibility as to allow measurements on a wide range of screen types.

At the end of the war, the equipment was decommissioned because of lack of interest and the general slowing down from the high-gearred war effort. It remained in storage for nearly two years, until the summer of 1947, when it was put back in good operating order by the author, in order to continue investigations of phosphor characteristics.

TABLE 1

DESCRIPTION OF TUBES MEASURED

MANUF. DESIG.	RMA DESIG.	SERIAL OF MANUF. DESIG.	REMARKS	SCREEN COMPOSITION <sup>19</sup>	REFLECTED COLOR	LUMINESCENCE COLOR	PHOSPHOR. COLOR	DECAY TYPE
GE	- - -	4633	GE Phosphor P4 Comp.	ZnS:CdS:Ag(.01)	Yellow-white	Light Yellow-green	Light Yellow-green	t <sup>n</sup>
GE	- - -	4665	Patterson Phosphor P4 Comp.	ZnS:CdS:Ag(.01)	Yellow-white	Yellow-green	Yellow-green	t <sup>n</sup>
GE	- - -	4609	Patterson Phosphor P4 Comp.	α*-ZnS:Ag(.01)	White	Light blue	Light blue	t <sup>n</sup>
RCA	5FP4 A	1	Regular Product	α*-ZnS:Ag(.01) + ZnS:CdS:Ag(.01)	White	White	White	t <sup>n</sup>
RCA	5FP14 A	6331	Poured Cascade Screen, Made-147	β*-ZnS:Ag(.015) on ZnS(73):CdS:Cu(.004)	Light Yellow-orange	Purple-White	Light Orange	t <sup>n</sup>
RCA	5FP14	3940-18	Syphoned Cascade Screen, Made-145	" " " " " " " "	" " " " " " " "	" " " " " " " "	" " " " " " " "	t <sup>n</sup>
GE	5FP14	672745	Cascade Screen	" " " " " " " "	" " " " " " " "	" " " " " " " "	" " " " " " " "	t <sup>n</sup>
RCA	5FP7 A	1 and 2	Regular Product Cascade Screen	β*-ZnS:Ag(.015) on ZnS(86):CdS:Cu(.0073)	Light Yellow-green	Blue white	Light yellow	t <sup>n</sup>

## II. CONSIDERATIONS FOR THE ESTABLISHMENT OF SCREEN SPECIFICATIONS

There are many factors upon which the operating characteristics, both electrical and luminescent, of CRT depend. Some of these characteristics must be chosen as representative, in order to provide a means of production control. There are several screen characteristics which might be used for standardization and control, of which some are satisfactory, and some are not. The chemical composition of the phosphor screen provides merely a descriptive specification, which is inadequate because of variations in phosphor properties with manufacturing techniques. The color or spectral energy characteristic can be used, but is not completely satisfactory. Confusion now exists in the field of color specification because of the incompleteness of the general knowledge concerning the value and limitations of spectral-radiometric data for the evaluation and specification of color appearance. The light emitting characteristics of the phosphor screen, including fluorescence, flash, buildup, and persistence of phosphorescence, provide other factors allowing classification. The persistence characteristic, i.e. the decay of phosphorescence as a function of time, is a fundamental property of phosphors, and is, therefore, of importance. However, the rapidity of the decay alone is not a sufficient characteristic for production control. Since it is quite possible to produce a phosphor of slow decay without a high buildup, and since high buildup is a requirement dictated by the use to which slow decay screens are put, the buildup must be specified in addition to the persistence. Although the buildup ratio

is not a good measure of what can be expected from a cathode ray tube screen in observed contrast when a signal or pip is applied upon a cyclic background, e.g. "snow" or noise on a PPI radar screen, it does indicate the properties of the phosphor and its general method of application, and is therefore useful for manufacturers' inspections.<sup>7</sup> The fluorescence value is of interest to indicate the brightness of the screen during continuous scanning. The flash value is of some interest, but it is of little value in the control of useful screen performance.

It was agreed on May 2, 1945, at the meeting of the JEETEC\* Sub-committee on Cathode Ray Tube Phosphors and Screen Characteristics, that phosphor screens for cathode ray tubes be defined by the following data and curves:

- (1) Brightness measured in foot lamberts as a function of both screen current and screen voltage, on linear plots.
- (2) I.C.I. trichromatic color coefficients for P4 and P6; spectral energy characteristic or color, relative energy as a function of wavelength in angstroms, on linear plots, for all other phosphors.
- (3) Persistence characteristic, light output in foot lamberts as a function of time after excitation, on semi-log plots for P1, P3, and P12 phosphors, and on log-log plots for remaining phosphors.

These data are not complete as yet.

The CRT screens as designated by the RMA data bureau, with the exception of the P8, which has been replaced by the P7, and the P9, the registration of which has been cancelled, may be divided into five groups with respect to their persistence characteristics:

\* Joint Electron Tube Engineering Council of the Radio Manufacturers' Association, and the National Electrical Manufacturers' Association.

- (1) Exponential decay\* screens -- P1, P3, P12, and P13.
- (2) Long persistence inverse power law decay screens -- P2, P7, and P14.
- (3) Medium persistence combination exponential and inverse power law decay screen -- P4.
- (4) Short persistence inverse power law decay screens -- P5, P6, and P11.
- (5) Very long variable persistence dark trace screen -- P10.

Characteristics of these phosphors, as registered with the RMA Data Bureau, are given in Table 2.

\* Exponential and inverse power law decay discussed in III-1.

---



TABLE 2

NOMENCLATURE OF RMA REGISTERED SCREEN TYPES<sup>19,30</sup>

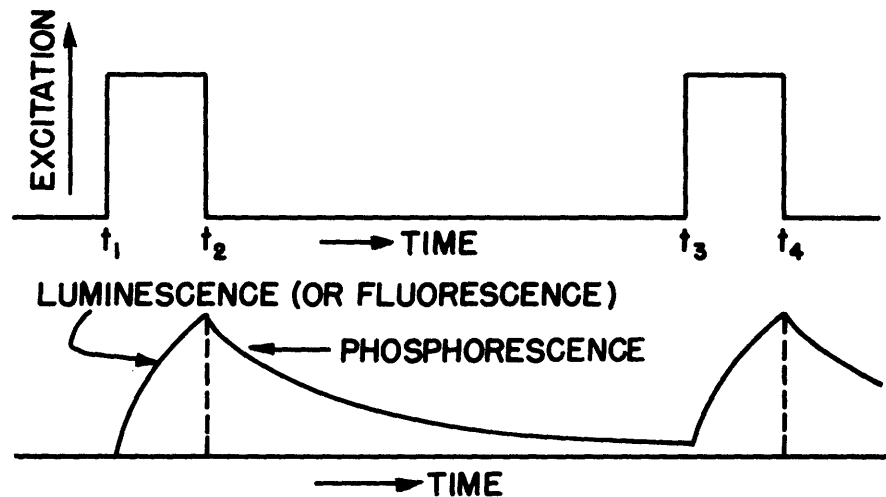
<u>PHOSPHOR</u>	<u>COMPOSITION</u>	<u>FLUORESCENT COLOR</u>	<u>PHOSPHORESCENT COLOR</u>	<u>PERSISTENCE</u>
P1	Willemite $Zn_2SiO_4:Mn(\alpha)$	Green	Green	Medium
P2	$ZnS:Cu(Ag)(\beta^*)$	Blue-green	Green	Long
P3	$Zn_8BeSi_5O_{19}:Mn$	Yellow	Yellow	Medium
P4**	$\alpha^*-ZnS:Ag +$ $Zn_8BeSi_5O_{19}:Mn$	White	White	Medium
P5	Scheelite $CaWO_4:W$	Blue	Blue	Very Short
P6	$ZnS:Ag +$ $ZnS:CdS:Ag$	White	White	Short
P7	$\beta^*-ZnS:Ag$ on $ZnS(86):CdS:Cu$ Cascade	Blue-white	Light yellow	Long
P10	KCl	Magenta (Dark Trace Tube)		Variable
P11	$\alpha^*-ZnS:Ag$	Blue	Blue	Short
P12	$Zn(Mg)F_2:Mn$	Orange	Orange	Medium
P13	$MgO \cdot SiO_2:Mn$	Light Red	Light Red	Medium
P14	$\beta^*-ZnS:Ag$ on $ZnS(75):CdS:Cu$	Purple White	Light Orange	Medium Long

\*\* Newer P4 has  $ZnS:CdS:Ag$  instead of the silicate.

### III. THEORETICAL CONSIDERATIONS AND GENERAL INFORMATION

#### III-1. Buildup and Decay of Screen Luminescence.

All luminescent materials useful as cathode ray tube phosphor screens emit light after the end of the electronic excitation. Fig. 1



THE RISE AND FALL OF SCREEN LUMINANCE UNDER PULSE EXCITATION

Figure 1

schematically illustrates the rise and fall of luminescence. Here it is assumed that the electronic excitation of the screen is constant from time  $t_1$  to time  $t_2$ , off until  $t_3$ , etc. When the electrons strike the screen, the luminescence or fluorescence increases rapidly, and follows the buildup curve characteristic of the phosphor. At  $t_2$ , when the excitation is discontinued, the light output immediately begins

to fall, and follows the phosphorescence decay characteristic of the phosphor.

For a double layer or cascade screen, e.g. P7, the picture is changed somewhat. The blue phosphor of the P7 is directly excited by the electron beam, emitting blue light by fluorescence during the excitation, and by phosphorescence after the cessation of excitation in the manner shown in Fig. 1. The first layer is practically opaque to electrons. Thus the second, or yellow layer of the P7 is excited chiefly by the light from the first layer. The excitation of the second layer by the luminescence of the blue phosphor causes a delay of about one microsecond after the end of electronic excitation before the peak light intensity is emitted by the cascade screen.

The buildup of the luminescence of cathode ray tube phosphors is very rapid, and increases in rapidity for larger excitations. The buildup under steady scanning is difficult to measure because of this rapidity, so a method of "cyclic excitation" was introduced by Bradfield and Garlick.<sup>12</sup> This method involved a series of rasters applied to the screen at intervals of one second. As adopted by the MIT Radiation Laboratory and for this report, cyclic excitation was used in defining the buildup ratio, which is the ratio of the light output one second after N pulses to the light output one second after one pulse.

The three recognized decay laws for CRT screens are given by Leverenz<sup>19</sup>, as the exponential, hyperbolic, and power-law types. The first is generally known as the "mono-molecular" decay, and is associated with conditions in which the number of transitions that take place per

unit of time is directly proportional to the number of active particles, and is analogous to a single impurity trap depth of the type shown in Fig. 3, p. 14. The hyperbolic decay is analogous to multiple trap levels of uniform distribution. The third type decay law results from assuming multiple trap levels of exponential distribution.

The fact that the observed decay characteristics differ so radically from those expected on the basis of any of the above decay laws is a direct indication of the fact that the concentration of electrons in the conduction levels continues to be replenished by the feeding of electrons up from the traps into the conduction level.<sup>29</sup>

In general, sulphide phosphors follow the inverse power law type, while fluoride or oxide phosphor lifelines are exponential, perhaps developing  $t^{-n}$  tails. There is, of course, no reason to exclude a representation of decay characteristics by various other combinations of exponential and inverse power law functions. Initial portions of exponential decays are practically unaffected by intensity variations, while the  $t^{-n}$  decays are accelerated in proportion to their luminescences at the time of cessation of excitation.

Plots of inverse power law and exponential decay laws are included, Fig. 2, drawn on a log log graph so that they may be easily compared with measured decay characteristics. The slope of the decay curve, corresponding to any decay law, must exceed one ultimately, in order to fulfill the condition that the integral of all power radiated remain finite. However, there is no theoretical reason why the slope cannot be less than one initially, as it often is. This condition

PLOTS OF

$$I = I_0 e^{-t/t_0}$$

$$I = I_0 \frac{a}{a+t^n}$$

	$t_0$
1.	1
2.	0.01

	$a$	$n$
3.	$10^{-1}$	1
4.	$10^{-1}$	2
5.	$10^{-4}$	1
6.	$10^{-4}$	2

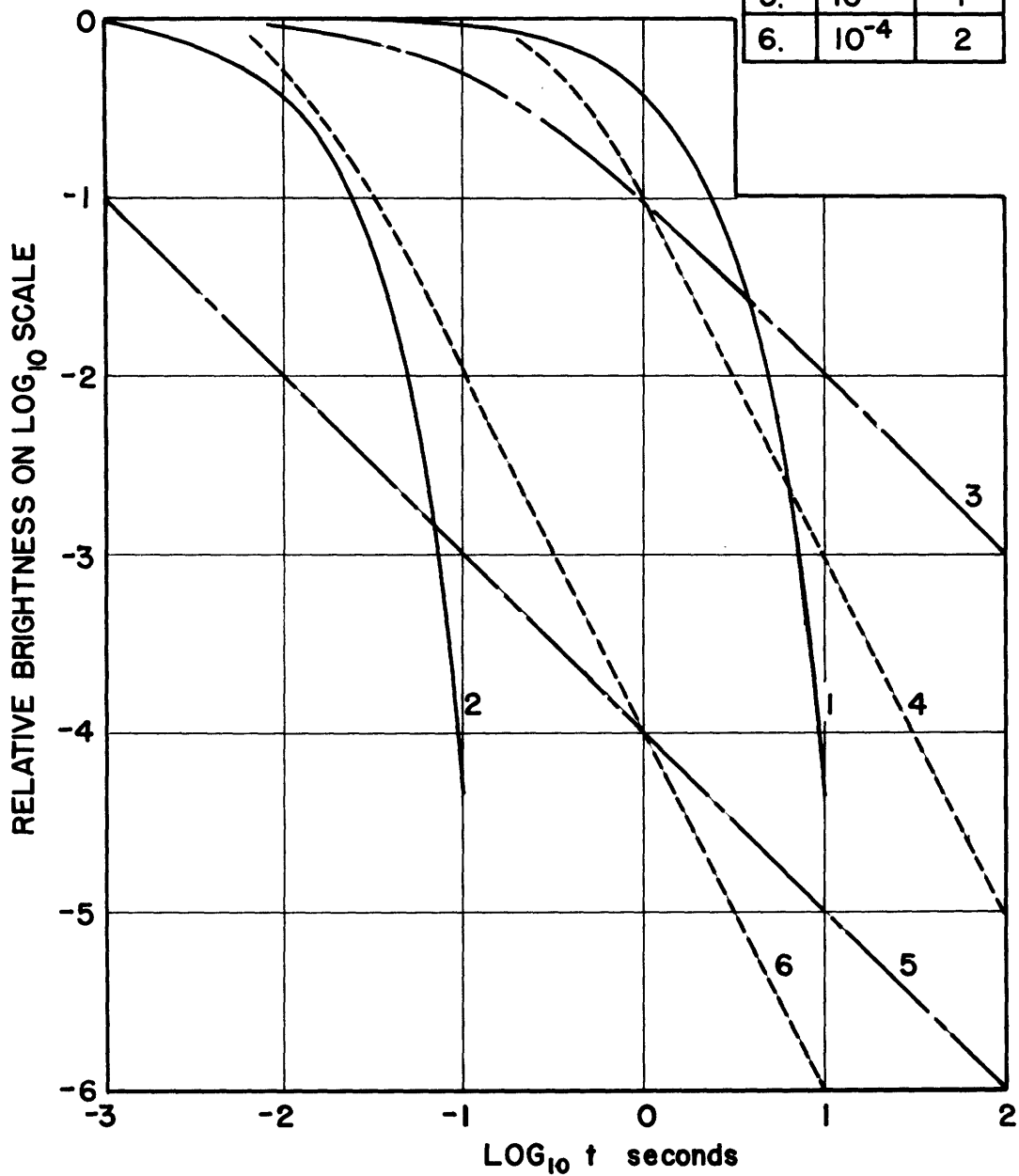


Figure 2

merely requires, for example, that the value of the negative exponent of the power law decay be greater than unity at large values of time.

It has been found experimentally that the following equation represents the dependence of luminescence,  $L$ , during excitation on the electron energy, or the anode voltage,  $V_a$ :

$$L = K (V_a - V_0)^n,$$

where  $K$  is a constant of proportionality, and  $V_0$  is the so-called "dead voltage".  $V_0$  is small and is usually zero. The exponent  $n$  has been observed to vary from 1.4 to 3, with many cases of values that are approximately 2.<sup>20-21</sup>

Luminescence during excitation is directly proportional to the current density of the electron beam over an extremely wide range of values. Phosphors are usefully operative over a range of at least  $10^{12}$  in current densities for normal positive modulation.<sup>19</sup>

---

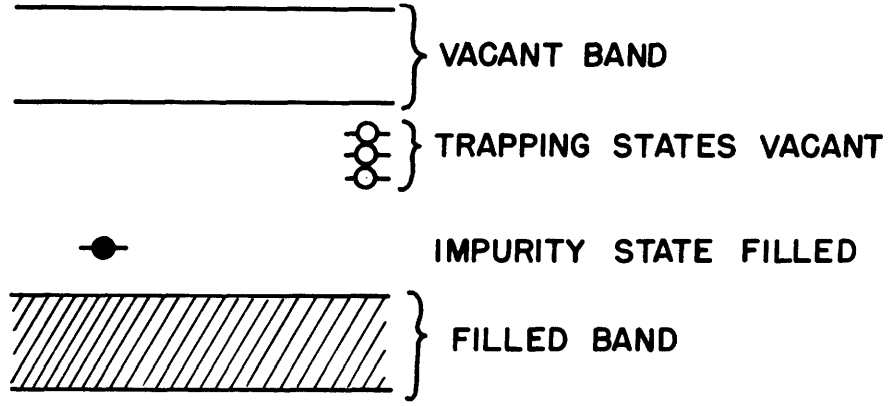
### III-2. Qualitative Mechanism of Phosphorescence.

A simplified model mechanism of excitation of a sulphide phosphor by light is given in Fig. 3. This figure is a copy of a diagram shown by Johnson.<sup>28</sup> The unexcited state of the crystal is shown in Fig. 3a. It is assumed that there is a band of completely filled electronic energy levels, and another band which is partially vacant and which might be thought of as a conduction band. It is also assumed that there is a separation of two or three electron volts between these bands of energy levels. The model shows the presence of metastable states distributed throughout the crystal which serve to trap the electrons which have arrived in the conduction band. The impurity state represents a level of the "activator" element such as silver.

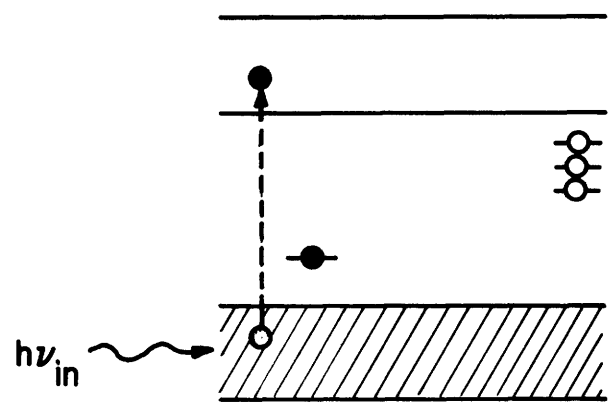
If light is incident on the phosphor, the light quantum lifts an electron from the filled band to the conduction band, as represented in Fig. 3b. A "hole" is left in the filled band. The electron then has the possibility of returning to the hole or of going into a trapping state. Apparently there is a very small probability of the first alternative.

The next step takes place extremely rapidly. The electron, which had been lifted to the upper band, falls to one of the lower levels of the band, and the hole of the lower filled band moves to an upper part of that band, and the condition shown in Fig. 3c is brought about. Immediately thereafter, two more changes occur, which need not take place simultaneously, and result in the status shown in Fig. 3d. The electron in the upper band has fallen to one of the metastable levels, and the

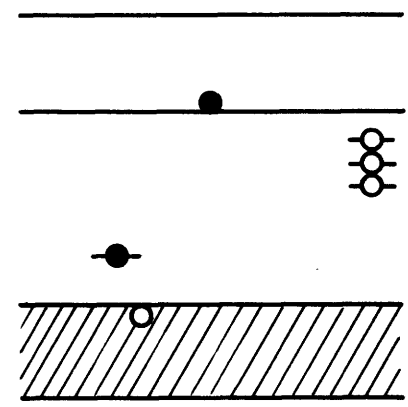
MODEL MECHANISM  
OF  
EXCITATION OF A PHOSPHOR BY LIGHT



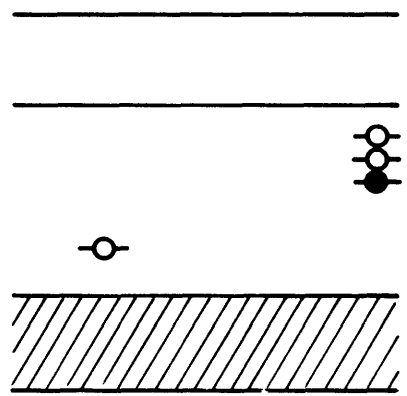
(a)



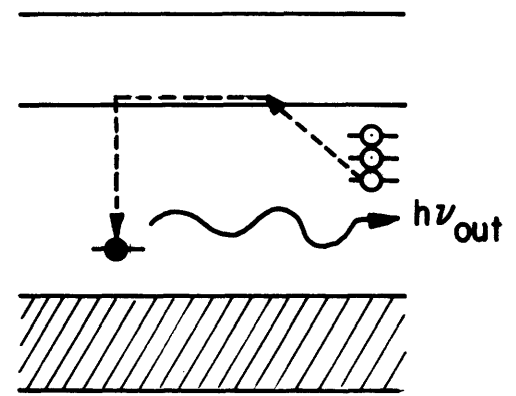
(b)



(c)



(d)



(e)

Figure 3



electron in the impurity state has dropped into the hole in the lower band. The elapsed time at this stage is of the order of ten microseconds or less.

Several seconds, or even minutes, elapse while the electron remains in the metastable state. The time, of course, depends upon the type of phosphor. Upon leaving the metastable level, as represented by Fig. 3e, the electron will go into the conduction band, flow through it, and fall into the vacant impurity level. Light is emitted when the electron falls.

Since the electrons may be excited to the conduction band and then returned to the hole in the filled band while further excitation is still going on, the model may represent both phosphorescence and fluorescence.<sup>1</sup>

This model is a simplification of the problem, and allows only a qualitative picture. However, there are a number of complicating factors which are not well understood, and so a more quantitative discussion is beyond the scope of this work.

III-3. Brief Remarks on the Centibel Scale.

The centibel scale was introduced by Nottingham in 1941. In his "Notes on Photometry, Colorimetry and an Explanation of the Centibel Scale"<sup>8</sup>, he presents a complete discussion of the problem of the centibel, and the adaptation of such a logarithmic scale to photometry and to the actual measurement of CRT screens.

The centibel scale is defined by the following relation:

$$cb = 100 \log_{10} (I_0/I),$$

where  $(I_0/I)$  is the ratio of the light intensities.

Photometry demands the detailed recognition of the spectral characteristics of the source and the receiver, which must be incorporated into the basic unit, and the concept of the zero level. Therefore the basic unit must be power per unit range in wave-length per unit area, instead of just power per unit area alone, as in acoustics. Using this basic unit, the zero level was taken arbitrarily to be  $10^{-16}$  watt  $\times$  cm<sup>-2</sup>  $\times$  A<sup>-1</sup>, where A = the unit of wave-length = 1 Angstrom =  $10^{-8}$  cm. The result of this choice gives the relative energy level of 0 cb as approximately equivalent to the minimum constant brightness which the completely dark adapted eye can detect.

The energy measurements on the centibel scale may be converted readily to visual units such as foot lamberts, since the physical dimensions and spectral energy characteristics of the source, filters, and receiver are known. The conversion factor for the standard P7 test conditions is:

$$\text{Foot Lamberts} = 2 \times 10^{-6} \times 10^{cb/100}.$$

#### IV. DESCRIPTION OF EQUIPMENT

##### IV-1. General.

The equipment<sup>22-27</sup> provides the voltages and currents necessary for the operation, screen excitation and de-excitation, for both electromagnetic and electrostatic type cathode ray tubes, including heater current, control and accelerating grid voltages, focusing and deflection currents for e.m. tubes, focusing and deflection plate voltages for e.s. tubes, and final anode or intensifier voltage. The equipment further includes a photomultiplier tube and associated amplification and light measuring circuits, with necessary power supplies and regulators, standardization circuits, and photometric calibration circuits. The standardization circuits utilize a potentiometer method which employs an electronic eye as a null indicator to allow accurate adjustment of the CRT anode voltage, the currents for the standard calibrating lamps, and various other voltages. A simplified block diagram of the equipment is given in Fig. 4.

### SIMPLIFIED BLOCK DIAGRAM NOTTINGHAM CATHODE RAY TUBE SCREEN TEST EQUIPMENT

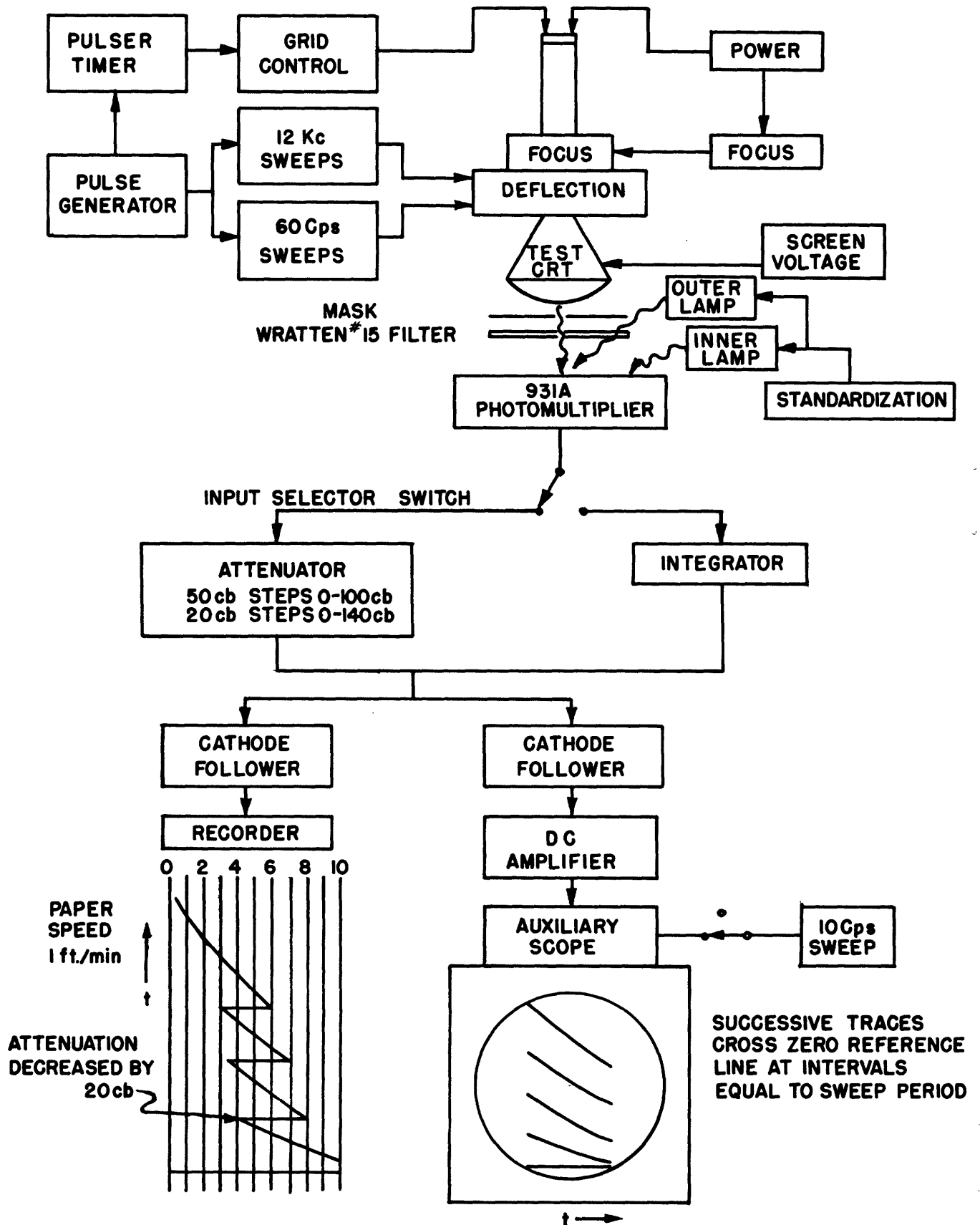


Figure 4

IV-2. Screen Excitation and Light Measurement.

After completion of all the adjustments necessary for the proper operation of these circuits, including the calibration of the light measuring circuits, and the adjustments necessary for the desired operation of the cathode ray tube to be measured, the screen of this CRT is de-excited by red light. The de-excitation is necessary since the luminescence of a phosphor depends, in a complicated manner, upon the past history of its excitation, if the influence of this past excitation is not removed. The CRT is then excited by a 50 cm<sup>2</sup> or 25 cm<sup>2</sup> raster formed by a horizontal 60 cycle sweep and a 12 kilocycle vertical sweep. The excitation may be steady, as for fluorescence measurements; or pulsed, for flash, buildup, and decay measurements, by applying a 1/60 sec positive square wave of voltage to the CRT grid at intervals of one second.

The light emitted as a result of this excitation passes through a Wratten 15 filter and falls upon the cathode of a 931A photomultiplier tube placed at a standard distance of 30 cm from the CRT screen. The CRT and the 931A are contained in a light tight housing.

The output current of the phototube develops a voltage across a high resistance load in the form of an accurately calibrated attenuator, except in the case of the flash measurement. For that measurement, the output current charges a condenser, thus performing an integration of the light incident on the photocathode up to the instant of recording.

The attenuator or condenser output is applied to the grid of a cathode follower which acts as an impedance transformer between the

931A and a GE high speed recorder<sup>22</sup>. The output signal from the cathode follower deflects the basic element in the recorder, which deflects the pen by a photoelectric coupling. The recorder has a basic microammeter element of 250 microamp sensitivity. The recorder paper is moved at the rate of 1 ft/min by a synchronous motor. The pen requires about 0.2 sec to reach deflection equilibrium, but its deflection is not very accurate for times less than 0.5 sec after a rapid change in deflection such as occurs in the early portions of decaying phosphor luminescence. Therefore, the one second decay point is the earliest measured using the recorder.

The output of the attenuator is also fed to a second similar cathode follower, which in turn drives one stage of DC amplification. The resulting signal is applied to the DC amplifier input of a DuMont type 208 oscilloscope. The oscilloscope is used with an externally supplied 10 cycle sweep, and internal sweeps of 60 cycles, 300 cycles, and 600 cycles, which allow the measurement of light intensities at times from 1.7 ms to 1 sec. The sweeps are synchronized from the pulse generator.

IV-3. Calibration of the Light Measuring Circuits.

The light measuring circuits are provided with a calibrated range in gain of ten million fold, and allow the accurate measurement of light intensities ranging from 160 cb to about 900 cb. Although the human eye responds over a range of  $10^{10}$  in brightness<sup>19</sup>, i.e. from about 0 to 1000 on the cb scale, the light measuring circuits cover the brightness range practical for usage in cathode ray tubes.

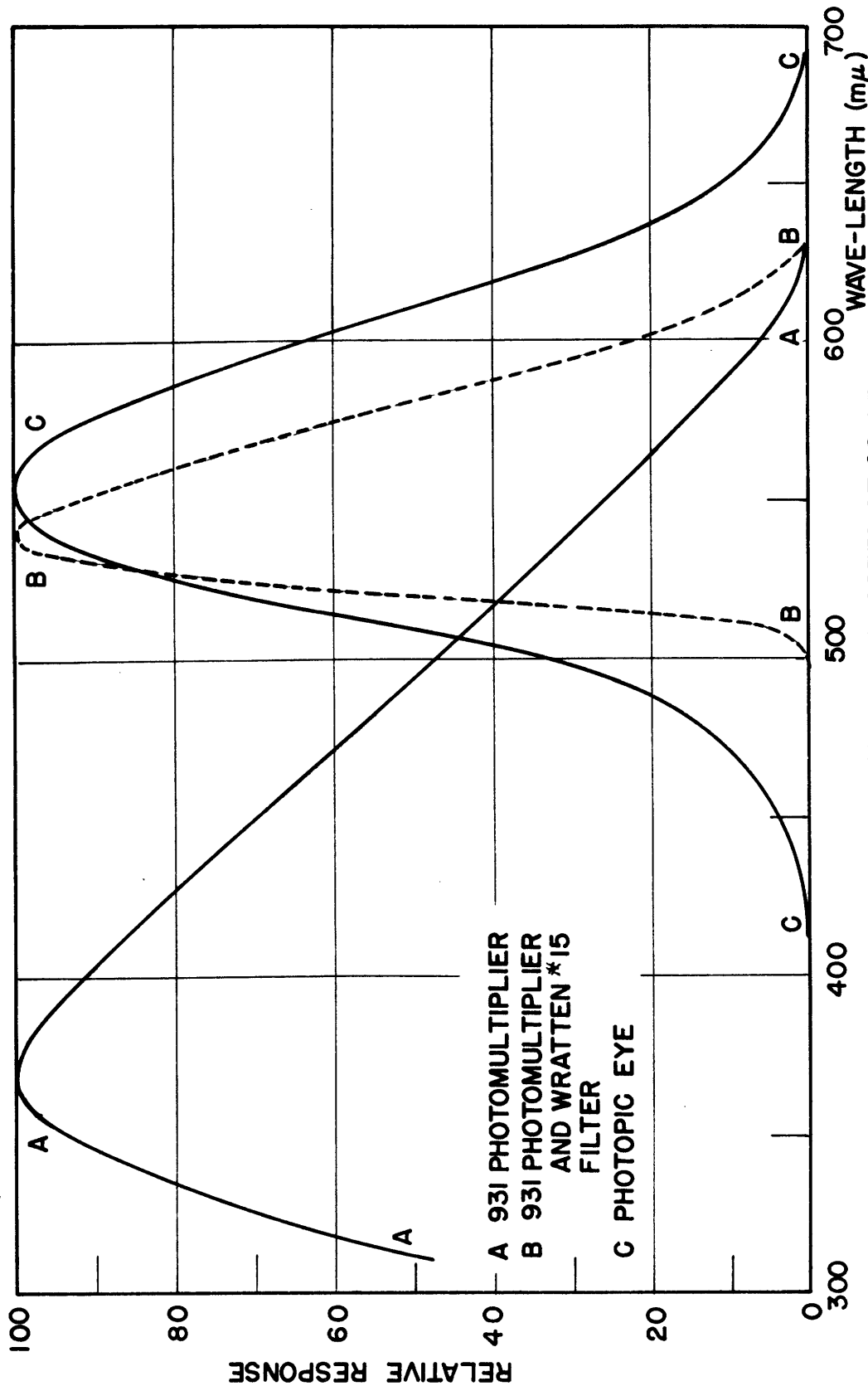
The basic standard for calibration of the photometric circuits was a ribbon filament lamp, calibrated by the Bureau of Standards, which was used with suitable slits and filters to establish a known value on the centibel scale.<sup>8</sup> The practical standard used for calibrating the light measuring circuits is a Leeds and Northrup straight filament pyrometer lamp and filter calibrated against the basic standard. The filter is a clear glass cell containing a water solution of copper sulphate. This L and N standard lamp, called "outer lamp", is mounted at a predetermined distance from the photocathode on an arm pivoted on an axis through the 931A, and is set at the angular position giving maximum multiplier response for calibrating the light measuring circuits. In this position, with standard current through it, set by the electronic potentiometer, and with its light passing through a Wratten 15 filter, this source supplies a relative energy level of 500 cb at the photocathode. Its spectral energy distribution is like that of the P7 screen. Under these conditions, the light measuring circuits require a gain of 400 cb to give full scale deflection of 10 divisions on the recorder. That is, 0.1 full scale corresponds to an energy level of 400 cb, and

full scale corresponds to 500 cb. With the gain set at the 400 cb scale, the current through a 110 volt pilot "inner lamp", located in the same housing with the photomultiplier, is adjusted so that its irradiance falling upon the photocathode will duplicate the full scale deflection produced by the outer lamp. After this exact duplication is accomplished, the inner lamp current can be re-established with high accuracy by matching an IR drop obtained over a fixed resistance to the voltage of the standard cell by means of the electronic potentiometer. The calibration of gains above and below the 400 cb scale are accomplished by using the inner lamp in conjunction with the calibrated attenuator steps.



IV-4. Spectral Response.

The spectral response of the Nottingham Cathode Ray Tube Screen Testing Equipment, Fig. 5, approximates that of the eye, except in the red and blue, where in both cases the response is low. Thus measured values on screens of these colors will be relatively low compared with visual observations. The calibration of the equipment is based on the spectral energy distribution of the P7 screen, so that when the spectral energy distribution of the source being measured differs from that of a P7 screen, the absolute cb values will be in error by a constant amount, but the ratios of light outputs will be correct. In other words, there will be an error in the measured light level, but there will be none in the slopes of the decay characteristics, nor in the buildup ratios.



A 931 PHOTOMULTIPLIER  
B 931 PHOTOMULTIPLIER  
AND WRATTEN \*15  
FILTER  
C PHOTOPIC EYE

RESPONSE CHARACTERISTICS OF  
931 PHOTOMULTIPLIER WITH AND WITHOUT FILTER AND OF PHOTOPIC EYE

Figure 5

## V. METHODS OF MEASUREMENT

### V-1. Phosphorescence.

Phosphorescence is the luminescence emitted by the screen after the cessation of excitation. To measure the phosphorescence or persistence characteristic, it is necessary to de-excite the screen by red light, excite the screen in the desired manner, remove the excitation, and measure the light values at various times after the end of excitation. The decays studied here are all decays after one raster. All data were taken at two values of screen voltage:  $V_a = 4$  kv and 6 kv; and at three values of the current density:  $Q = 10, 20, \text{ and } 40 \text{ } \mu\text{coulombs/cm}^2$ .

One 1/60 sec raster was applied to the screen after de-excitation by red light, and the light values of the decaying phosphorescence were recorded for convenient times. Zero time is at the end of excitation. For the RCA P4, the two RCA P14's, the GE P14, and the two RCA P7's, all of which have octal bases, a raster area of  $50 \text{ cm}^2$  was used. For the GE 4633, the GE 4665, and the GE 4609 tubes with P4 component screens, a  $50 \text{ cm}^2$  raster was used for the 4 kv excitation, but it was necessary to use a smaller raster for the 6 kv excitation. These three tubes have the new type seven pin duodecal base which is slightly larger in diameter than the regular octal base. This necessitated the use of different deflection coils for these tubes than were used for the previously mentioned tubes. The new set of coils produced a very noticeable non-linearity in the 60 cycle sweep for a  $50 \text{ cm}^2$  raster for the 6 kv excitation. By using a smaller raster,  $25 \text{ cm}^2$  in area, this difficulty

was removed. Beam current was also reduced to maintain the same  $Q$  values of 10, 20, and 40 as for the 50 cm<sup>2</sup> raster. Since the luminescence is directly proportional to the area of the screen excited, a correction of 30 cb was added when the unmasked\* 25 cm<sup>2</sup> raster was used so that the 6 kv data for these tubes would be comparable to the rest of the data.

For times greater than one second after the end of excitation, the photoelectric recorder was used. The time scale for the recorder is provided by a synchronous motor which moves the recorder paper at a speed of one ft/min. The multiplier gain was set in such a way that the one second point on the decay curve would give a deflection of about 3 divisions, i.e. about 0.3 of full scale, with the maximum of 140 cb attenuation in the circuit. As the phosphorescence decayed, the attenuation was removed by steps of 20 cb to follow the decay. Since the lowest energy level which can be measured accurately with this equipment is 160 cb, which corresponds to 0.1 of full scale with multiplier gain at its maximum value, the lifeline was followed to a time when the light value had fallen 140 cb from the value at 1 sec, but no lower than 160 cb.

For times less than one second, the auxiliary DuMont oscilloscope with a P7 CRT was used. An external sweep of 10 cps, and internal 60 cycle, 300 cycle, and 600 cycle sweeps were used, which allowed measurement of light intensities at times from 1.7 ms to 1 sec. Sweeps were synchronized from the pulse generator. Light values at intervals

\* Masking technique is described on the following page.

of one sweep length, i.e. 100 ms, 16.7 ms, 3.3 ms, and 1.7 ms, were obtained by observing where successive traces on the auxiliary scope screen crossed the zero line as the luminescence decayed. As in the case of the recorder, the attenuation was removed in steps of 20 db to observe successive traces, and follow the decay.

Light measurements at times shorter than 50 ms required a shorter excitation than the 17 ms given by the standard raster. A mask containing a slit parallel to the raster lines placed over the CRT face shortened the excitation time and decreased the screen area viewed by the photocathode. A slit width of 1 mm was used, reducing the raster area by a factor of 70, giving an effective excitation time of  $1/70 \times 1/60 = 0.24$  ms approximately. The measured intensities would thus be expected to be 185 db lower, because of the decrease in area, for a 50 cm<sup>2</sup> raster, and 200 db lower for a 25 cm<sup>2</sup> raster. However, the slit width and raster area exposed were not known accurately enough to allow this addition. Instead, the correction was determined by plotting and matching the sections of the characteristics as measured with the mask to the sections obtained with the full raster.

Since the cathode ray beam is not blanked during the backtrace of the 60 cycle sweep of the raster, spurious excitation of the screen is produced. A method of eliminating this backtrace effect was necessary. For the points from 1.7 ms to 5.0 ms, the slit was placed near the center of the raster, thus the excitation due to the backtrace occurred about 8 ms after the pulse due to the sweep itself. For the points from 6.7 ms to 50 ms, the slit was placed near the righthand edge of the raster.

### BACKTRACE EFFECT ON MEASURED DECAY CHARACTERISTIC FOR VARIOUS SLIT POSITIONS

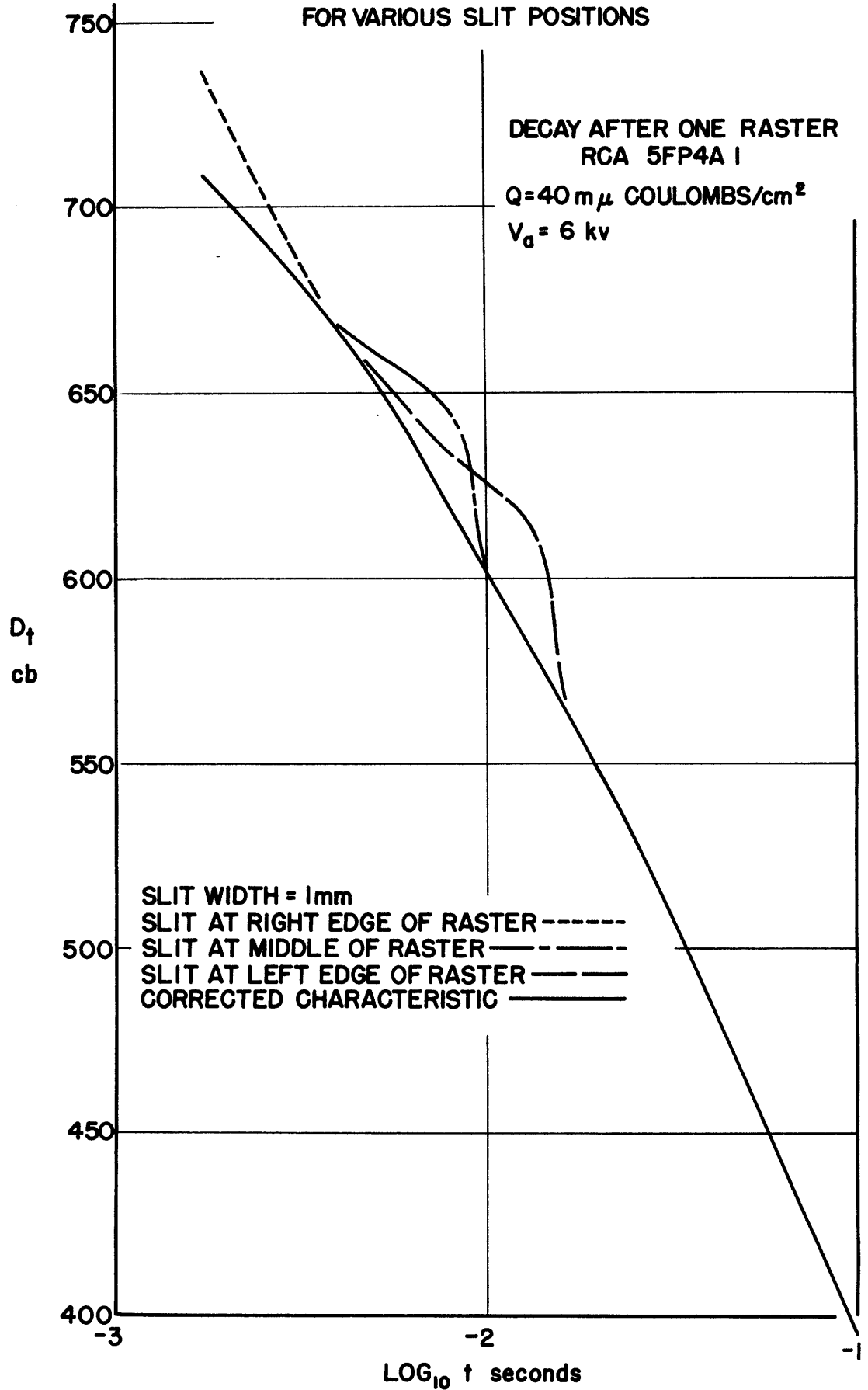


Figure 6

As the sweep is from left to right, the spurious excitation occurred about 2 ms after the desired pulse. This involved the assumption that the effect of the backtrace pulse is negligible after 4 or 5 ms. The validity of this assumption is demonstrated by the plot of Fig. 6 for the P4 screen, which, because of its rapid decay, shows the effect of the backtrace quite markedly.

The measurements of light output during decay were plotted on the logarithmic graph  $D_t$  vs  $\log_{10} t$ , where  $D_t$  indicates the cb value on the decay characteristic at time  $t$  seconds after the end of screen excitation. The decay characteristics are shown, in Fig. 7 through 24, for the six excitation conditions, and each characteristic represents the decay after one 1/60 sec raster. The accuracy of the measurements is such that the width of the line used to represent the results is greater than the uncertainty in the values obtained. This statement is made in order to indicate that the detailed nature of the decay characteristics shown is as complex as indicated. The small variations are not an indication of experimental error, but are characteristic of the particular phosphor, and depend somewhat on the concentration and velocity of the exciting electrons.

The decay curves can be analyzed by studying their variations in slope, and using plots of the slope values to recognize the character of single curves, or to compare decays from the different screen excitations or from different phosphors. Such slope analyses make the differences in decay properties more evident than direct inspection of the decay curves. They also normalize the decay properties so that direct

numerical comparisons may be made without considering light output levels.

The slope values of the decay characteristics were plotted as functions of  $\log_{10} t$ , Fig. 25 through 36. The slope values used are actually the average values for small intervals along the time axis, i.e. slope =  $(D_b - D_a)/(\log b - \log a) = \Delta cb/\Delta \log t$ . Increments of about 0.5 in  $\log_{10} t$  values were used.

Even though the maximum error in cb values is not greater than 5 cb, and is small enough so that the true decay characteristic is within the line width of the curve plotted as such, no special significance may be assigned to the detailed structure of the slope plots, since each plot results from only one particular test on one particular tube. For an increment of 0.5 in  $\log_{10} t$ , a range of  $\pm 5$  cb in  $D_t$  results in a range of  $\pm 10\%$  in calculated slope. A series of tests on many screens of the same type would be necessary to determine accurately such details in the slope curves. However, some conclusions may be drawn from the general shape and tendency of the plots.

For a general indication of the rapidity of the decay, the average slope of the persistence characteristic was computed by finding the straight line that has approximately the least square deviation from the actual decay characteristic.



V-2. Buildup.

Eleven standard 1/60 sec 50 cm<sup>2</sup> rasters were applied to the screen at one second intervals. The light values one second after the first pulse, the fifth pulse, and the tenth pulse were computed, and denoted as  $cb_1$ ,  $cb_5$ , and  $cb_{10}$ , and plotted as functions of the number of pulses, Fig. 37 through 41, to show buildup. These values were also plotted as functions of the logarithm of the beam current,  $i_p$ , Fig. 42 through 46. The buildup ratio is defined by the relation:

$$G_{N:1} = \text{antilog} \left( \frac{cb_N - cb_1}{100} \right).$$

V-3. Integrated Flash and Fluorescence.

Integrated flash is the averaged fluorescence during excitation of the screen by the electron beam plus the phosphorescence during the eye's integration time of about 0.1 sec after excitation. For measurement of integrated flash, the light output resulting from one 1/60 sec 50 cm<sup>2</sup> raster was integrated to 1 sec, this time being marked by the appearance of the next succeeding raster. To convert to 0.1 sec, 100 cb was added to the computed value. For the screens studied, this is a good approximation, since most of the light was emitted before 0.1 sec.

Fluorescence is the luminescence of the phosphor during excitation. A steady excitation by a continuous 50 cm<sup>2</sup> raster was applied and the light output was allowed to build up to equilibrium, which was measured as the fluorescence value, cb<sub>f</sub>. For the P4 and P4 component screens, the equilibrium values measured are approximately 10 cb lower than the actual fluorescence value, because of significant decay during excitation, between successive sweeps.

Integrated flash and fluorescence values were plotted, Fig. 47 through 55, on the cb scale as functions of the logarithm of the beam current for each value of the screen voltage.

## VI. ANALYSIS OF MEASUREMENTS BY SCREEN TYPE

### VI-1. GE 4633.

The decay characteristics of this zinc-cadmium sulphide, silver activated screen, Fig. 7 and 8, are extremely steep compared to the RMA designated screens studied. This becomes quite evident when Fig. 7 and 8 are compared with Fig. 13 through 24 for the RMA screens. The slope curves for this P4 component screen, Fig. 25 and 26, compared with the slope curves in Fig. 30 through 36, also make this fact evident. The average slopes of the decay curves of the GE 4633 screen vary from 2.24 to 2.54 for the various excitation conditions, and decrease with greater excitation.

The plots of the decay characteristics for the six excitation conditions studied are similar in general. Each curve has a noticeable increase in downward curvature in the early portions of the decay, and an opposite effect towards upward curvature for times near 0.1 sec. The initial portion of the characteristic is least different from a straight line for the highest excitation, i.e.  $Q = 40$ ,  $V_a = 6$  kv. The curves are somewhat further apart in the latter portions than initially. At the initial reading of 1.7 ms, an increase in  $Q$  by a factor of two increases the phosphorescence by an average of 30 cb, and thus the light output 1.7 ms after the end of excitation is directly proportional to  $Q$ . Near the end of the measured decay at 0.1 sec, doubling  $Q$  produces an average change of 40 cb in the light output. This greater separation indicates that the slope of the decay curve decreases as  $Q$  increases.

Increasing the screen voltage from 4 kv to 6 kv produces an average increase of 35 cb in light output at 1.7 ms. At 0.01 sec the same change in voltage produces an average increase of 45 cb for  $Q = 10$  and 20 curves, and an increase of 9 cb for the  $Q = 40$  condition. At 0.1 sec, the increase in voltage from 4 kv to 6 kv increases the light output by an average of 17 cb for the  $Q = 10$  and 40 excitations, and by 4 cb for the  $Q = 20$  case. The relation between phosphorescence and anode voltage may be expressed as follows:\*

$$\left(\frac{V_a'}{V_a}\right)^n = \text{antilog}\left(\frac{cb' - cb}{100}\right),$$

i.e. the phosphorescence is proportional to  $V_a^n$ , where  $n$  for this particular case lies between 0.21 and 2.55. The low value of  $n$  is for the  $Q = 20$  condition for times near 0.1 sec. There is some uncertainty in the low value. However, the values of  $D_t$  for times near 0.1 sec were remeasured and found in agreement with previous data. Measurements were repeated with  $V_a = 4$  kv with a 25 cm<sup>2</sup> raster first. Immediately thereafter, and without changing the multiplier gain, the values of  $D_t$  for the 6 kv condition were remeasured with a 25 cm<sup>2</sup> raster. This provided a check on the method of using a 50 cm<sup>2</sup> raster for 4 kv and a 25 cm<sup>2</sup> raster for 6 kv, as discussed on pp. 25 and 26. Time limitations prevented closer checking of these data. The author feels that further investiga-

\* Here the exponent is determined by two points only. A more detailed study<sup>20,21</sup> of the dependence of luminescence on anode voltage indicates the linearity of the relationship and so allows the determination of the exponent of the anode voltage by two points only.

tion is necessary to establish definitely the validity of the low value of  $n$ .

The slope curves, Fig. 25 and 26, show that the slope decreases with increasing  $Q$  for times less than 0.01 sec, and that for times greater than 0.02 the slope increases with increasing  $Q$ . The slopes range from initial values of 1.52 to 1.97 at 3.3 ms, to maxima of 2.65 to 2.98 at times between 0.01 and 0.03 sec. The decrease in slope after the maximum is not so fast as the increase before the maximum. The slopes decrease to values ranging from 1.94 to 2.48 at 0.1 sec.

The plots of fluorescence and integrated flash, Fig. 47, are very nearly straight lines, of approximately unit slope. This indicates the direct proportionality between beam current and light output. Increasing  $V_a$  from 4 kv to 6 kv increases the fluorescence by 29 cb. Thus fluorescence is proportional to  $V_a^{1.65}$ . The measured fluorescence value for this screen is about 10 cb lower than the actual value because of significant decay, during excitation, between successive sweeps. Integrated flash is 33 cb greater at 6 kv than at 4 kv, or  $cb_i$  is proportional to  $V_a^{1.88}$ . That this change in  $cb_i$  is larger than the change in  $cb_f$  for the increase in voltage, would be expected because of the slower decay resulting from the increased excitation, as the decay slope decreases with greater excitation for the early portions of the decay. The smaller slope at the greater value of excitation produces an increase in phosphorescence in addition to the increase directly attributable to the increase in excitation, resulting in a larger value of the integration of light out to 1 sec after excitation, and thus a larger value for  $cb_i$ .

This screen has no useful buildup.

VI-2. GE 4665.

The decay characteristics of this zinc-cadmium sulphide, silver activated screen, Fig. 9 and 10, are extremely steep compared to the RMA designated screens studied, and only slightly less steep than the similar phosphor of the GE 4633 tube. The rapid decay becomes quite evident when Fig. 9 and 10 are compared with Fig. 13 through 24 for the RMA screens. The slope curves for this P4 component screen, Fig. 27, compared with the slope curves of Fig. 30 through 36, also make this fact evident. The average slopes of the decay curves of the GE 4665 screen vary from 1.79 to 1.95 for the various excitation conditions, and increase with greater excitation.

The plots of the decay characteristics are similar in general, with downward curvature as the predominating feature. However, the 6 kv curves and the  $Q = 40$ , 4 kv curve have a slightly upward curvature initially, while the  $Q = 10$  and 20, 4 kv decays increase in slope throughout the range of time studied. The trend towards downward curvature is evident for all the curves for later times. The curves for the 6 kv excitation are approximately straight lines for the early parts of the decay, but curve quite noticeably after 0.1 sec. Doubling the value of  $Q$  increases the value of the phosphorescence by an average of 23 cb. At 1.7 ms, an increase in the anode voltage from 4 kv to 6 kv increases phosphorescence by an average of 47 cb. At 0.01 sec, the average increase is 30 cb for the same change in voltage. At 0.3 sec, the same voltage change results in an increase in light output of 51 cb for the  $Q = 10$  condition, 33 cb for the  $Q = 20$  condition, and 6 cb for the  $Q = 40$

condition. Thus phosphorescence is proportional to  $V_a^{0.34}$  to 2.9. The low value of the exponent is for the  $Q = 40$  excitation for times near 0.3 sec. There is some uncertainty in the low value of  $n$ .\*

The slope curves, Fig. 27, show that the slope decreases with greater current density for a screen voltage of 4 kv, and that the slope increases with greater current density for a screen voltage of 6 kv. The slopes have initial values of 1.51 to 1.93. For the two lowest current densities, i.e.  $Q = 10$  and 20, for the 4 kv excitation, the slopes increase from these values at a fairly uniform rate. The remaining curves tend toward minima of 1.46 to 1.79 at about 0.01 sec. The values of the slopes increase thereafter to 2.06 to 2.16 at 0.3 sec.

The plots of fluorescence and integrated flash, Fig. 48, are very nearly straight lines of approximately unit slope. This indicates the direct proportionality between beam current and light output. Increasing  $V_a$  from 4 kv to 6 kv increases fluorescence by 24 cb. Thus fluorescence is proportional to  $V_a^{1.37}$ . The measured fluorescence value for this screen is about 10 cb lower than the actual value because of significant decay, during excitation, between successive sweeps. Integrated flash is 30 cb greater at 6 kv than at 4 kv, or  $cb_i$  is proportional to  $V_a^{1.71}$ .

This screen has no useful buildup.

\* See p. 34.

VI-3. GE 4609.

The decay characteristics of this zinc sulphide, silver activated screen, Fig. 11 and 12, are extremely steep compared to the RMA designated screens studied. This becomes quite evident when Fig. 11 and 12 are compared with Fig. 13 through 24 for the RMA screens. The slope curves for this P4 component screen, Fig. 28 and 29, compared with the slope curves of Fig. 30 through 36, also make this fact evident. The decay of this zinc sulphide screen is somewhat slower than that of the two zinc-cadmium sulphide screens previously discussed. The average slopes of the decay curves of the GE 4609 screen vary from 1.58 to 1.71 for the various excitation conditions, and decrease with greater excitation.

The lifelines for the six excitation conditions are similar among themselves, but are quite different from other decay characteristics measured, in that their variations from a straight line are much more noticeable. Each curve has a slight downward curvature initially, with a following region of greatly accelerated decay. The latter portions of the decay have decided upward curvature, and the decay is of about the same rapidity near the end of the measured decay as initially.

An increase in  $Q$  by a factor of two increases the phosphorescence by an average of 20 cb. Increasing the screen voltage from 4 kv to 6 kv produces an average increase of 25 cb in light output at 1.7 ms for the  $Q = 10$  and 20 conditions, and an average increase of 41 cb for the  $Q = 40$  excitation. At 0.01 sec, the same voltage change increases the light value by an average of 18 cb for the two lower current densities, and 31 cb for the higher current density. The same voltage change



increases the light output by an average of 27 cb at 0.3 sec. Thus the decay curves are somewhat closer together at late times near the end of the measured decay, than initially. Phosphorescence is proportional to  $V_a^{1.42}$  to  $2.57$ .

The slope curves, Fig. 28 and 29, show that the slope decreases with increasing  $Q$  for times less than 0.01 sec, but that for times greater than 0.05 sec the slope increases with increasing  $Q$ . The slopes range from initial values of 1.07 to 1.41 at 3.3 ms, to maxima of 2.2 to 2.54 at 0.1 sec. The 6 kv slope curves decrease initially by about 0.1, forming minima at about 0.01 sec, and then increase to the aforementioned maxima. The decrease in slope after the maximum is slightly faster than the increase before the maximum. The slopes decrease to values ranging from 1.27 to 1.44 at 0.3 sec.

The plots of fluorescence and integrated flash, Fig. 49, are very nearly straight lines of approximately unit slope. This indicates the direct proportionality between beam current and light output. Increasing  $V_a$  from 4 kv to 6 kv increases fluorescence by 35 cb. Thus fluorescence is proportional to  $V_a^{1.98}$ . The measured fluorescence value for this screen is about 10 cb lower than the actual value because of significant decay, during excitation, between successive sweeps. Integrated flash is 38 cb greater at 6 kv than at 4 kv, or  $cb_i$  is proportional to  $V_a^{2.16}$ . That the change in  $cb_i$  is greater than in  $cb_f$ , for the increase in voltage, would be expected because of the slower decay resulting from the increased excitation, as the decay slope decreases with greater excitation for the early part of the decay.

This screen has no useful buildup.

VI-4. RCA 5FP4 A.

The decay characteristics of the P4 screen, Fig. 13 and 14, are much steeper than those for the other RMA screens measured, as seen by direct comparison of the decay curves for the P4 with the curves in Fig. 15 through 24 for the other screens. The slope curves, Fig. 30 and 31 for the P4, compared with Fig. 32 through 36, also make this fact evident. The average slopes of the decay curves of the P4 vary from 1.67 to 1.91 for the various excitation conditions, and increase with greater excitation.

The lifelines for the six excitation conditions studied are similar inasmuch as their slopes increase rapidly from low values for early times to maxima at approximately 0.1 sec, and decrease thereafter. The decay curves deviate increasingly from straight lines as  $Q$  is increased. The lifeline for the lowest excitation,  $Q = 10$ ,  $V_a = 4$  kv, is a close approximation to a straight line, while for the highest excitation,  $Q = 40$ ,  $V_a = 6$  kv, the lifeline shows a noticeable curvature, especially at early times. The latter portions of the decay curves are much closer together than the early portions. At the initial reading at 1.7 ms, an increase in  $Q$  by a factor of two increases phosphorescence by an average of 40 cb. At 0.3 sec, the average increase in phosphorescence is 15 cb when  $Q$  is increased from 10 to 20, and 35 cb when  $Q$  is increased from 20 to 40. This indicates that the slope of the decay curve increases as  $Q$  increases. The slope curves, Fig. 30 and 31, also show that the slope increases as  $Q$  increases, with a possible exception for small values of times. Initially the slope may

decrease as  $Q$  increases, but the evidence here is inconclusive.

Increasing the screen voltage from 4 kv to 6 kv produces an average increase in phosphorescence of 40 cb at 1.7 ms and 25 cb at 0.3 sec. Phosphorescence is proportional to  $V_a^n$ , where  $n$  for this case lies between 1.4 and 2.51.

Slopes range from low values, 1.14 to 1.48, at 3.3 ms, to maxima of 1.88 to 2.34 at about 0.1 sec. The decrease in slope after the maximum is about as fast as the increase before 0.1 sec. The slope decreases to a value of 1.75 to 2.14 at 0.3 sec.

The plots of fluorescence and integrated flash, Fig. 50, are very nearly straight lines of approximately unit slope, and thus indicate the direct proportionality between beam current and light output. Increasing  $V_a$  from 4 kv to 6 kv increases fluorescence by 33 cb. Thus fluorescence is proportional to  $V_a^{1.87}$ . The measured fluorescence value for this screen is about 10 cb lower than the actual value because of significant decay, during excitation, between successive sweeps. Integrated flash is 27 cb greater at 6 kv than at 4 kv, or  $cb_i$  is proportional to  $V_a^{1.53}$ . That this change in  $cb_i$  is smaller than the change in  $cb_f$  for the increase in voltage, would be expected because of the more rapid decay resulting from the increased excitation, as the decay slope increases with greater excitation. The equilibrium value, measured as  $cb_f$ , is increased solely by the increase in fluorescence. The integrated flash value, being determined by integration of light out to 1 sec after excitation, is affected by the increase in phosphorescence, brought about by the increase in the magnitude of the excitation; but

the increase is reduced somewhat by the simultaneous acceleration of decay.

This screen has no useful buildup.

VI-5. RCA 5FP14 A 6331.

The average slopes of the decay characteristics, Fig. 15 and 16, for this screen, are in the region between 1.12 and 1.22, and are smaller for larger excitations.

The decay curves are very nearly straight lines, tending to have increasing slopes initially, decreasing in steepness at intermediate times, and again increasing near the end of the measured decay. The differences in slopes for the different excitation conditions are apparent from the greater separation of the decay characteristics at later times than initially. The average increase in phosphorescence due to an increase in current density by a factor of two is 22 cb at 1.7 ms and 38 cb at 10 sec. The separation of the characteristics taken at two screen voltages, 4 kv and 6 kv, is approximately the same as the separation between curves for the different Q's, as evidenced by the similarity of the  $Q = 20, V_a = 4$  kv curve to the one for the  $Q = 10, V_a = 6$  kv condition. Thus phosphorescence is proportional to  $V_a^{1.3}$  to  $2.2$ .

The decay slopes, Fig. 32, increase initially for the 4 kv excitations, but change little for early times for the 6 kv excitations. All the slope curves tend toward lower values at intermediate times with increasing slopes at later times. The initial slopes at 4 kv range from 0.97 to 1.07, increase to values between 1.14 and 1.31 at about 0.03 sec, pass through variations at somewhat smaller values, for intermediate times, creating not very clearly defined minima, and finally increase after about 3 sec to values between 1.29 and 1.4 at 10 sec. The 6 kv group has initial slopes in the range between 1.08 and 1.2, followed by

a decrease to minima of 0.98 to 1.02 for times between 0.1 sec and 3 sec. The increase after the minima brings the slope values to 1.35 to 1.4 at 10 sec. Here again, an increase in  $Q$  decreases the slope of the early part of the decay, but increases the slope of the later part. The change from the condition in which the slope decreases as  $Q$  increases, to that in which the slope increases as  $Q$  increases, takes place earlier for greater excitations. Slope values on the tails of the decay curves tend to increase and approach equality as the excitation is increased.

The very nearly straight line plots of approximately unit slope of Fig. 51, for fluorescence and integrated flash, indicate the direct dependence of  $cb_f$  and  $cb_i$  on beam current. The fluorescence value for 6 kv is 27 cb above the value for 4 kv, while the two  $cb_i$  curves are 31 cb apart. Thus fluorescence is proportional to  $V_a^{1.5}$ , and  $cb_i$  is proportional to  $V_a^{1.7}$ . That the change in  $cb_i$  is greater than in  $cb_f$  for the increase in voltage, would be expected because of the slower decay resulting from the increased excitation, as the decay slope decreases with greater excitation for the early part of the decay.

Fig. 37, buildup plots, shows that the phosphor approaches saturation rapidly when excited by repeated pulses. The buildup ratio  $G_{5:1}$  decreases from 6.8 for the  $Q = 10$ ,  $V_a = 4$  kv case, to 2.4 for the  $Q = 40$ ,  $V_a = 6$  kv excitation. For the same two conditions,  $G_{10:1}$  decreases from 10.5 to 2.7. Doubling the current density produces a smaller change in light output 1 sec after excitation than increasing the anode voltage by a factor of 1.5.

The plots in Fig. 42, of  $cb_1$ ,  $cb_5$ ,  $cb_{10}$  as functions of beam

current, have slopes ranging from 1.3 to 0.75. The two  $cb_1$  curves have slopes greater than unity, indicating that  $cb_1$  increases more rapidly than  $\log_{10} i_p$ . Now since  $cb_f$  is directly proportional to  $Q$ , this shows that the total decay in the first second after excitation by one raster decreases with increasing  $Q$ . On the other hand, the slopes of the  $cb_5$  and  $cb_{10}$  curves are less than unity, indicating that the total decay in the first second after excitation by five to ten rasters is greater for greater current density. The smaller separation of the curves for the greater excitations on this plot demonstrates the decrease in buildup ratios.

VI-6. RCA 5FP14 C7570N 3940-18.

The average slopes of the decay characteristics, Fig. 17 and 18, of this screen, are reduced by increasing excitation, and lie in the range between 1.1 and 1.18.

An inspection of the plots of the slopes of the decay curves, Fig. 33, reveals the existence of slope minima as the characteristic common to the decays of the various excitations studied. These minima are also indicated by the greater separation of the curves for different Q values at intermediate times than at initial times. Doubling the value of Q results in an average increase of 25 cb in phosphorescence at 1.7 ms, 38 cb at 0.3 sec, and 33 cb at 10 sec. Increasing the anode voltage from 4 kv to 6 kv increases phosphorescence about 5 cb more than doubling the current density, at all points along the decay characteristic. Thus phosphorescence is proportional to  $V_a^{1.7}$  to  $2.5$ .

The decay slopes decrease from initial values of 1.28 to 1.34, to minima of 0.96 to 1.02 at times between 0.03 and 3.0 sec, and increase to 1.11 to 1.33 at 10 sec. The time of the minimum is shifted to earlier times for increased current density or increased screen potential. The slope plots for the 6 kv group are quite similar in general appearance, much more so than the 4 kv group, indicating that for larger excitations the slopes tend towards the same value, and the decay characteristics become more nearly parallel. The early parts of the decays are steeper for smaller excitations, while the later parts are steeper for larger excitations. The change from the condition in which the slope decreases as Q increases to that in which the slope



increases as  $Q$  increases, takes place earlier for the 6 kv characteristics than for the 4 kv characteristics.

The plots of fluorescence and integrated flash in Fig. 52 are very nearly straight lines of approximately unit slope, indicating the direct proportionality of light output upon current density. The  $cb_f$  curve for 6 kv is 23 cb above that for 4 kv, while the two  $cb_1$  curves are 32 cb apart. Thus fluorescence is proportional to  $V_a^{1.3}$ , and  $cb_1$  is proportional to  $V_a^{1.8}$ . That the change in  $cb_1$  is greater than the change in  $cb_f$  for the increase in voltage, would be expected, because of the slower decay resulting from the increased excitation, as the slope decreases with greater excitation for the early part of the decay.

The buildup plots of Fig. 38 show the rapid approach of saturation as the phosphor is excited by repeated pulses. The buildup ratio  $G_{5:1}$  decreases from 5.75 for the  $Q = 10$ ,  $V_a = 4$  kv case, to 1.95 for the  $Q = 40$ ,  $V_a = 6$  kv excitation. For the same two excitations,  $G_{10:1}$  decreases from 7.6 to 2.1. As for the previous tubes discussed, doubling the current density produces a smaller change in light output 1 sec after excitation than increasing the voltage by a factor of 1.5.

The plots in Fig. 43 of  $cb_1$ ,  $cb_5$ ,  $cb_{10}$  as functions of beam current have slopes ranging from 1.4 to 0.5. The two  $cb_1$  curves have slopes greater than unity\*, indicating that the total decay in the first second after excitation by one raster decreases with increasing  $Q$ . On the other hand, the slopes of the  $cb_5$  and  $cb_{10}$  curves are less than

\* See p. 45.

unity, indicating that the total decay in the first second after excitation by five or ten rasters is greater for greater current density. The smaller separation of the curves for the greater excitations on this plot demonstrates the decrease in buildup ratio.

VI-7. GE 5FP14 C72745.

The decay characteristics of this screen, Fig. 19 and 20, have average slopes which lie between 0.93 and 1.06, and decrease with greater excitation. In general, the characteristics decrease in slope in the early portions of the decays, reach slope minima at intermediate times, and increase in steepness near the end of the measured decay. These variations in slope become smaller for greater excitations, so that the curve for the  $Q = 40$ ,  $V_a = 6$  kv condition is a fair approximation to a straight line initially, but has a noticeable increase in steepness after about 1 sec. The minima in slope values are made evident from the decay curves by the greater separation of the characteristics for the various excitation conditions at the intermediate times than for earlier and later times. At the initial reading, 1.7 ms, the separation of the curves for the different  $Q$ 's averages 25 cb; at 0.1 sec this separation averages 50 cb; and at 1 sec it averages 45 cb. The separation of the characteristics taken at the two screen voltages, 4 kv and 6 kv, is approximately the same as the separation between the curves for the different  $Q$ 's. Note the marked resemblance of the  $Q = 20$ ,  $V_a = 4$  kv curve to the one for  $Q = 10$ ,  $V_a = 6$  kv curve. This indicates that doubling the current density gives nearly the same effect as increasing the voltage by a factor of 1.5, and thus that phosphorescence is proportional to  $V_a^{1.4}$  to  $2.8$ .

The decay slopes, Fig. 34, decrease initially from values of 0.88 to 1.27, to minima of 0.81 to 0.87 at times between 0.05 sec and 1.0 sec, then increase to values ranging from 1.02 to 1.19 at 10 sec.

Note that the range in slope values for the 6 kv group is quite small at the end of the measured decay, indicating that for large excitations, the slopes tend towards the same value at the tails of the decay characteristics, even though the initial slopes may vary considerably. The minima of the slopes of the decay curves occur earlier at greater excitations. An increase in  $Q$  decreases the slope of the early part of the decay, but increases the slope of the later part of the decay. The change from the condition in which the slope decreases as  $Q$  increases to that in which the slope increases as  $Q$  increases, takes place earlier for characteristics taken at 6 kv than for those at 4 kv.

The plots of fluorescence and integrated flash in Fig. 53 are very nearly straight lines of approximately unit slope, and indicate the direct proportionality of light output and current density. The  $cb_f$  curve for 6 kv is 32 cb above that for 4 kv, while the two  $cb_i$  curves are 40 cb apart. Thus fluorescence is proportional to  $V_a^{1.8}$ , and  $cb_i$  is proportional to  $V_a^{2.3}$ . That the change in  $cb_i$  is greater than the change in  $cb_f$  for the increase in voltage, would be expected because of the slower decay resulting from the increased excitation, as the decay slope decreases with greater excitation for the early part of the decay.

Fig. 39, buildup plots, shows that the phosphor approaches saturation rapidly when excited by repeated pulses. The buildup ratio  $G_{5:1}$  decreases from 10.8 for the  $Q = 10$ ,  $V_a = 4$  kv case, to 2.4 for the  $Q = 40$ ,  $V_a = 6$  kv excitation. For the same two conditions,  $G_{10:1}$  decreases from 15.1 to 2.6. As for the other P14's, an increase in current density by a factor of two produces a smaller change in light

output 1 sec after excitation than an increase in voltage by a factor of 1.5.

The plots of  $cb_1$ ,  $cb_5$ ,  $cb_{10}$  in Fig. 44 have slopes ranging from 1.7 for  $cb_1$  at 4 kv to 0.62 for  $cb_{10}$  at 6 kv. The slopes of the two  $cb_1$  curves are both greater than unity. This indicates that the total decay in the first second after excitation by one raster decreases with increasing  $Q$ .\* On the other hand, the slopes of the  $cb_5$  and  $cb_{10}$  curves are less than unity. This indicates that the total decay in the first second after excitation by five or ten rasters is greater for greater  $Q$ . The smaller separation of the curves for the greater excitations on this plot demonstrates the decrease in buildup ratios.

\* See p. 45.

VI-8 and 9. RCA 5FP7 A, 1 and 2.

The P7 screen has the longest persistence of the tubes measured, so that the decay characteristics in Fig. 21 through 24 have the lowest slope values, although the average slopes are only slightly lower than those for the P14 screens. The average slopes of the decay curves of the two P7 screens vary from 0.9 to 1.04 for the various excitation conditions, and decrease with greater excitations.

The two P7 screens are at roughly the same light levels along the decay characteristics. At 1.7 ms, the phosphorescence values of the P7 1 are an average of 13 cb above those for the P7 2. At 0.1 sec, the light output of the P7 2 is an average of 5 cb higher than the P7 1. At 10 sec and 30 sec, the P7 2 is an average of 2 cb higher than the P7 1.

The similarity of the P7 decay curves can best be seen by comparisons of the slope plots, Fig. 35 and 36. There is some tendency for the slope to increase in the beginning from its initial value, but the increase is smaller for greater excitations. The chief characteristic of the slope curves, however, is the appearance of minima in the intermediate parts of the measured decays, followed by an increase in the slopes. These variations in slope along the lifelines are also evident from the decay plots, where the curves are closer together at earlier times than at later times. The minima in the slope curves correspond to the initial upward curvature of the decay characteristics, followed by the increase in slope evident from the downward curvature near the later portions of the measured decays. The  $Q = 10$ ,  $V_a = 4$  kv

curves, Fig. 21 and 23, are very nearly straight lines, but the curves for higher excitations, Fig. 22 and 24, differ increasingly from linearity with increasing excitation.

For the P7 1, doubling the value of  $Q$  results in an average increase of 25 cb in phosphorescence at the 1.7 ms decay point, 35 cb at 0.1 sec, and 38 cb at 10 sec. For the P7 2, doubling the value of  $Q$  results in average increases of 15 cb at 1.7 ms, 30 cb at 0.1 sec, and 36 cb at 10 sec. Thus the P7 2 is influenced somewhat less by the increased current density. The general trend of greater separation for the later portions of the decay, together with the sequence of slope plots, indicates that the slope decreases when the excitation increases.

Increasing the screen voltage of the P7 1 from 4 kv to 6 kv results in an average increase of phosphorescence of 32 cb at the initial reading of 1.7 ms, 48 cb at 0.1 sec, and 42 cb at 10 sec. Thus phosphorescence is proportional to  $V_a^{1.8}$  to  $2.7$  for the P7 1. For the P7 2, increasing the screen voltage from 4 kv to 6 kv results in an average increase of phosphorescence of 24 cb at 1.7 ms, 38 cb at 0.1 sec, and 39 cb at 10 sec. So for the P7 2, phosphorescence is proportional to  $V_a^{1.37}$  to  $2.21$ . As for the increase in  $Q$ , the P7 2 is influenced less by the increased voltage than the P7 1. These comparisons show that the decay curves for the two values of screen voltage also increase in separation at intermediate times, but tend together again near the end of the measured decay. That is, the slope decreases more for an increase in screen voltage at intermediate times than at earlier or later times.

For the P7 1, decay slope values range from 0.97 to 1.24

initially, decrease to minima of 0.81 to 0.95 at times between 0.3 sec and 1 sec, and increase thereafter to values of 1.08 to 1.21 at 30 sec. For the P7 2, the initial slopes range from 0.79 to 1.07, decrease to minima of 0.73 to 0.96 at times between 0.03 sec and 0.1 sec. After the minima, the slopes increase to 1.08 to 1.17 at 30 sec. The average slope of the P7 1 varies from 0.95 to 1.04, while the average slope of the P7 2 varies from 0.9 to 1.03. Thus the average slopes of the two screens are very nearly the same, although the P7 2 decays somewhat more slowly. The time of the minimum in the slopes is earlier for increased current density or increased screen potential. The time of the slope minimum is also much earlier for the P7 2 than for the P7 1.

Fig. 54 and 55 indicate the direct proportionality of screen excitation to light output by the very nearly straight line plots of approximately unit slope of fluorescence and integrated flash vs the logarithm of the beam current. The  $cb_f$  curve of the P7 1 for 6 kv is 25 cb above the one for 4 kv, while the two  $cb_i$  curves for this tube are 35 cb apart. The  $cb_f$  curve of the P7 2 for 6 kv is 22 cb above that for 4 kv, while the two  $cb_i$  curves are 32 cb apart. Thus fluorescence is proportional to  $V_a^{1.4}$  for the P7 1 and to  $V_a^{1.25}$  for the P7 2. Integrated flash is proportional to  $V_a^2$  for the P7 1 and to  $V_a^{1.82}$  for the P7 2. Measured fluorescence values for the P7 2 are an average of 9 cb above the corresponding values for the P7 1. The measured  $cb_i$  values for the two tubes are less than 2 cb apart on the average, again with the P7 2 somewhat larger than the P7 1.

That the change in  $cb_i$  is greater than the change in  $cb_f$  for



the increase in voltage, would be expected because of the slower decay resulting from the increased excitation, as the decay slope decreases with greater excitation.

The buildup plots, Fig. 40 and 41, show that even at the greatest excitation used,  $Q = 40$ ,  $V_a = 6$  kv, the phosphor was only beginning to reach saturation. Buildups for the P14 screens, cf. Fig. 37 through 39, are much faster than for the P7's. The buildup ratios decrease with increasing  $Q$ , since, of course, a greater current density brings the light output closer to that of the saturated condition. The buildup ratio  $G_{5:1}$  for the P7 1 decreases from 7.2 for the  $Q = 10$ ,  $V_a = 4$  kv excitation, to 3.4 for the  $Q = 40$ ,  $V_a = 6$  kv excitation. For the same conditions,  $G_{10:1}$  for the P7 1 decreases from 11.5 to 4.4. For the same conditions again,  $G_{5:1}$  for the P7 2 decreases from 5.25 to 3.55, and  $G_{10:1}$  decreases from 9.1 to 4.16. From the plots, it is also seen that an increase in current density by a factor of two, with constant  $V_a$ , produces a smaller change in light output 1 sec after excitation than an increase in voltage by a factor of 1.5, with constant  $Q$ .

The plots of  $cb_1$ ,  $cb_5$ ,  $cb_{10}$  vs  $\log_{10} i_p$  for the P7 1, Fig. 45, have average slopes ranging from 1.0 to 1.4. For the P7 2, Fig. 46,  $cb_1$  and  $cb_5$  have slopes ranging from 1.02 to 1.3. Slopes of the  $cb_{10}$  plots for the P7 2 are less than unity, and are 0.92 and 0.85 for the 4 kv and 6 kv conditions, respectively. When the slope is greater than unity, i.e. for excitations by one to ten rasters for the P7 1, and by one to five rasters for the P7 2, the total decay in the first second after

excitation decreases with increasing  $Q$ .\* When the slope is unity, i.e. for a ten raster excitation of the P7 1 at 6 kv, this one second total decay is not changed when  $Q$  changes. When the slope is less than unity, i.e. for excitation of the P7 2 screen by ten rasters, the total decay in the first second after excitation increases with increasing  $Q$ . The slopes of these  $cb_N$  curves decrease with increasing  $Q$ . The decrease in buildup ratios with increasing excitations is evidenced in these plots by the decreasing separation of the curves at the higher levels of excitation.

\* See p. 45.

## VII. ANALYSIS OF MEASUREMENTS BY COMPARISONS AMONG TUBE TYPES

### VII-1. Phosphorescence.

The decay characteristics provide a comparison of persistence times. The tubes have been discussed in the order of increasing persistence. The three GE tubes, GE 4633, GE 4665, GE 4609, with screens composed of P4 components, decay the most rapidly of the tubes studied, as the decay plots in Fig. 7 through 12 indicate. The P4 screen, Fig. 13 and 14, decays nearly as fast. The three P14 screens, Fig. 15 through 20, are considerably slower in decay than any of these, and the P7's, Fig. 21 through 24, are somewhat slower than the P14's. Table 3 is included in order to present a comparison of light levels among the screen types, at various times, for excitation of the phosphor by a current density of 20  $\mu\text{coulombs}/\text{cm}^2$  with an anode voltage of 4 kv. This value of excitation was chosen as representative. Note that the three GE P4 component screens and the P4 screen decay about 200 cb between 0.01 sec and 0.1 sec. This is equivalent to saying that the phosphorescence level decreases by a factor of about 100 during that time interval, and that the slope of the decay curves for these screens is about two in that interval. For the remaining screens, the decay between 0.01 sec and 0.1 sec is about 100 cb, a decrease in phosphorescence by a factor of about 10. Thus the P14's and the P7's have decay slopes near unity.

The decay characteristics of the GE 4633 screen, Fig. 7 and 8, and the GE 4665 screen, Fig. 9 and 10, are noticeably different, although

TABLE 3

CONDENSED DATA ON DECAY AND SLOPES

for:  $Q = 20 \text{ micoulombs/cm}^2$   
 $V_a = 4 \text{ kv}$

<u>TUBE</u>	<u>D<sub>0.01</sub></u> <sup>*</sup>	<u>S<sub>0.01</sub></u> <sup>**</sup>	<u>D<sub>0.1</sub></u>	<u>S<sub>0.1</sub></u>	<u>D<sub>1.0</sub></u>	<u>S<sub>1.0</sub></u>	<u>D<sub>10</sub></u>	<u>S<sub>10</sub></u>
GE 4633	449	2.98	229	1.94	----	----	----	----
GE 4665	531	1.56	344	1.88	----	----	----	----
GE 4609	499	1.21	294	2.52	----	----	----	----
RCA 5FP4 A	521	1.52	317	2.12	----	----	----	----
RCA 5FP14 A 6331	565	1.15	440	1.21	334	1.15	207	1.39
RCA 5FP14 3940-18	566	1.23	453	1.12	355	0.98	243	1.21
GE 5FP14	531	1.18	442	0.83	351	0.94	248	1.10
RCA 5FP7 A 1	542	1.21	437	0.98	350	0.82	261	0.96
RCA 5FP7 A 2	541	1.08	443	1.00	359	0.81	267	0.98

\* D indicates the cb value on the decay characteristic at the time in seconds, indicated by the subscript, after the end of screen excitation.

\*\* S indicates the slope of the decay characteristic at the time in seconds indicated by the subscript.

their phosphor compositions are nominally the same. Both tubes have zinc-cadmium sulphide, silver activated screens, with phosphors manufactured by the General Electric Company and the Patterson Screen Company respectively. Both screens have yellow green luminescence, with the GE 4633 somewhat lighter in shade. Although the fluorescence values for these two tubes are less than 10 cb apart, with the GE 4665 having the higher value, the difference in light levels is quite large for short times after the end of excitation. For example, as shown in Table 3, the GE 4665 is 115 cb higher than the GE 4633 at 0.1 sec.

The third P4 component screen, the GE 4609 tube, differs markedly from the other screens. It has a zinc sulphide, silver activated screen which emits light blue luminescence. Its measured fluorescence is less than one-tenth as bright as the other two P4 component screens. However, a part of the difference in measured values is caused by the variation in the multiplier-filter response with wave-length, Fig. 5. The decay characteristics, Fig. 11 and 12, are unusual in their rather extreme variation from straight lines. This variation consists of the initial downward curvature of the lifelines, followed by regions of greatly accelerated decay at intermediate times, and a marked decrease in slope near the end of the measured decay.

The decay of the P4 screen, Fig. 13 and 14, is less rapid than any of the screens having components of the P4 phosphor. Of the three P14 screens, the GE tube, Fig. 19 and 20, has the slowest decay, although its phosphorescence is lowest for early times. The two RCA P14's, Fig. 15 through 18, emit very nearly the same light shortly after excitation,

but the 6331 tube, which has the newer type poured screen, decays somewhat faster.

Slope plots show the character of the lifelines much more readily than the decay plots. The slope plots fall into two categories: one in which the slope rises from a low value to a maximum; and a second in which the slope decreases to a minimum for intermediate parts of the decay, and increases for later times. The first type represents the decay curve which has downward curvature initially, followed by upward curvature. The second type of slope curve corresponds to the decay curve with initial upward curvature followed by downward curvature. The slope plots of the screens of the P4, Fig. 30 and 31, the GE 4633, Fig. 25 and 26, and the GE 4609, Fig. 28 and 29, belong to the first category, while those of the P7 and P14 screens, Fig. 32 through 36, and the GE 4665 screen, Fig. 27, are of the second type. Table 4 presents information taken from the slope plots of Fig. 25 through 36. The minima in the slopes of the decay characteristics of the P7 and P14 screens occur at intermediate times ranging from 0.03 to 3.0 sec. The minima in the slope plots of the GE 4665 occur at about 0.01 sec, except for the  $Q = 10$  and  $Q = 20$  curves at 4 kv, for which the slope increases over the entire range of measured decay. Since the minima are not evident on all curves, and since they are not as pronounced as for the other tubes when they do appear, the significance of these minima for the GE 4665 tube is uncertain. The maxima in the slopes of the decay characteristics of the P4 and GE 4609 occur at about 0.1 sec, while the maxima in slope for the GE 4633 occur between 0.01 and 0.03 sec.

TABLE 4

SOME DATA ON SLOPES OF DECAY CHARACTERISTICS

TUBE	ANODE VOLTAGE KV	APPROXIMATE VALUE OF t(sec) WHEN SLOPE IS:			
		MAX	MIN	DECREASING WITH Q	INCREASING WITH Q
GE 4633	4	0.01 - 0.03 *	-----	less than 0.01	greater than 0.02
	6	0.01 - 0.03	-----	" " 0.01	" " 0.02
GE 4665	4	-----	0.01 **	all	-----
	6	-----	0.01	-----	all
GE 4609	4	0.1	-----	less than 0.03	greater than 0.05
	6	0.1	0.01	" " 0.01	" " 0.03
RCA 5FP4 A	4	0.1	-----	-----	all
	6	0.1	-----	-----	all
RCA 5FP14 A 6331	4	-----	0.1 - 3.0	less than 1	greater than 5.0
	6	-----	0.1 - 3.0	" " 0.3	" " 2.0
RCA 5FP14 3940-18	4	-----	0.03- 3.0	less than 1	greater than 3.0
	6	-----	0.03	" " 0.03	greater than 0.5
GE 5FP14	4	-----	0.1 - 1.0	less than 0.3	greater than 0.5
	6	-----	0.05- 0.1	" " 0.05	" " 0.3
RCA 5FP7 A 1	4	-----	1.0	all	-----
	6	-----	0.3	all	-----
RCA 5FP7 A 2	4	-----	0.03- 1.0	all	-----
	6	-----	0.03- 0.1	all	-----

\* Where two figures appear, they represent the extremes of the locations of the minima or maxima for the three values of Q: 10, 20, and 40  $\mu\text{c}/\text{cm}^2$ .

\*\* Curves for Q = 10 and 20  $\mu\text{c}/\text{cm}^2$  show no minima, but are increasing initially.

The minima in the slope plots for the P7 and P14 screens are observed to shift to earlier times for increased excitation, as shown in Fig. 32 through 36. The minima for the GE 4665 screen, Fig. 27, and the maxima in the slopes of the P4, GE 4633, and GE 4609 screens, Fig. 25, 26, 28, and 29, appear to be at about the same time for all the excitations studied.

The magnitudes of the slopes of the characteristics of the P14's, Fig. 31 through 34, the GE 4633, Fig. 25 and 26, and the GE 4609, Fig. 28 and 29, decrease as  $Q$  increases at early times, but increase as  $Q$  increases at later times. This reversal occurs at earlier times for greater values of excitation. For the range in time studied, there is no such reversal in the case of the P4, Fig. 30, for which the slopes increase with  $Q$ ; nor in the case of the P7's, Fig. 35 and 36, for which the slopes decrease with  $Q$ . The GE 4665 is exceptional in that the slopes of its characteristics decrease with  $Q$  over the entire measured decay for the 4 kv condition, but increase with  $Q$  over the entire range for the 6 kv condition.

Data taken from the plots discussed above are presented in Table 4, which gives, approximately, times of maxima or minima in slopes, and times when slopes increase and decrease as  $Q$  increases.

Phosphorescence is directly proportional to  $V_a^n$ , where  $n$  varies from 1.3 to 2.9 over the range in time of the decays studied, for all the screens with the exception of the GE 4633 and the GE 4665. The lowest values of  $n$  were found to be 0.21 and 0.34 respectively for these screens. However, there is some uncertainty in these low values\*

\* See pp. 34, 37.



## VII-2. Buildup.

The buildup curves, Fig. 37 through 41, show that the buildup decreases with increasing excitation as the phosphor approaches the saturated condition.

Table 5 presents a tabulation of the average slopes of the  $cb_N$  vs  $\log_{10} i_p$  plots, Fig. 42 through 46, and Table 6, p. 67, gives some comparative data showing the decrease in buildup ratios for increasing excitations.

Here it is shown that the slopes of the  $cb_1$  vs  $\log_{10} i_p$  curves are greater than unity for the tubes measured. This means that the value of  $cb_1$  increases more rapidly than  $\log_{10} i_p$ , or that the light values at the one second decay points are superproportional to beam current. As shown in Table 4, this superproportionality decreases with increasing intensifier voltage. Flash and fluorescence values, on the other hand, are directly proportional to beam current.

This superproportionality, and the direct dependence of fluorescence on current density, indicate that the total decay, in the first second after excitation of these screens, decreases with increasing  $Q$ . Or, in other words, the average slope of the decay curve, computed from the maximum light value at the end of excitation to the light value at the one second point, decreases with increasing current density. It is found experimentally that the average slopes of the decay curves, determined from the straight lines that have approximately the least square deviation from the actual decay characteristics, decrease as the excitation increases, with the exception of the P4 and the GE 4665 screens.

TABLE 5  
AVERAGE SLOPES\* OF PLOTS OF  
" $cb_1$ ,  $cb_5$ ,  $cb_{10}$  AS FUNCTIONS OF BEAM CURRENT"

TUBE	$cb_1$		$cb_5$		$cb_{10}$	
	4 kv	6 kv	4 kv	6 kv	4 kv	6 kv
GE 4633	No useful buildup					
GE 4665	No useful buildup					
GE 4609	No useful buildup					
RCA 5FP4 ▲	No useful buildup					
RCA 5FP14 A 6331	1.3	1.3	0.9	0.87	0.68	0.75
RCA 5FP14 3940-18	1.4	1.03	0.82	0.55	0.68	0.5
GE 5FP14	1.7	1.25	0.87	0.65	0.72	0.62
RCA 5FP7 A 1	1.4	1.35	1.15	1.05	1.05	1.0
RCA 5FP7 A 2	1.12	1.3	1.1	1.02	0.92	0.85

$$* \text{ Average Slope } = \frac{cb_N(i_p = 120 \mu a) - cb_N(i_p = 30 \mu a)}{\log_{10} (120/30)}$$

The values of  $cb_5$  and  $cb_{10}$  for the three P14 screens, and of  $cb_{10}$  for the P7 2 screen, are subproportional to beam current, showing the approach of saturation of the phosphor; whereas  $cb_5$  values for both P7's, and  $cb_{10}$  values as well for P7 1, are somewhat superproportional, indicating that these screens approach saturation more slowly. Because of the subproportionality existing for the P14 screens, the total decay in the first second after excitation of these screens by five or ten standard rasters at one second intervals would be expected to increase with increasing  $Q$ . This increase in the decay slope would be greater for ten pulse excitation than for five, and would be greater for greater final anode voltage.

VII-3. Integrated Flash and Fluorescence.

Plots of flash and fluorescence, Fig. 47 through 55, are very nearly straight lines, with slopes of approximately unity, indicating the direct proportionality between beam current, and flash and fluorescence, over the range tested. A comparison of values, given in Table 6, for the tubes studied, shows a rough correlation between decay slopes, integrated flash values, fluorescence values, and buildup ratios. Associated with rapid decay are high flash and fluorescence values and low values of the buildup ratio.

Fluorescence and integrated flash are proportional to  $V_a^n$ , where the exponent  $n$  varies from 1.25 to 1.98 for fluorescence, and from 1.7 to 2.3 for flash. Various values of the exponent for the tubes studied are given in Table 7.

TABLE 6

FLASH AND FLUORESCENCE CHARACTERISTICS

<u>TUBE</u>	V = Q <sup>a</sup> =	<u>cb<sub>i</sub></u>		<u>S<sub>0.1</sub></u>		<u>G<sub>5:1</sub></u>		<u>cb<sub>f</sub></u>	
		4 <u>10</u>	6 <u>40</u>	4 <u>10</u>	6 <u>40</u>	4 <u>10</u>	6 <u>40</u>	4 <u>10</u>	6 <u>40</u>
GE 4633		642	731	2.02	2.12	*		693	771
GE 4665		653	738	1.9	1.85	*		700	774
GE 4609		533	622	2.29	2.54	*		582	668
RCA 5FP4 A		591	671	1.88	2.25	*		661	746
RCA 5FP14 A 6331		560	648	1.19	0.98	6.8	2.4	653	728
RCA 5FP14 3940-18		571	662	1.23	1.00	5.8	2.0	668	742
GE 5FP14		528	633	1.06	0.97	10.8	2.4	646	727
RCA 5FP7 A 1		560	651	1.0	0.81	7.2	3.4	655	732
RCA 5FP7 A 2		562	643	0.98	0.79	5.25	3.55	668	736

cb<sub>i</sub> = integrated flash to 0.1 sec.

S<sub>0.1</sub> = slope of decay characteristic at the 0.1 sec. point.

G<sub>5:1</sub> = buildup ratio for five rasters

$$= \text{antilog} \frac{cb_5 - cb_1}{100} .$$

cb<sub>f</sub> = fluorescence.

\* No useful buildup.

TABLE 7

DEPENDENCE OF FLUORESCENCE AND FLASH ON ANODE VOLTAGE

<u>TUBE</u>	<u>EXPONENT OF <math>V_a</math></u>	
	<u>FLUORESCENCE</u>	<u>FLASH</u>
GE 4633	1.65	1.88
GE 4665	1.37	1.71
GE 4609	1.98	2.16
RCA 5FP4 A	1.87	1.53
RCA 5FP14 A 6331	1.5	1.7
RCA 5FP14 3940-18	1.3	1.8
GE 5FP14	1.8	2.3
RCA 5FP7 A 1	1.4	2.0
RCA 5FP7 A 2	1.25	1.82

## VIII. SUMMARY OF GENERAL CONCLUSIONS

The following conclusions can be reached regarding the properties of the particular screens studied herein, viz. the P4, P14, P7, ZnS:CdS, and ZnS phosphors; over the ranges of excitation used, viz.  $Q = 10$  to  $40 \text{ } \mu\text{coulombs/cm}^2$ ,  $V_a = 4 \text{ kv}$  and  $6 \text{ kv}$ ; through the range in times measured, viz.  $1.7 \text{ ms}$  to  $0.1 \text{ sec}$  for more rapid decays, and  $1.7 \text{ ms}$  to  $30 \text{ sec}$  for the slower decays.

### VIII-1. Phosphorescence.

The slopes of the decay characteristics fall into two broad categories:

- (1) Slope increases to maximum and then decreases.
- (2) Slope decreases to minimum and then increases.

The first type includes the shorter persistence screens, e.g. P4. The second type includes the intermediate and long persistence screens, e.g. P7.

The maxima of the slopes of the first type occur at about the same time for each excitation investigated.

In the slopes of the second type, the minima occur at earlier times for increased excitations.

The slopes of the decay characteristics of the P7 screens decrease with increasing  $Q$ . For the P4 screens, the slopes of the decay characteristics increase with increasing  $Q$ . For the other screens, the initial slopes are smaller for larger values of the excitation, but the slopes near the end of the measured lifelines are larger for increased

excitations; this shift from a decrease to an increase of slope with excitation occurs at earlier times for greater excitations.

Phosphorescence decays for various excitations are not uniformly separated. In general, if the slopes exhibit minima, the decay curves are closer together initially than at intermediate times; but for slopes which have maxima, the reverse is true. Phosphorescence, therefore, has a dependence on the anode voltage and the current density which varies with time from the end of excitation. It is directly proportional to  $V_a^n$ , where the value of  $n$  varies from 1.3 to 2.9 approximately. Its dependence on the current density is such that doubling  $Q$  increases the light level by a factor which varies from 1.4 to 3.2.

The luminescence, both during and after excitation, increases more for a change in anode voltage from 4 kv to 6 kv than for a change in  $Q$  from 10 to 20 or from 20 to 40  $\mu\text{coulombs/cm}^2$ .



VIII-2. Buildup.

The buildup ratio decreases for greater excitation for all the phosphors.

The value of the light output one second after one raster, i.e.  $cb_1$ , is superproportional to the logarithm of the current density for all the phosphors. The superproportionality decreases with increasing excitation. The values of  $cb_5$  and  $cb_{10}$  are subproportional to  $\log_{10} Q$ , with the exception of the P7. Superproportionality, and the direct dependence of fluorescence on current density, indicate that the total decay in the first second after excitation decreases with increasing  $Q$ . Subproportionality indicates that this decay increases with increasing  $Q$ .

VIII-3. Integrated Flash and Fluorescence.

The fluorescence and flash values are directly proportional to  $V_a^n$ . For fluorescence, the value of n varies from 1.25 to 1.98. For flash, the value of n varies from 1.7 to 2.3. Flash and fluorescence are directly proportional to Q.

There is some evidence that high flash and fluorescence values, and low values of the buildup ratio, are associated with rapid decays.

Acknowledgment. The author wishes to express his appreciation to Professor W. B. Nottingham for advice in the conduct of this research and in the preparation of this report.

APPENDIX

PLOTS

DECAY AFTER ONE RASTER  
GE 4633  
 $V_G = 6 \text{ kv}$

$Q = 10, 20, 40 \text{ m}\mu\text{ COULOMBS/cm}^2$

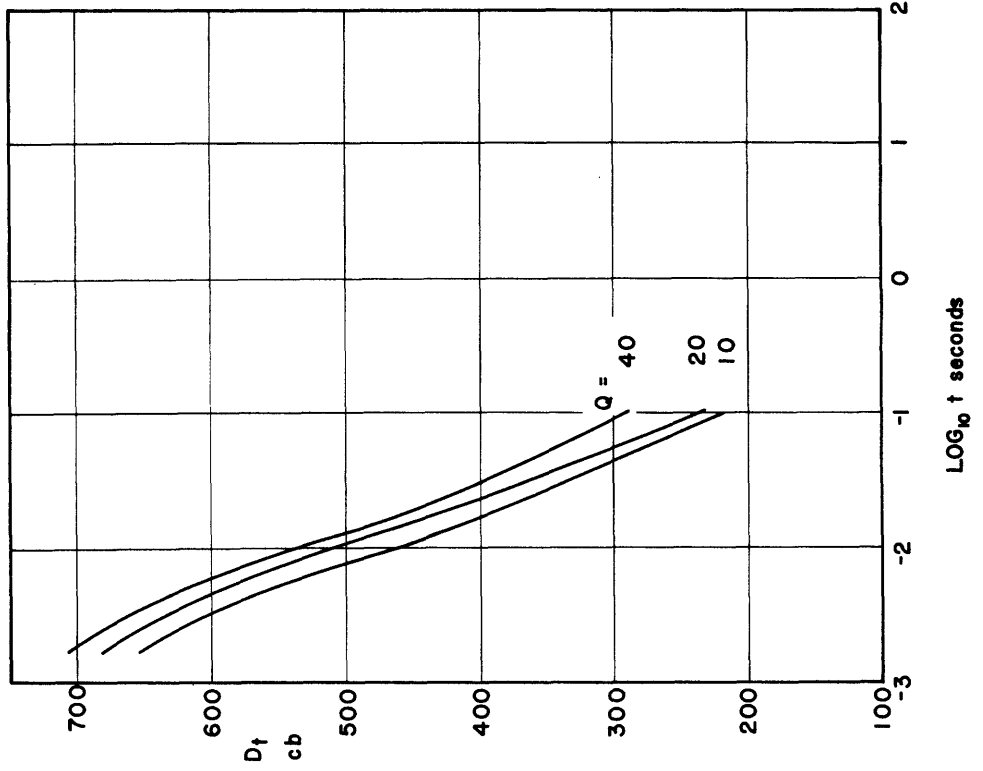


Figure 8

DECAY AFTER ONE RASTER  
GE 4633  
 $V_G = 4 \text{ kv}$

$Q = 10, 20, 40 \text{ m}\mu\text{ COULOMBS/cm}^2$

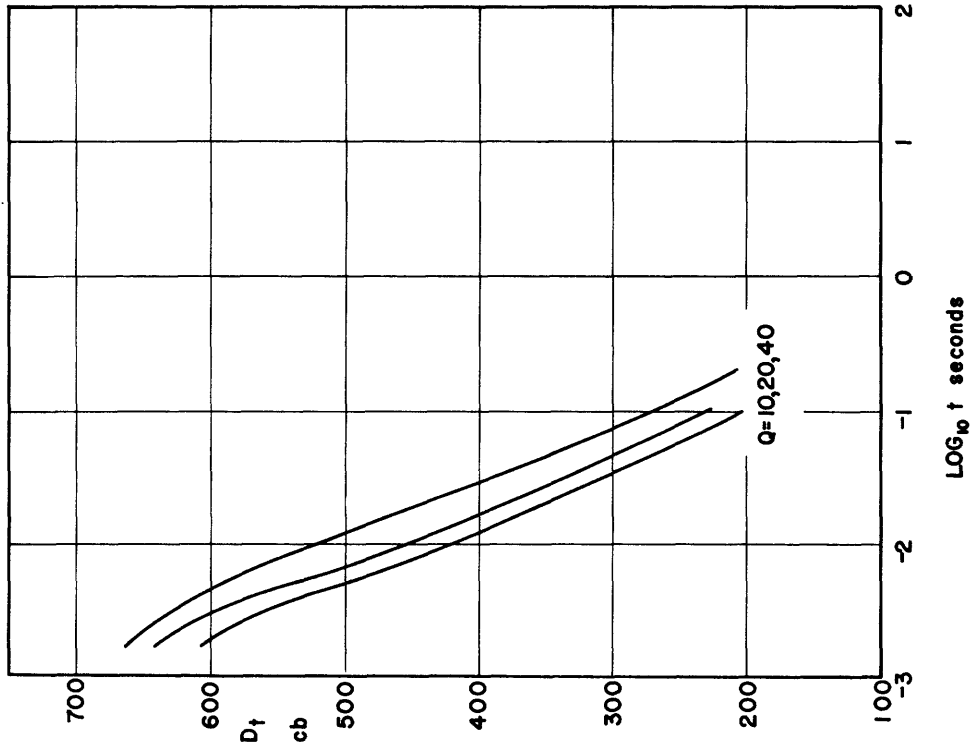


Figure 7

DECAY AFTER ONE RASTER  
GE 4665  
 $V_g = 6 \text{ kv}$   
 $Q = 10, 20, 40 \text{ m}\mu\text{ COULOMBS/cm}^2$

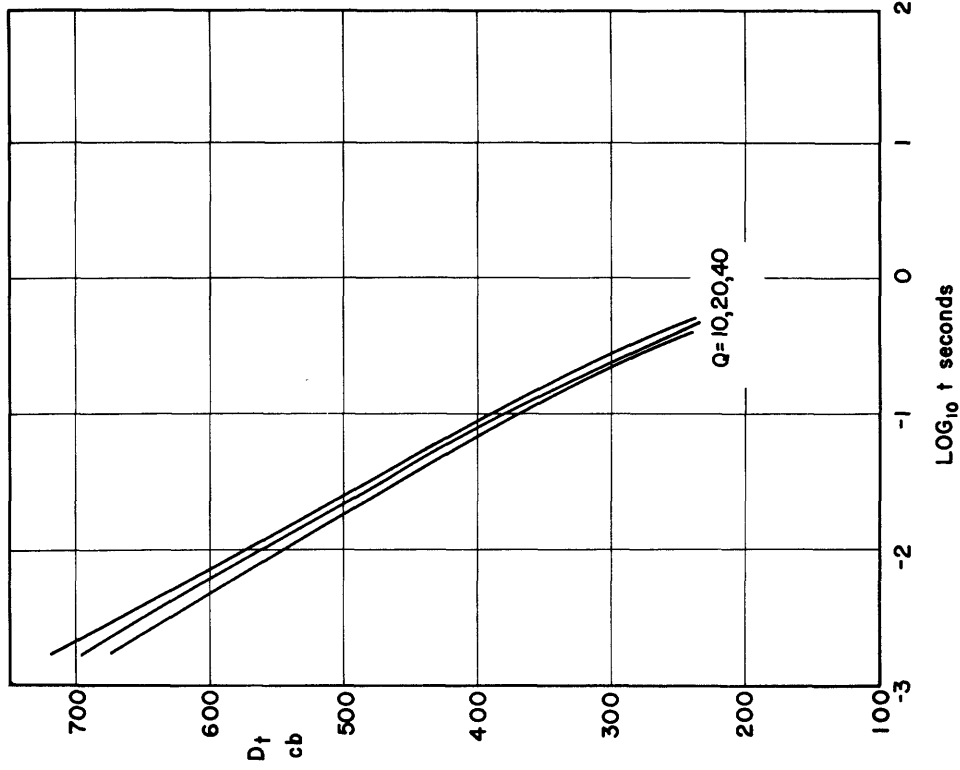


Figure 10

DECAY AFTER ONE RASTER  
GE 4665  
 $V_g = 4 \text{ kv}$   
 $Q = 10, 20, 40 \text{ m}\mu\text{ COULOMBS/cm}^2$

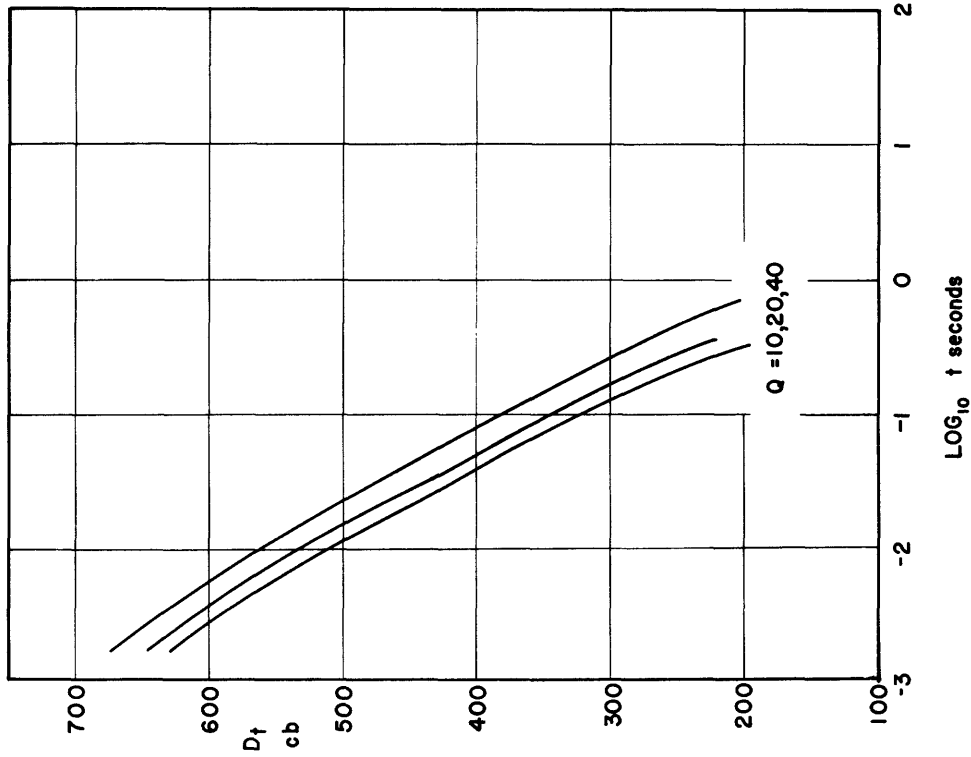


Figure 9

DECAY AFTER ONE RASTER

GE 4609

$V_d = 4 \text{ kv}$

$Q = 10, 20, 40 \text{ m}\mu\text{ COULOMBS/cm}^2$

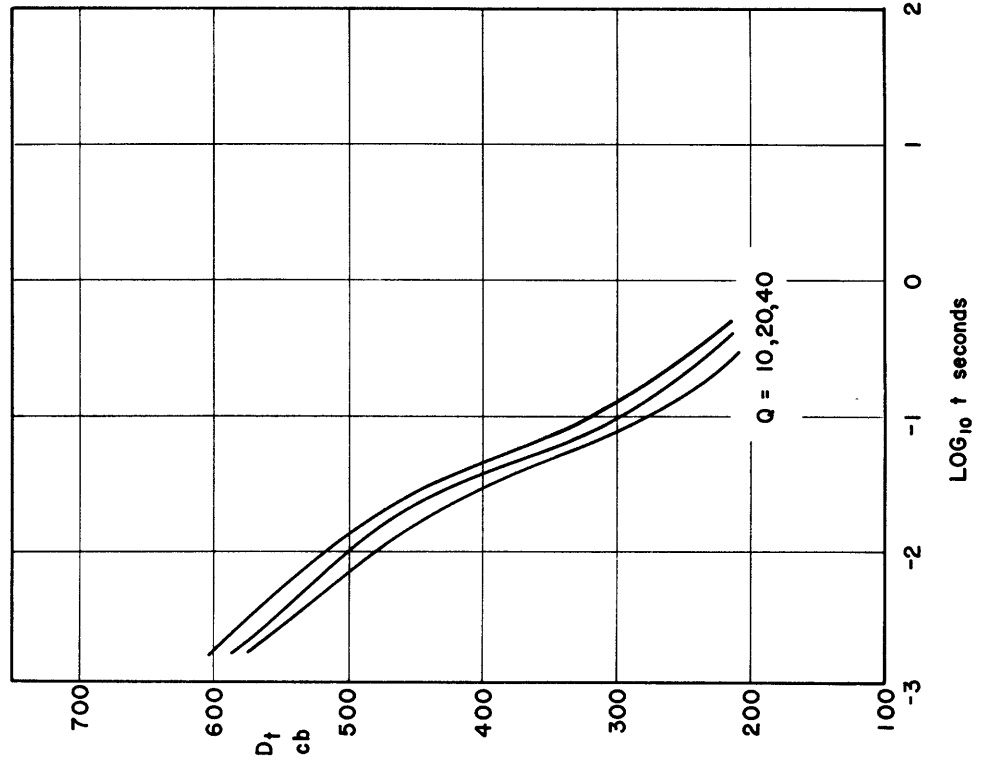


Figure 11

DECAY AFTER ONE RASTER

GE 4609

$V_d = 6 \text{ kv}$

$Q = 10, 20, 40 \text{ m}\mu\text{ COULOMBS/cm}^2$

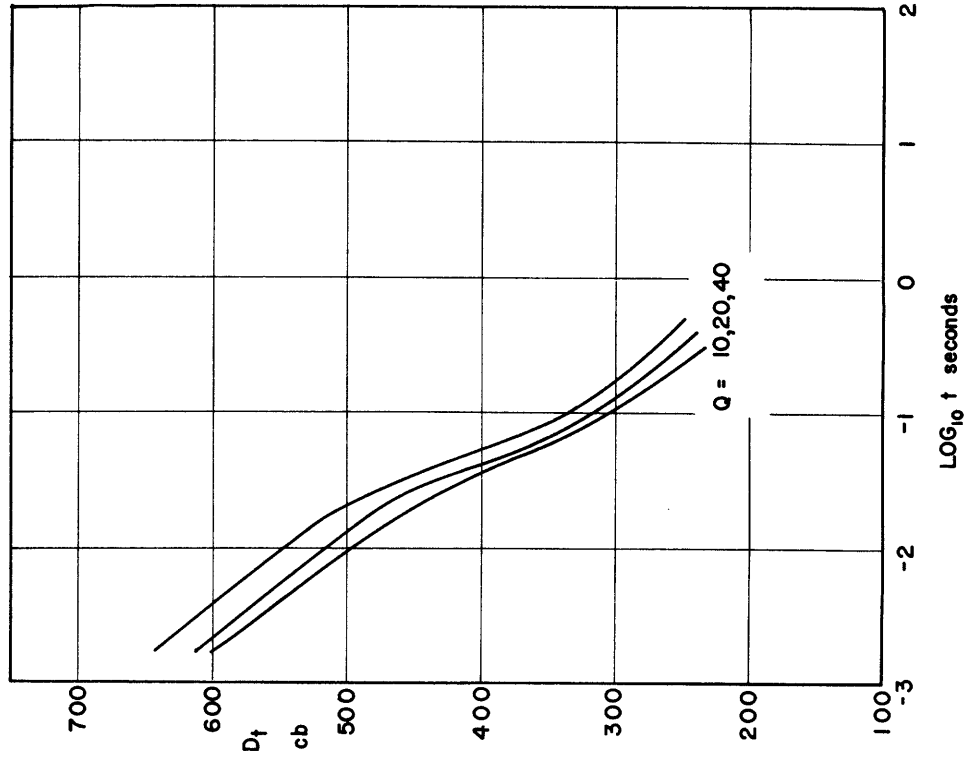


Figure 12

DECAY AFTER ONE RASTER  
RCA 5FP4A I  
 $V_g = 4 \text{ kv}$

$Q = 10, 20, 40 \text{ m}\mu \text{ COULOMBS/cm}^2$

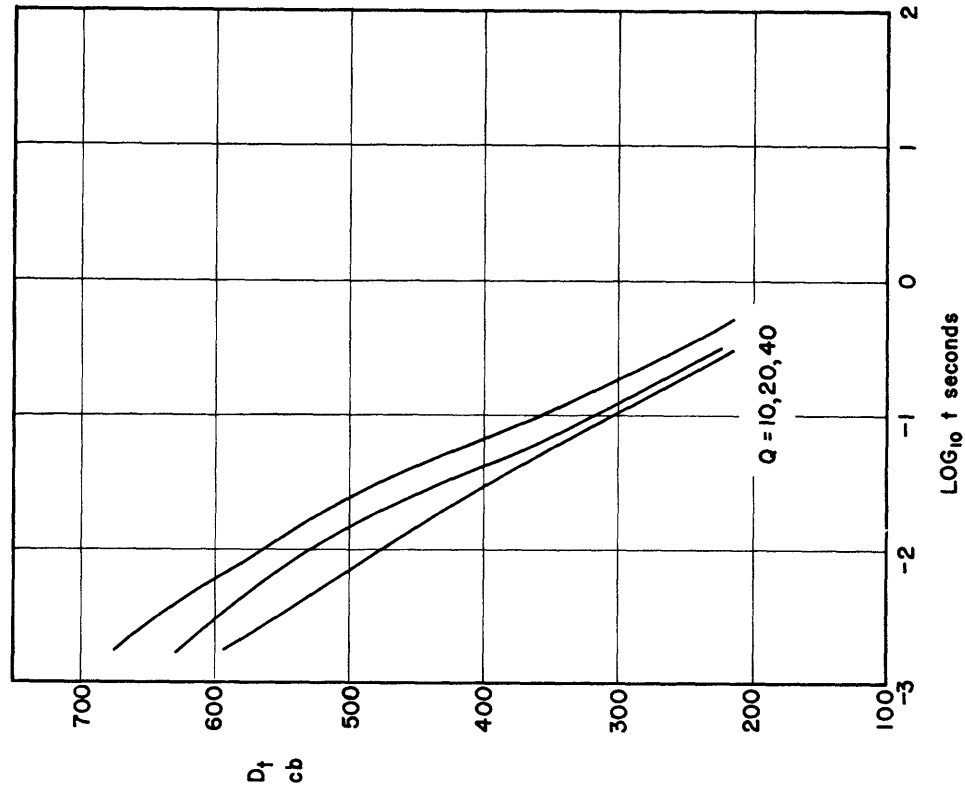


Figure 13

DECAY AFTER ONE RASTER  
RCA 5FP4A I  
 $V_g = 6 \text{ kv}$

$Q = 10, 20, 40 \text{ m}\mu \text{ COULOMBS/cm}^2$

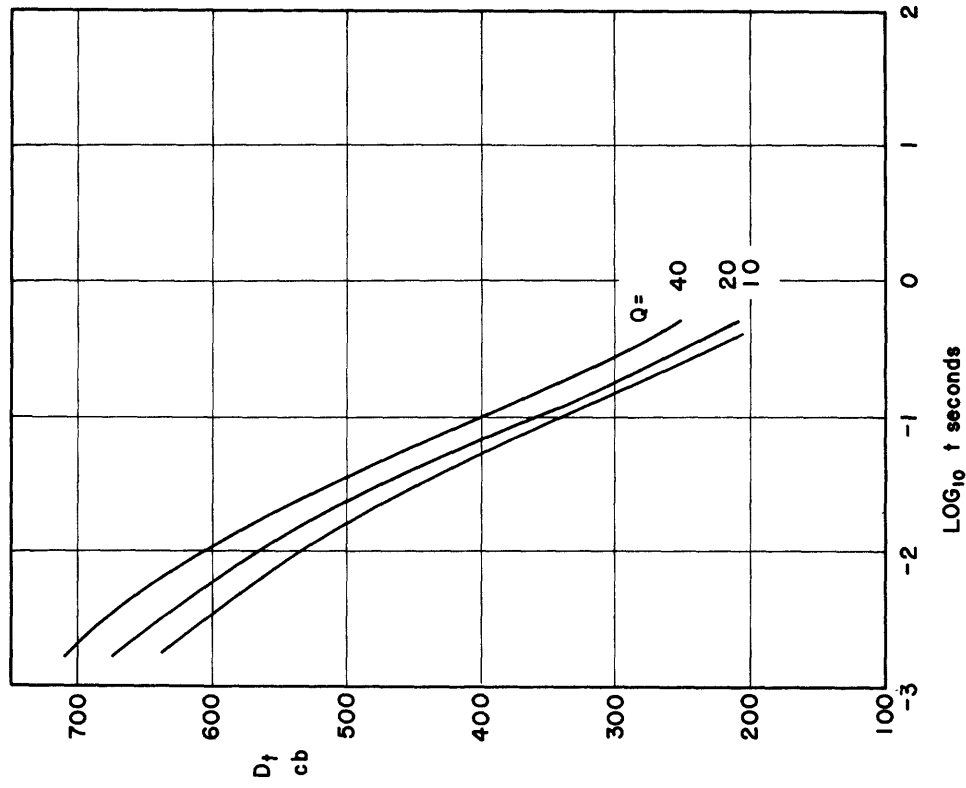


Figure 14

DECAY AFTER ONE RASTER  
RCA 5FPI4A 6331

$V_g = 6 \text{ kv}$

$Q = 10, 20, 40 \text{ m}\mu \text{ COULOMBS/cm}^2$

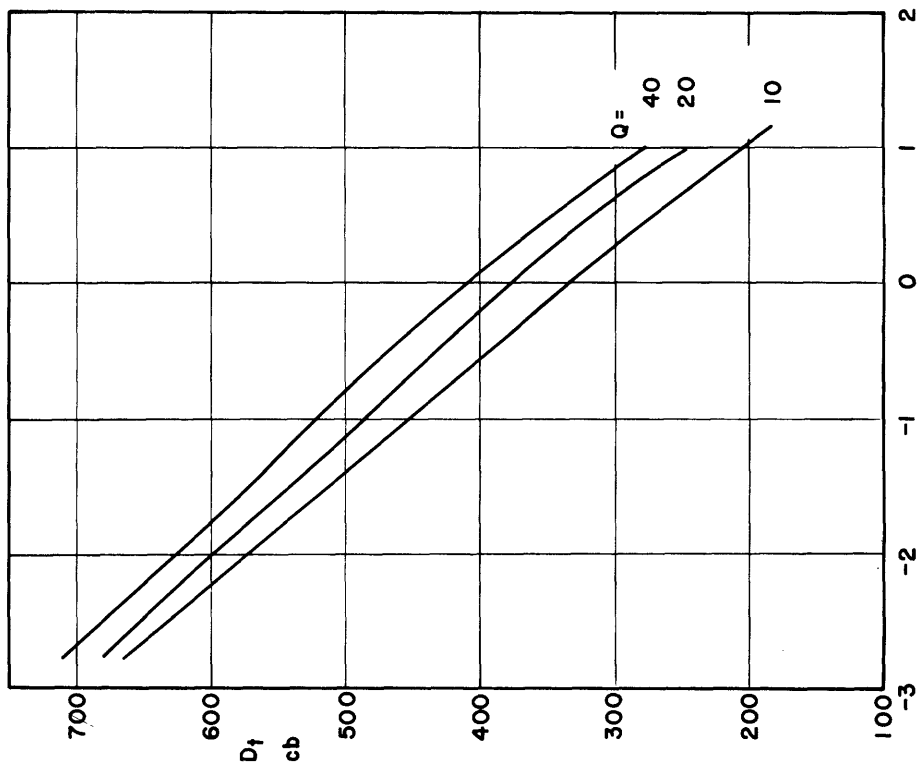


Figure 16

DECAY AFTER ONE RASTER  
RCA 5FPI4A 6331

$V_g = 4 \text{ kv}$

$Q = 10, 20, 40 \text{ m}\mu \text{ COULOMBS/cm}^2$

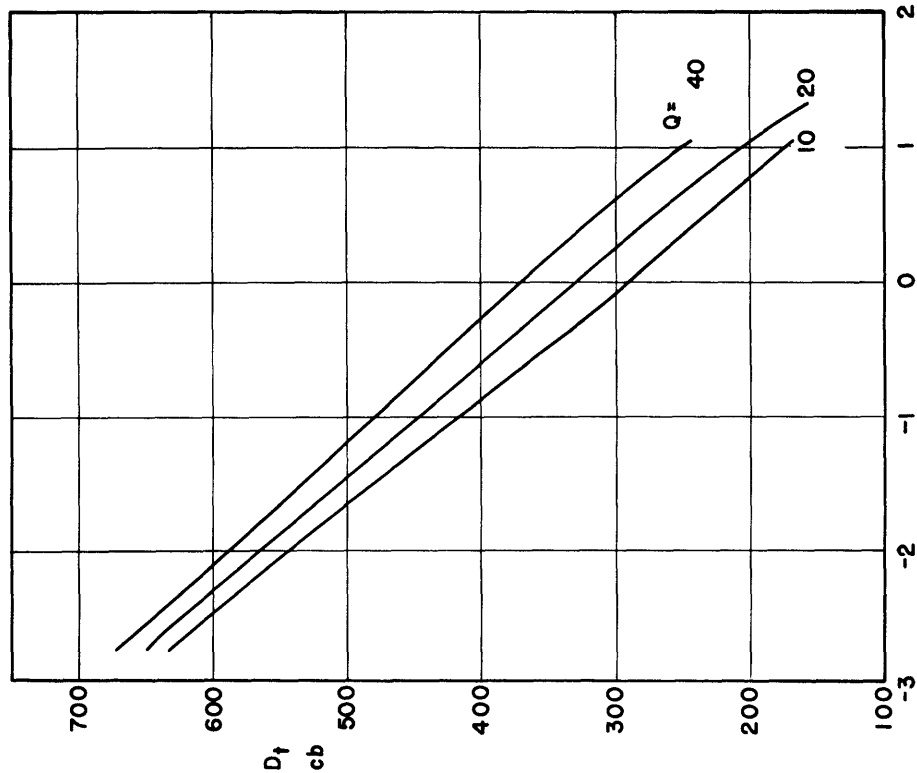


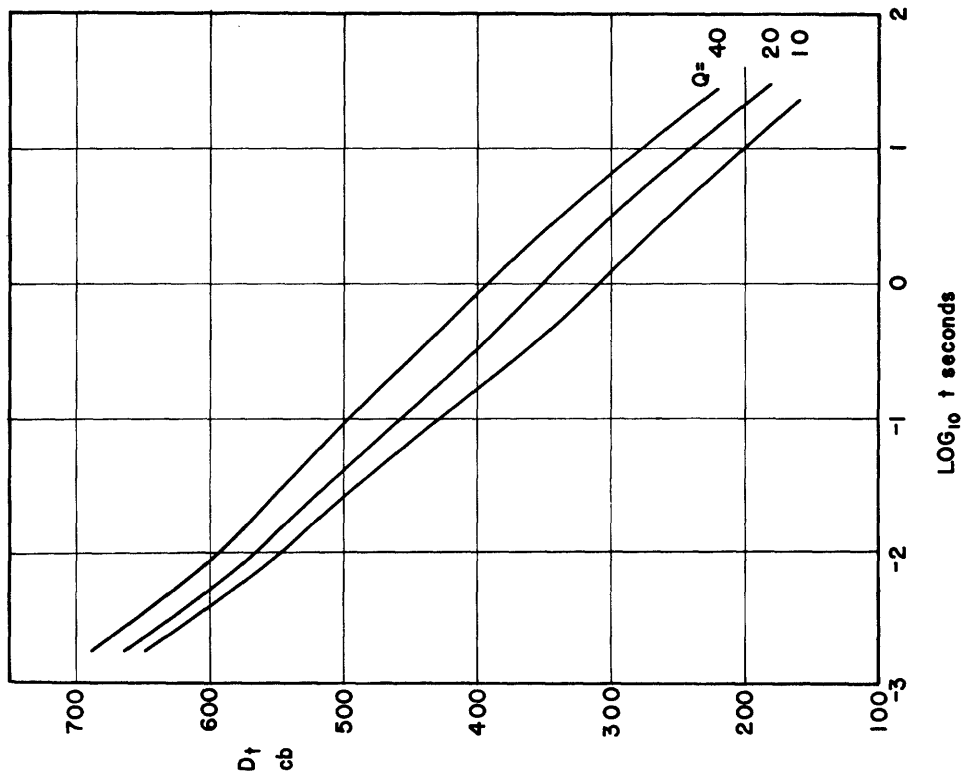
Figure 15



DECAY AFTER ONE RASTER  
RCA 5FP14 (C7570N) 3940-18

$V_g = 4 \text{ kv}$

$Q = 10, 20, 40 \text{ m}\mu\text{ COULOMBS/cm}^2$



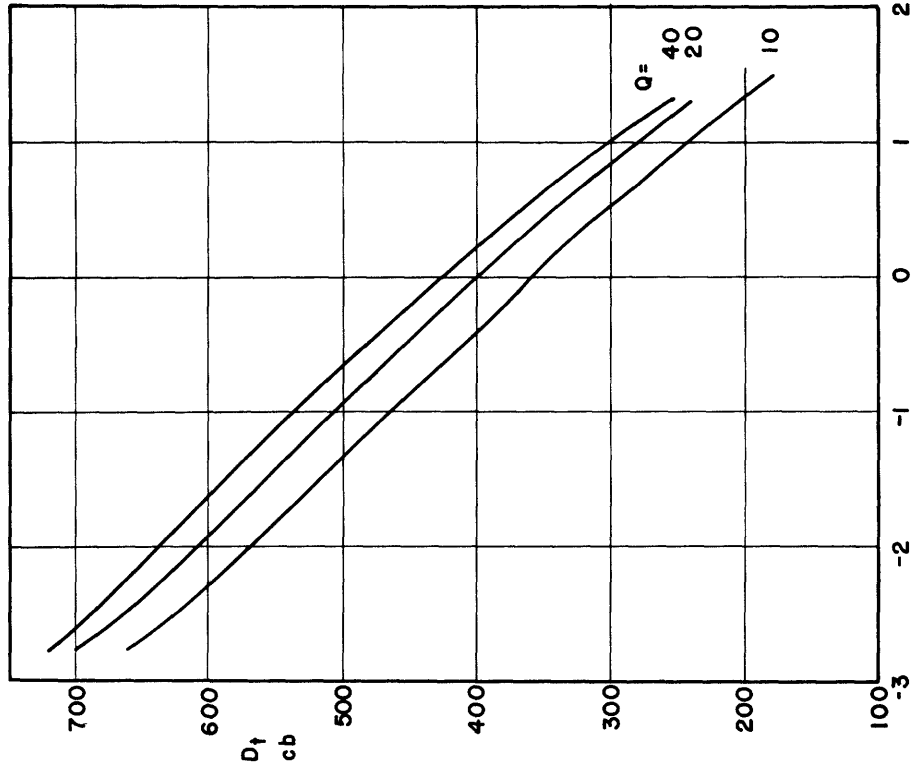
$\text{LOG}_{10} t \text{ seconds}$

Figure 17

DECAY AFTER ONE RASTER  
RCA 5FP14 (C7570N) 3940-18

$V_g = 6 \text{ kv}$

$Q = 10, 20, 40 \text{ m}\mu\text{ COULOMBS/cm}^2$



$\text{LOG}_{10} t \text{ seconds}$

Figure 18

DECAY AFTER ONE RASTER  
 GE 5FP14 C72745

$V_d = 4 \text{ kv}$

$Q = 10, 20, 40 \text{ m}\mu\text{ COULOMBS/cm}^2$

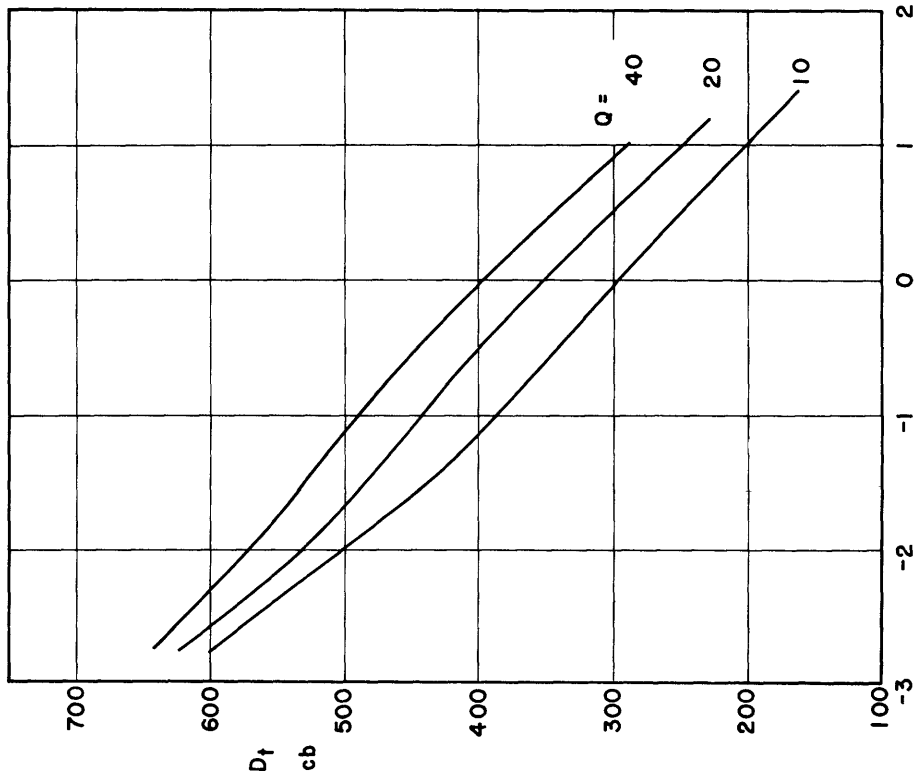


Figure 19

DECAY AFTER ONE RASTER  
 GE 5FP14 C72745

$V_d = 6 \text{ kv}$

$Q = 10, 20, 40 \text{ m}\mu\text{ COULOMBS/cm}^2$

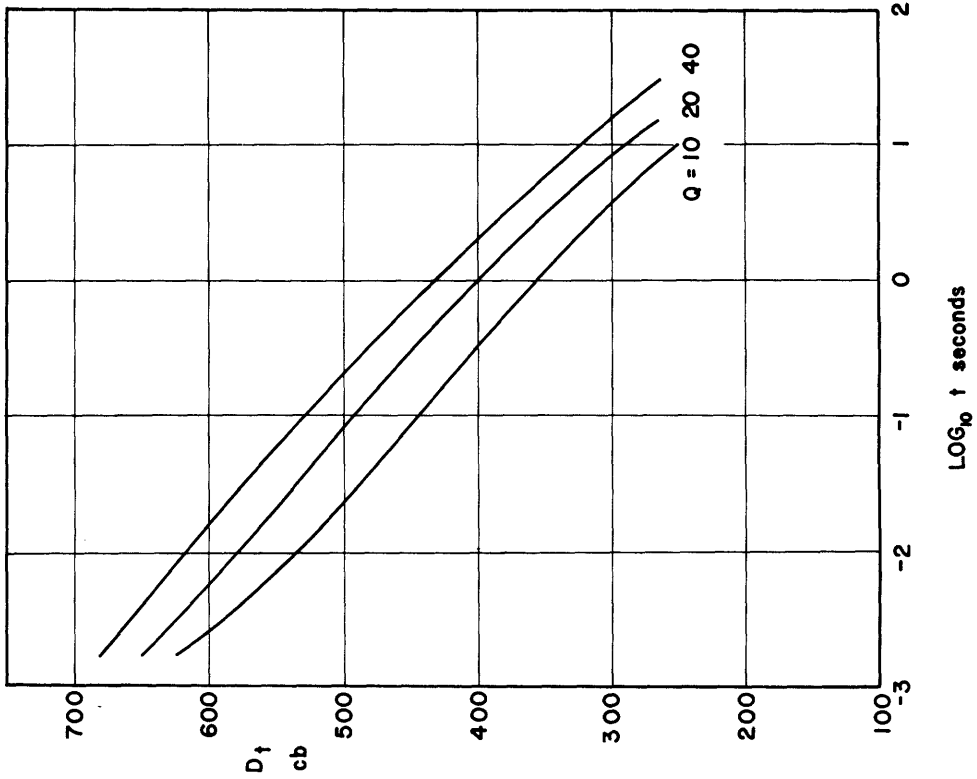


Figure 20

DECAY AFTER ONE RASTER  
RCA 5FP7A I  
 $V_g = 6 \text{ kv}$

$Q = 10, 20, 40 \text{ m}\mu \text{ COULOMBS/cm}^2$

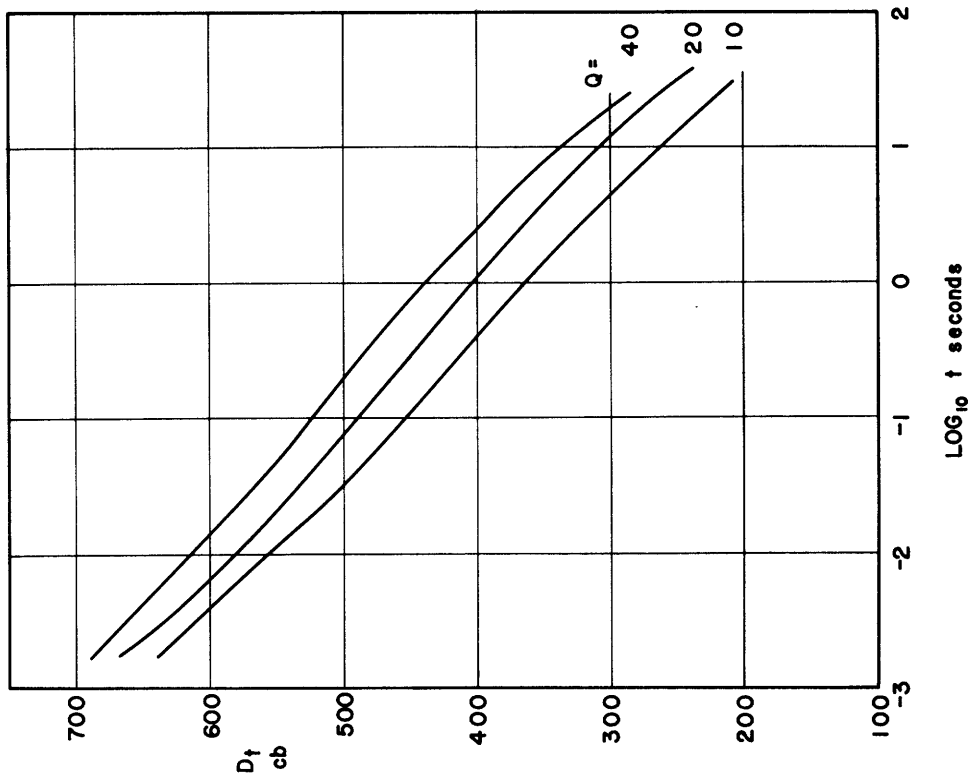


Figure 22

DECAY AFTER ONE RASTER  
RCA 5FP7A I  
 $V_g = 4 \text{ kv}$

$Q = 10, 20, 40 \text{ m}\mu \text{ COULOMBS/cm}^2$

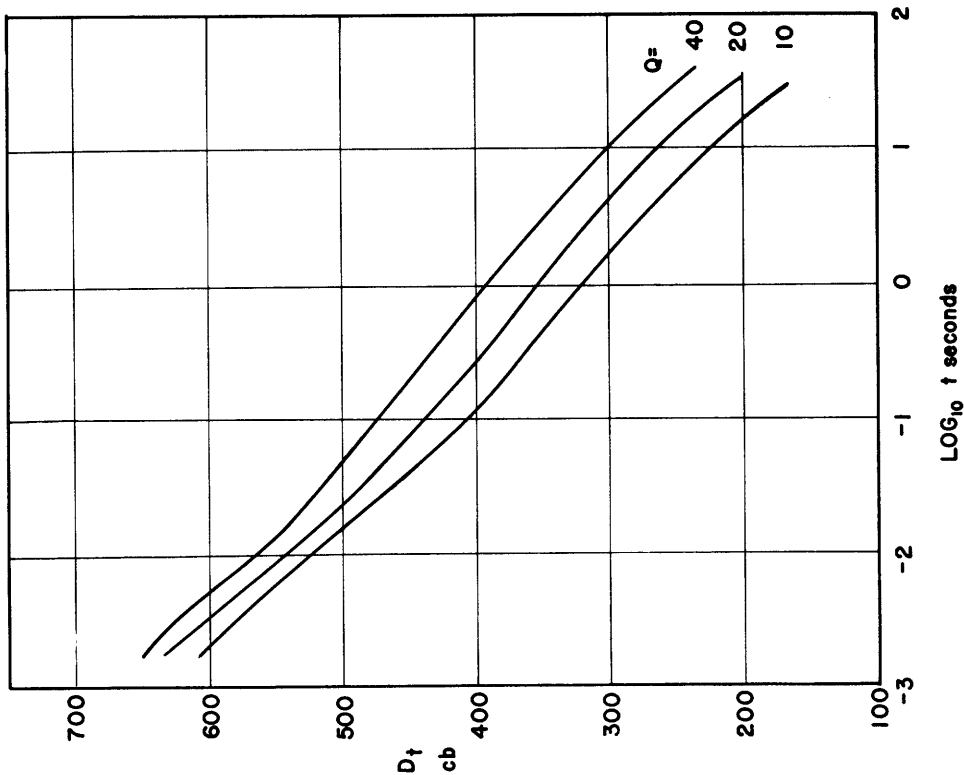


Figure 21

DECAY AFTER ONE RASTER  
RCA 5FP7 A 2  
 $V_g = 6 \text{ kv}$   
 $Q = 10, 20, 40 \text{ m}\mu\text{ COULOMBS/cm}^2$

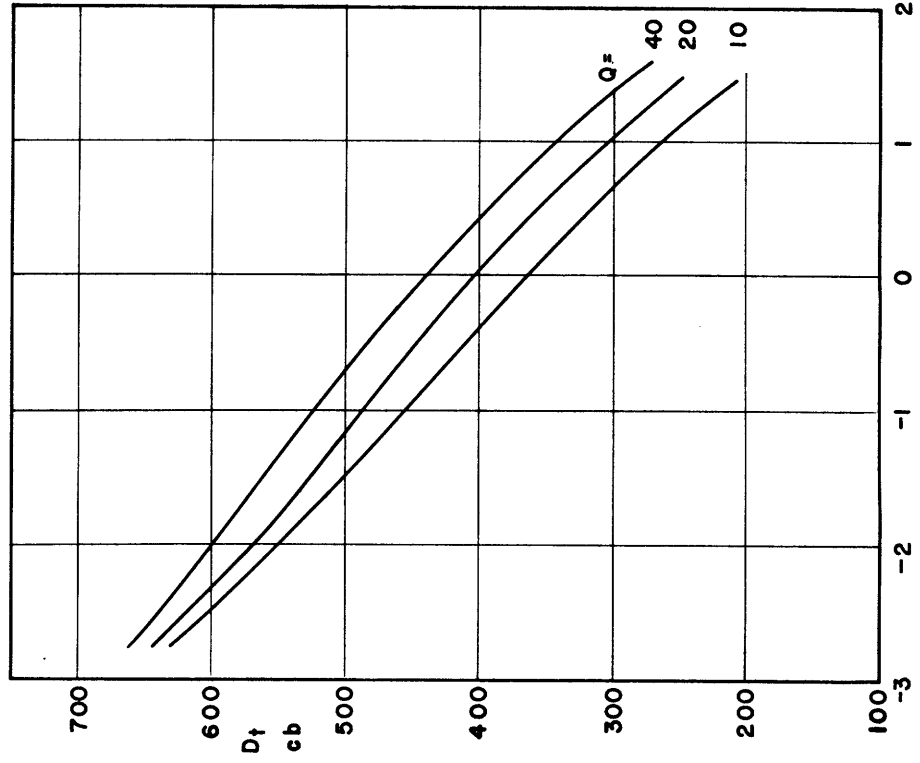


Figure 24

DECAY AFTER ONE RASTER  
RCA 5FP7 A 2  
 $V_g = 4 \text{ kv}$   
 $Q = 10, 20, 40 \text{ m}\mu\text{ COULOMBS/cm}^2$

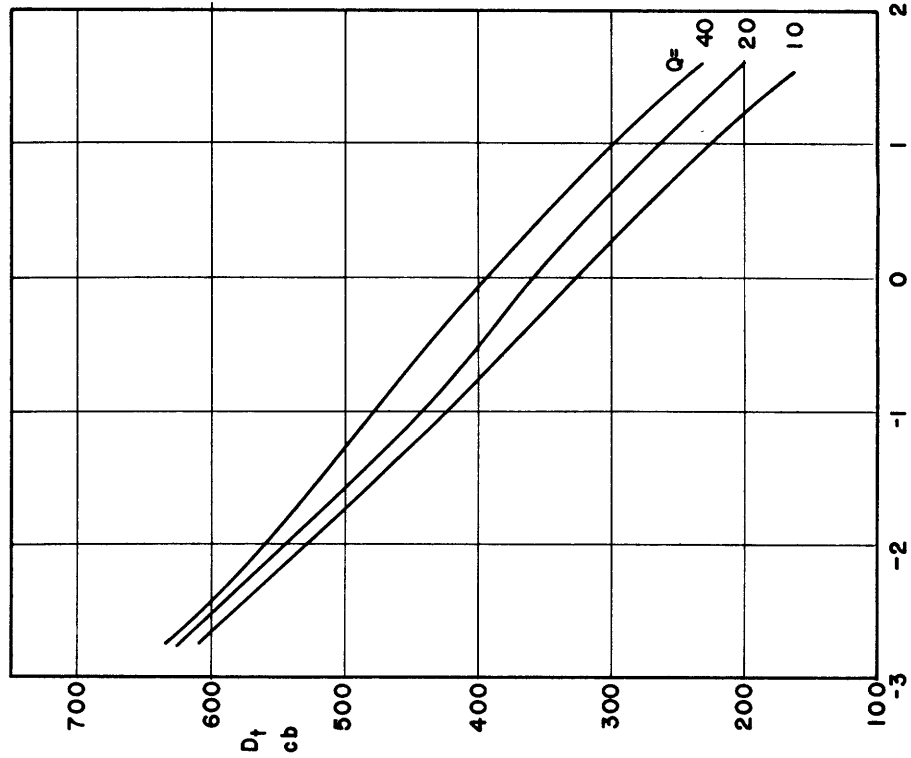


Figure 23

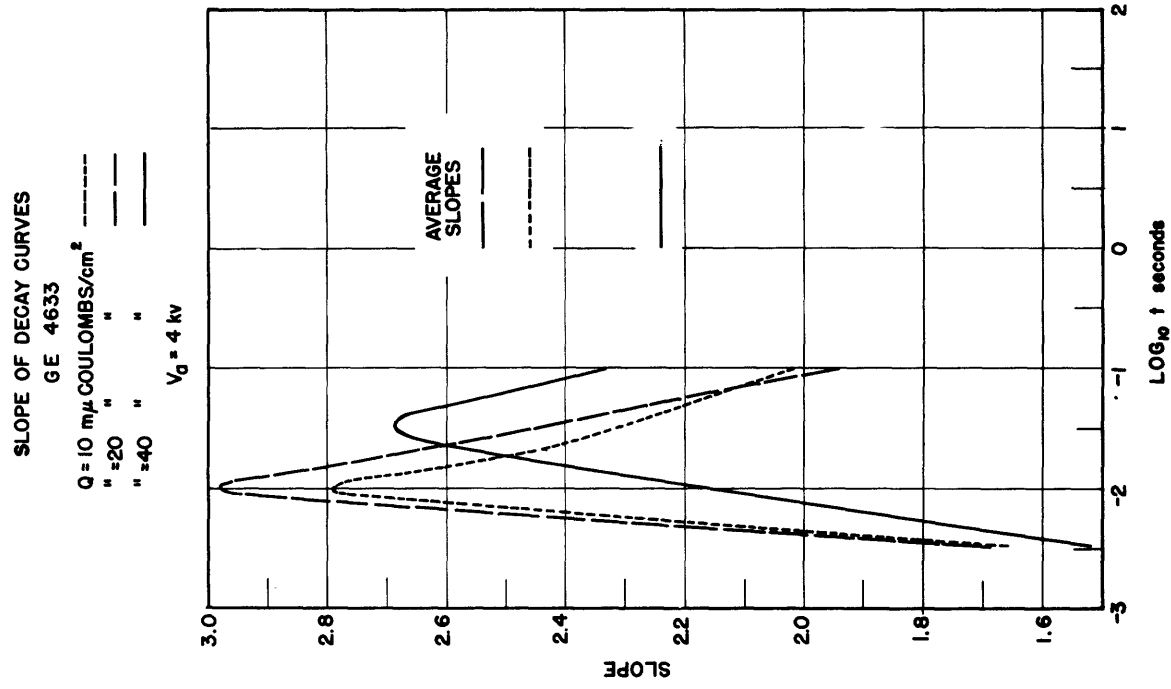


Figure 26

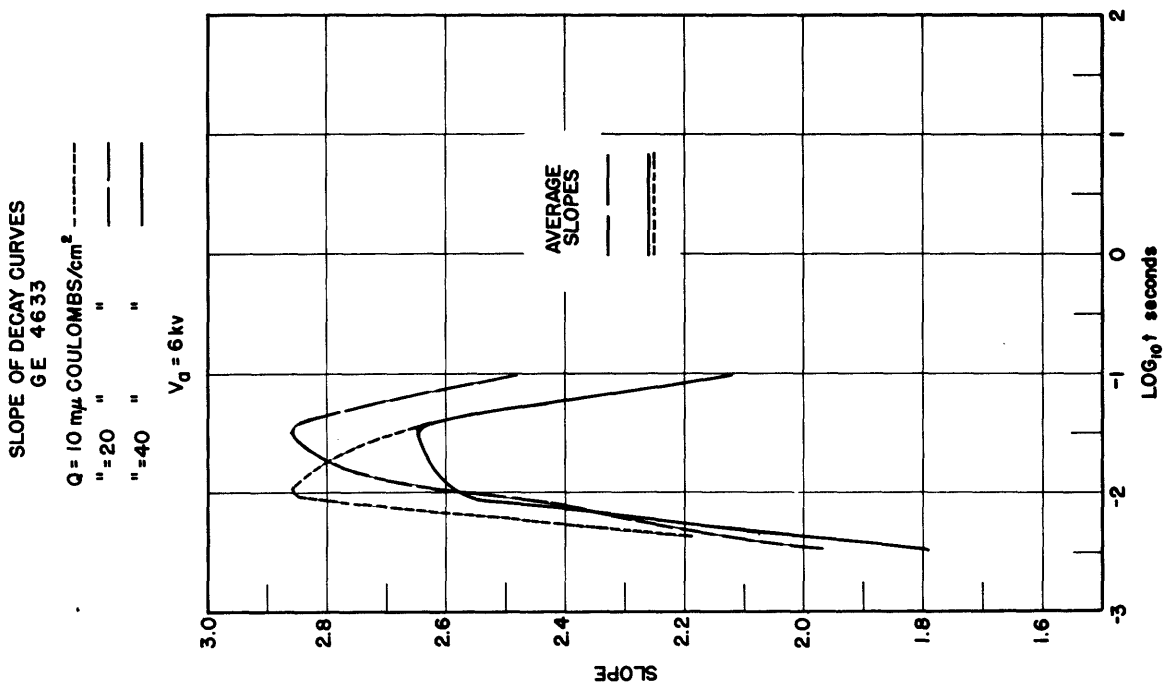


Figure 25

SLOPE OF DECAY CURVES  
GE 4665

Q = 10 m $\mu$  GOULOMBS/cm<sup>2</sup> -----  
" = 20 " " -----  
" = 40 " " -----

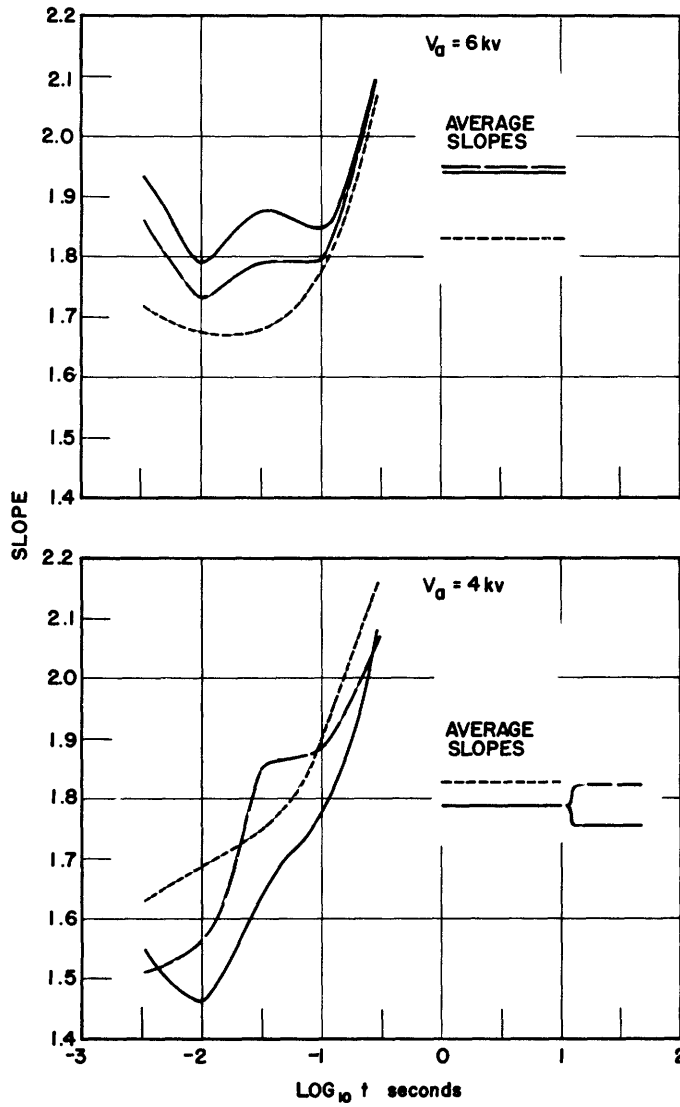


Figure 27

SLOPE OF DECAY CURVES  
GE 4609

Q = 10 m $\mu$  COULOMBS/cm<sup>2</sup> -----  
" = 20 " " -----  
" = 40 " " -----

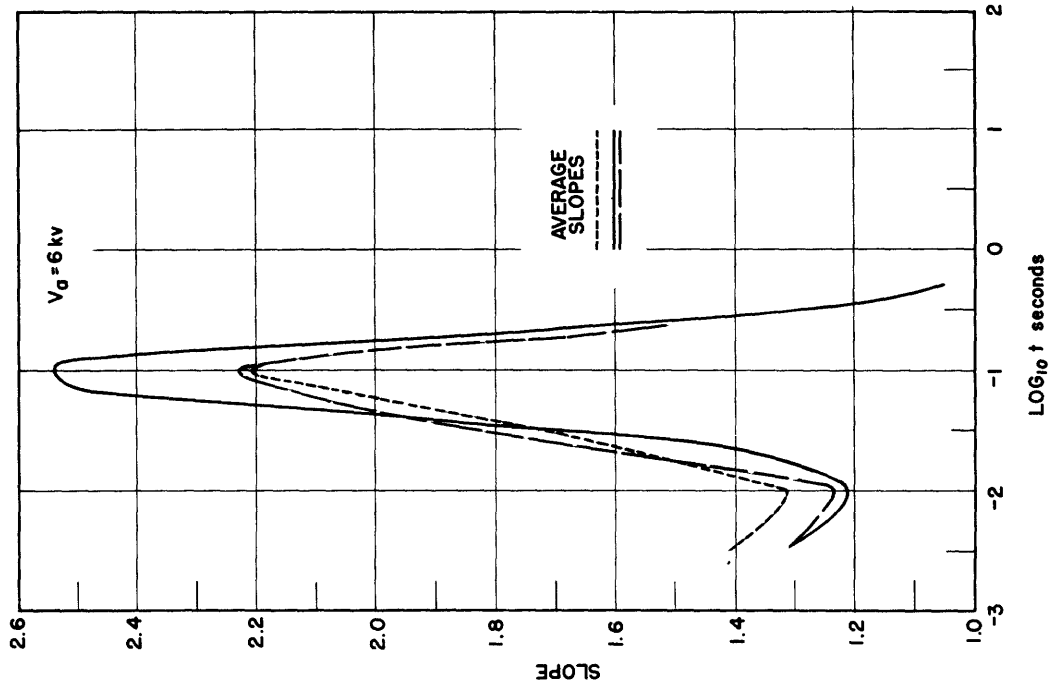


Figure 29

SLOPE OF DECAY CURVES  
GE 4609

Q = 10 m $\mu$  COULOMBS/cm<sup>2</sup> -----  
" = 20 " " -----  
" = 40 " " -----

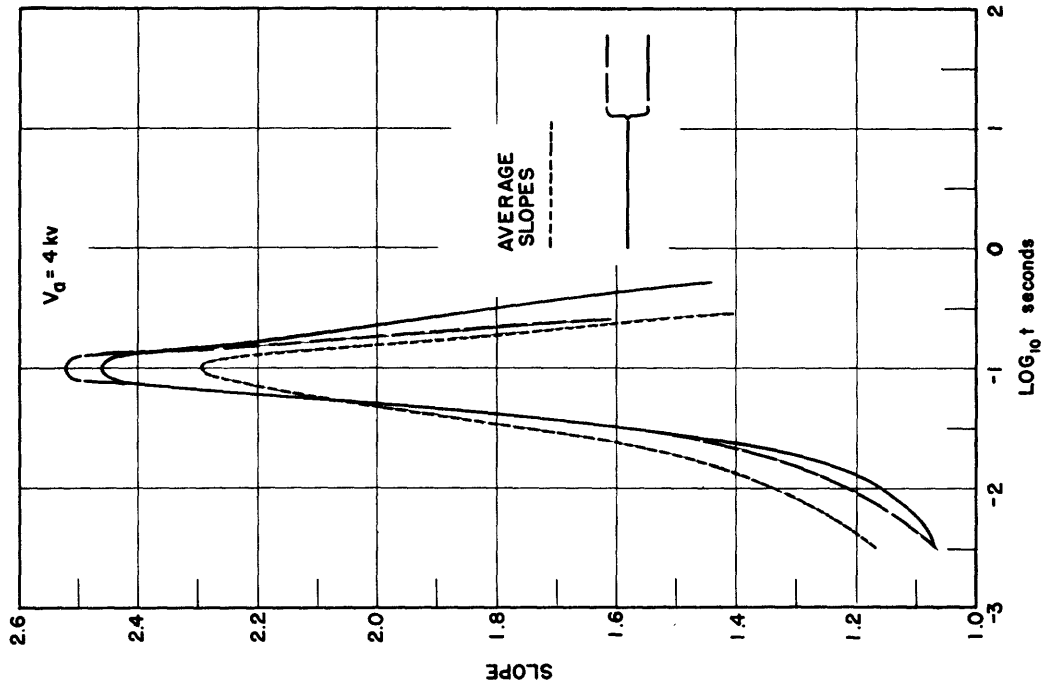


Figure 28

SLOPE OF DECAY CURVES  
RCA 5FP4A

Q = 10 m $\mu$  COULOMBS/cm<sup>2</sup> -----  
" = 20 " " -----  
" = 40 " " -----

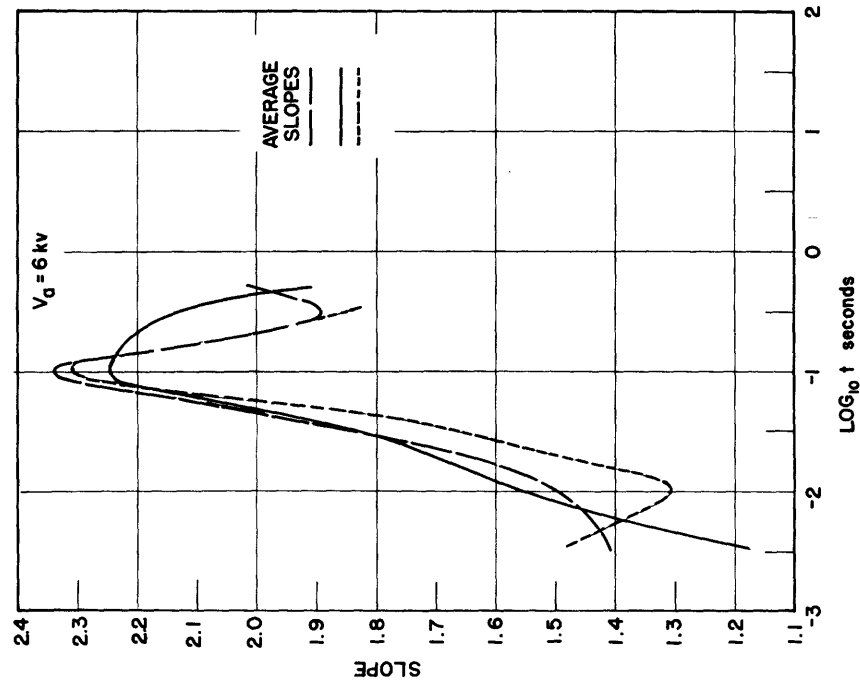


Figure 31

SLOPE OF DECAY CURVES  
RCA 5FP4A

Q = 10 m $\mu$  COULOMBS/cm<sup>2</sup> -----  
" = 20 " " -----  
" = 40 " " -----

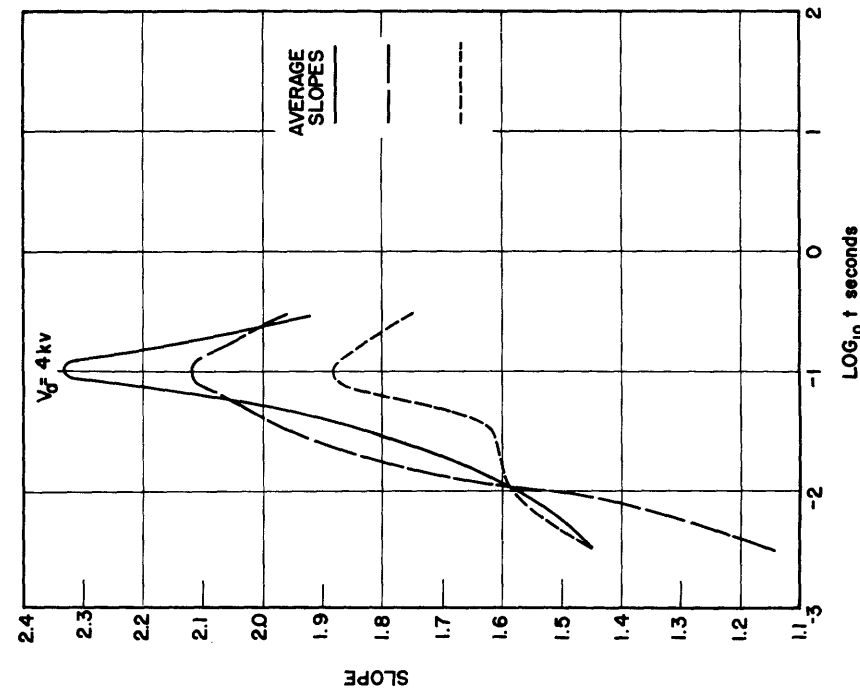


Figure 30



SLOPE OF DECAY CURVE  
RCA 5FPI4 C7570N 3940-18  
Q = 10 m $\mu$  COULOMBS/cm<sup>2</sup> -----  
" = 20 " " -----  
" = 40 " " -----

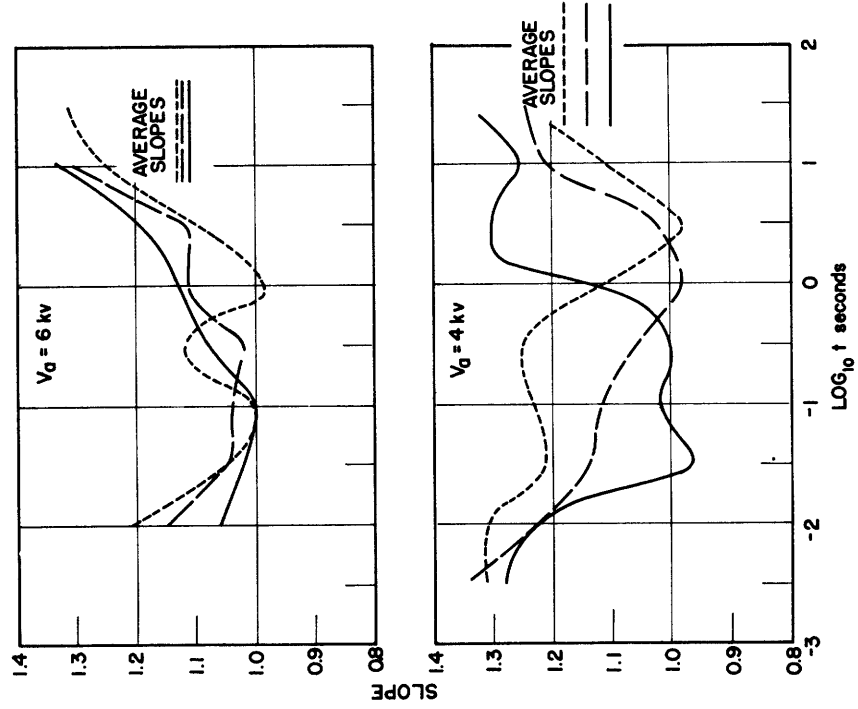


Figure 35

SLOPE OF DECAY CURVES  
RCA 5FPI4 6331  
Q = 10 m $\mu$  COULOMBS/cm<sup>2</sup> -----  
" = 20 " " -----  
" = 40 " " -----

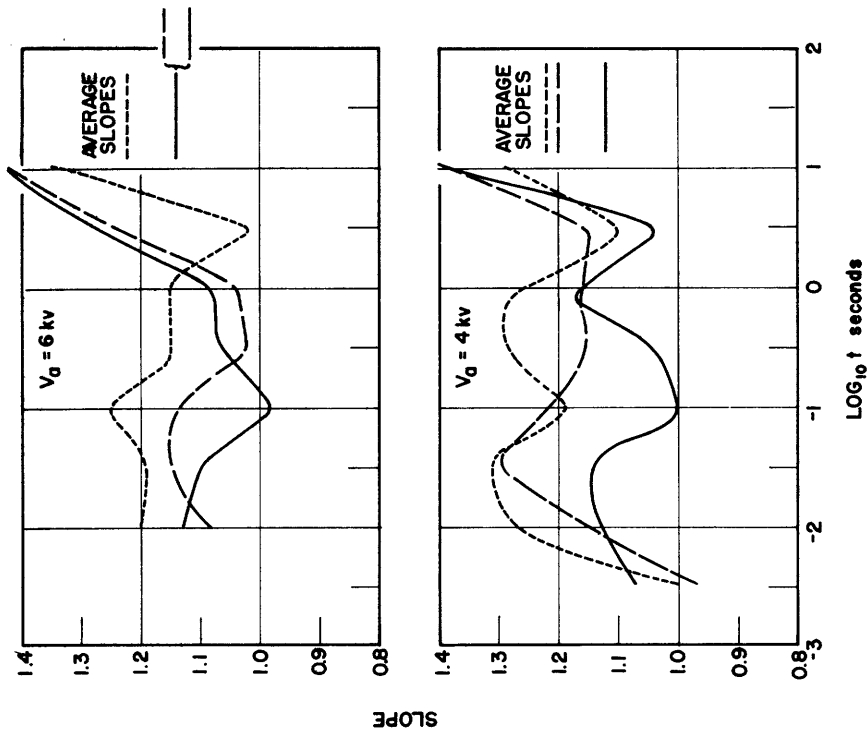


Figure 32

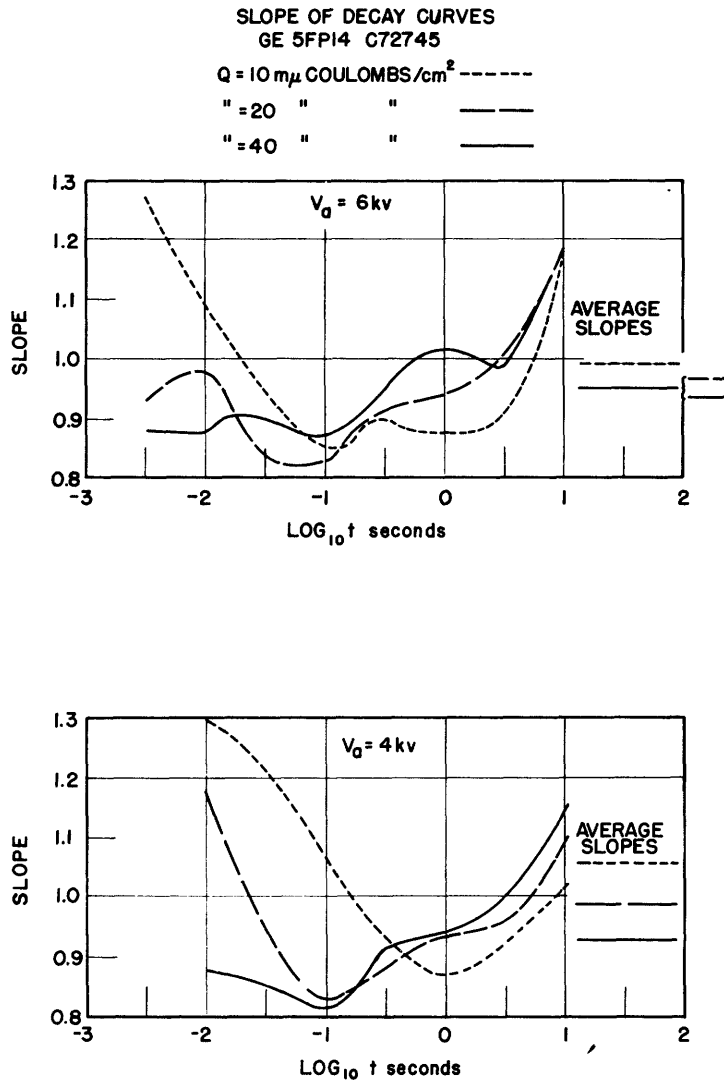
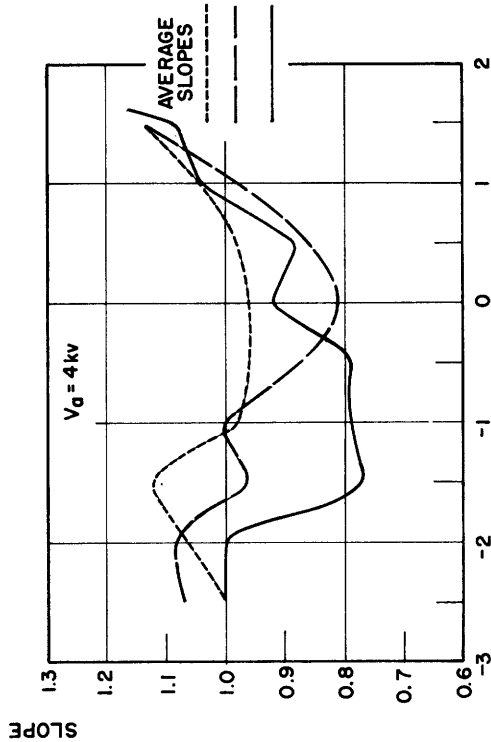
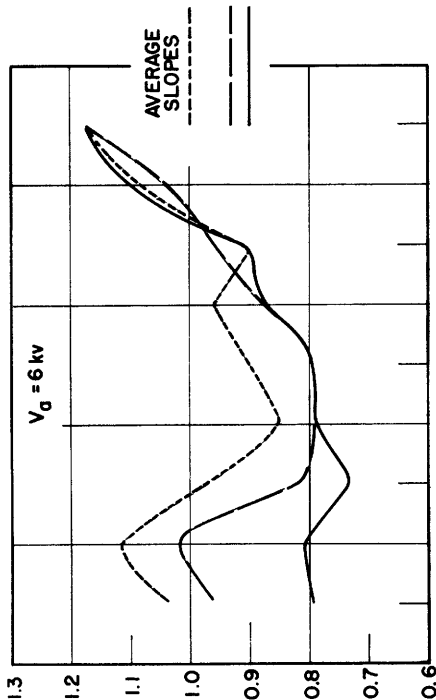


Figure 34

SLOPE OF DECAY CURVES

RCA 5FP7A 2  
Q = 10 m $\mu$ COULOMBS/cm<sup>2</sup> -----  
" = 20 " " -----  
" = 40 " " -----

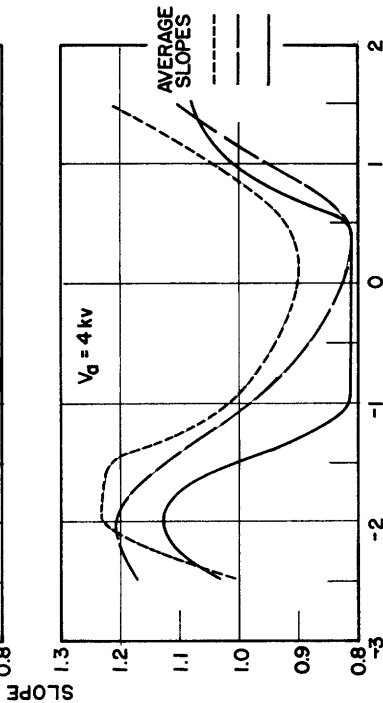
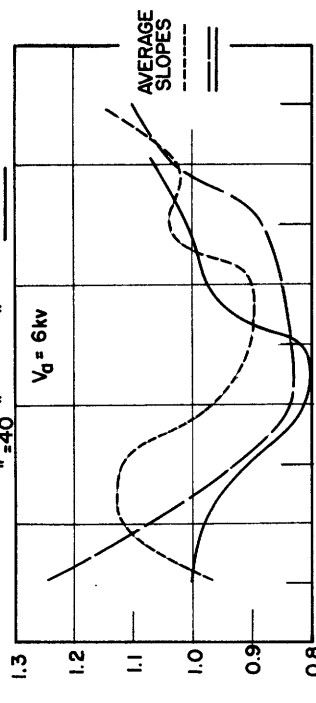


LOG<sub>10</sub> t seconds

Figure 36

SLOPE OF DECAY CURVES

RCA 5FP7A 1  
Q = 10 m $\mu$ COULOMBS/cm<sup>2</sup> -----  
" = 20 " " -----  
" = 40 " " -----



LOG<sub>10</sub> t seconds

Figure 35

BUILDUP  
RCA 5FP14A 6331

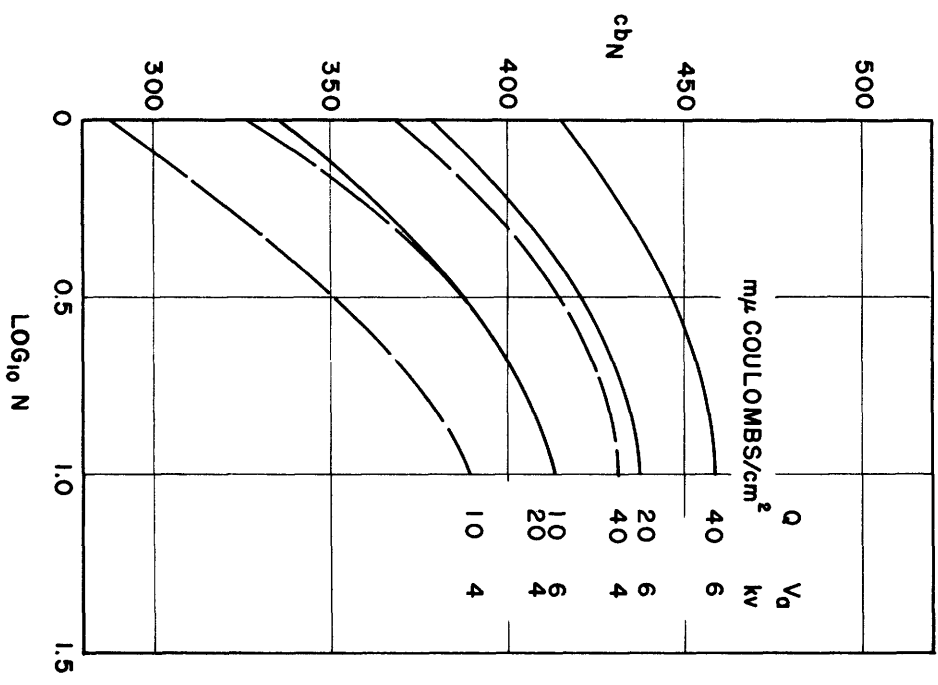


Figure 37

BUILDUP  
RCA 5FP14 C7570N 3940-18

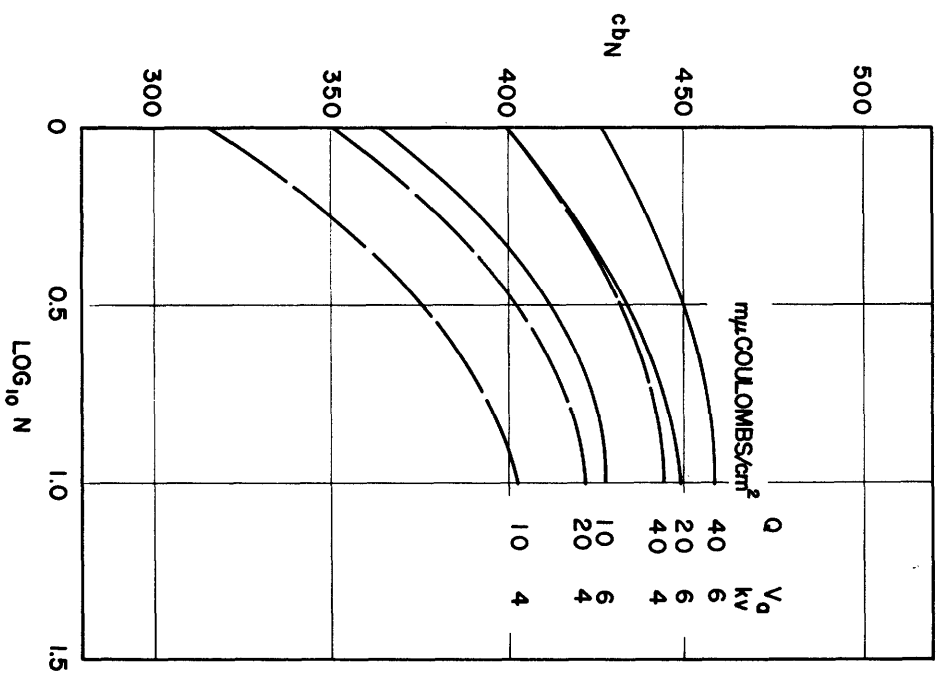


Figure 38

BUILDUP  
GE 5FPI4 C72745

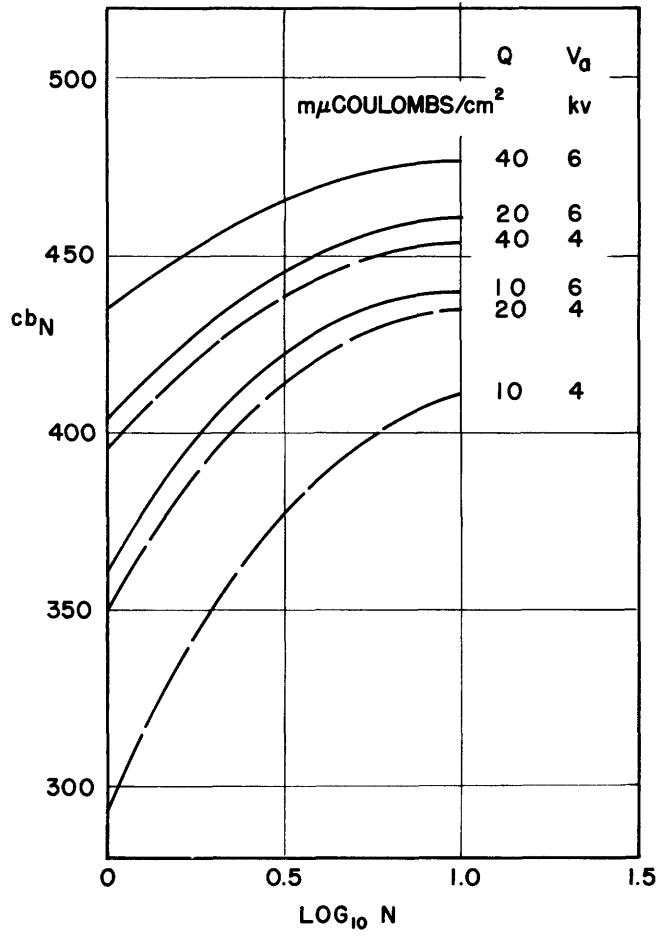


Figure 39

BUILDUP  
RCA 5FP7 A 2

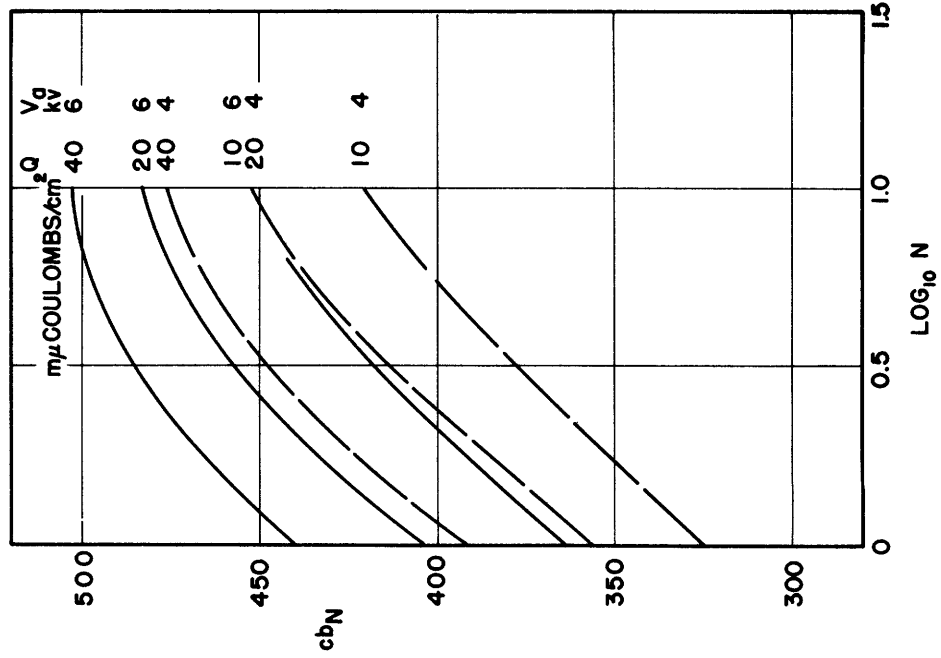


Figure 41

BUILDUP  
RCA 5FP7A 1

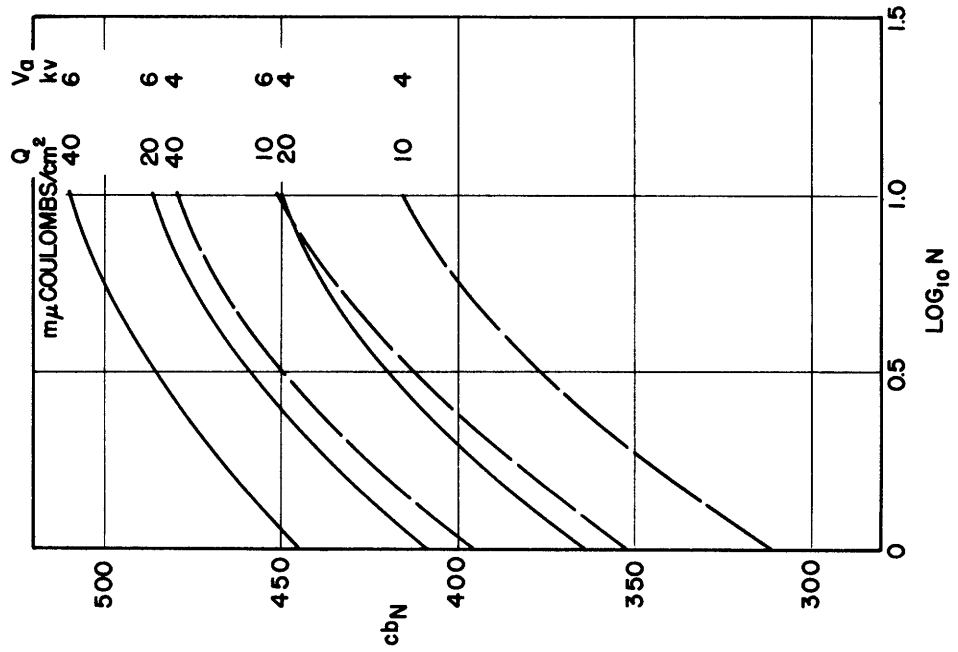


Figure 40

cb<sub>1</sub>, cb<sub>5</sub>, cb<sub>10</sub>

AS FUNCTIONS OF BEAM CURRENT

RCA 5FPI4 3940-1B

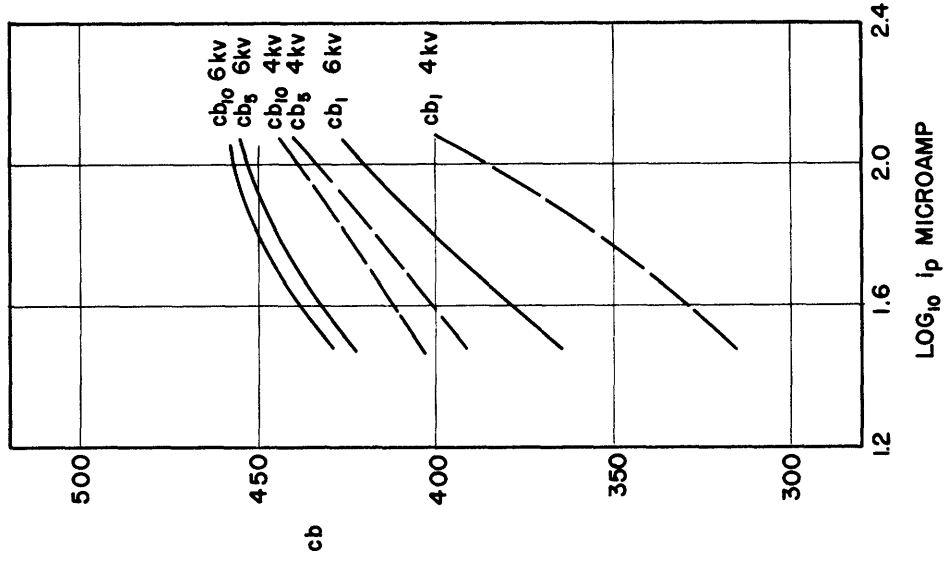


Figure 43

cb<sub>1</sub>, cb<sub>5</sub>, cb<sub>10</sub>

AS FUNCTIONS OF BEAM CURRENT

RCA 5FPI4A 6331

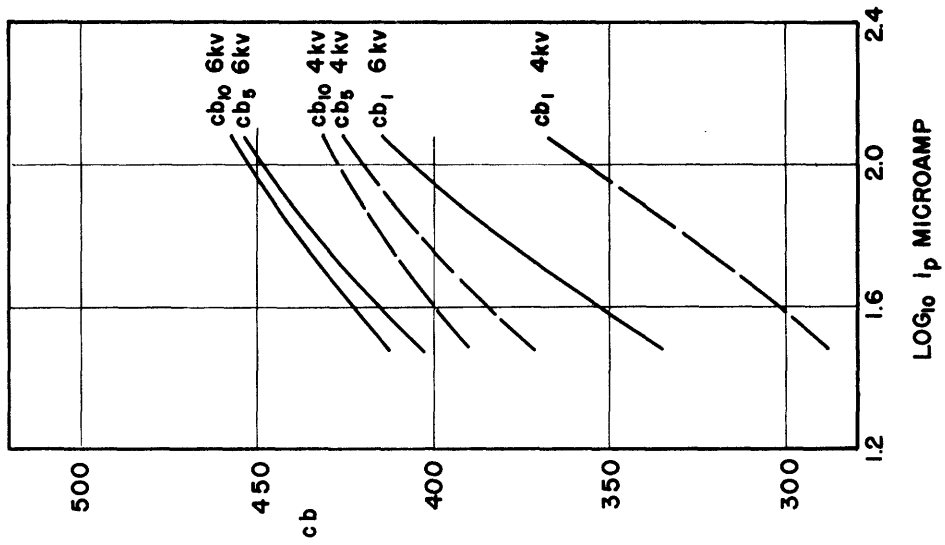


Figure 42

$cb_1, cb_5, cb_{10}$   
AS FUNCTIONS OF BEAM CURRENT  
GE 5FP14 G72745

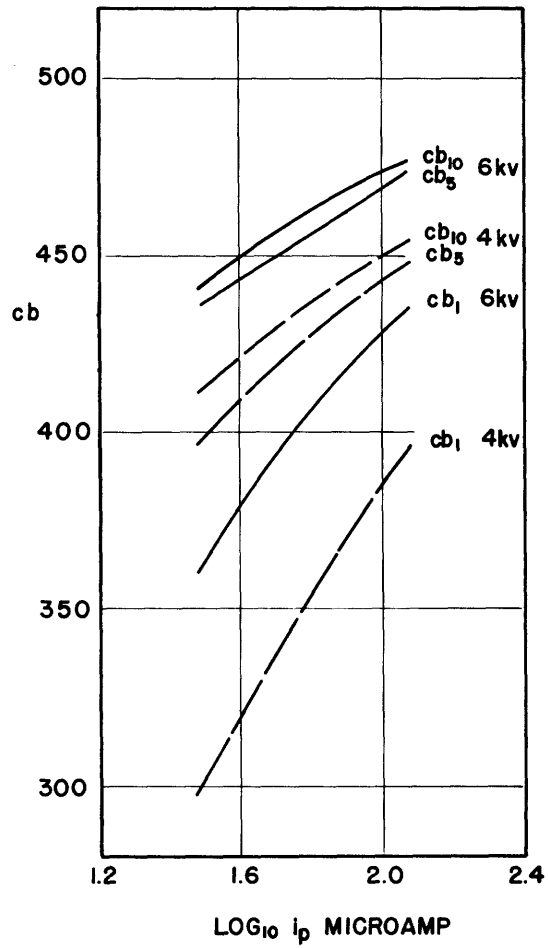


Figure 44



$cb_1, cb_5, cb_{10}$   
AS FUNCTIONS OF BEAM CURRENT  
RCA 5FP7A I

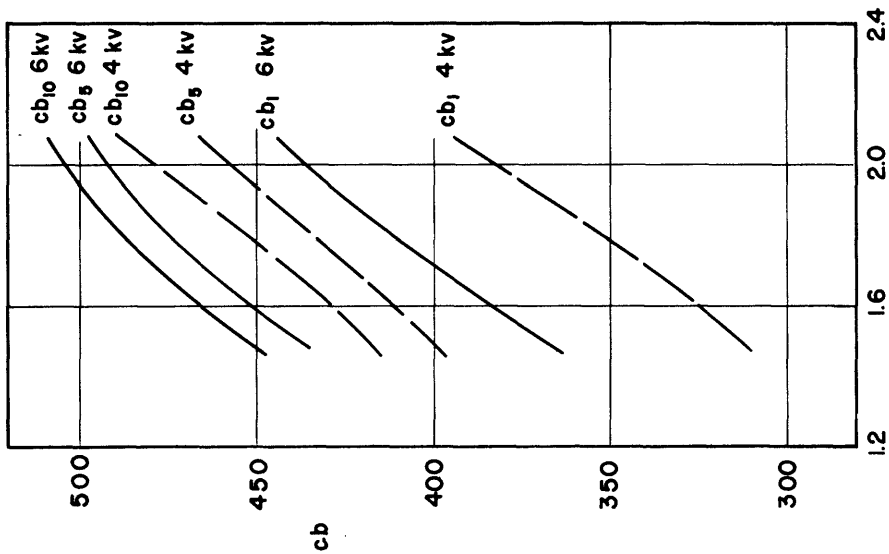


Figure 45

$cb_1, cb_5, cb_{10}$   
AS FUNCTIONS OF BEAM CURRENT  
RCA 5FP7 A 2

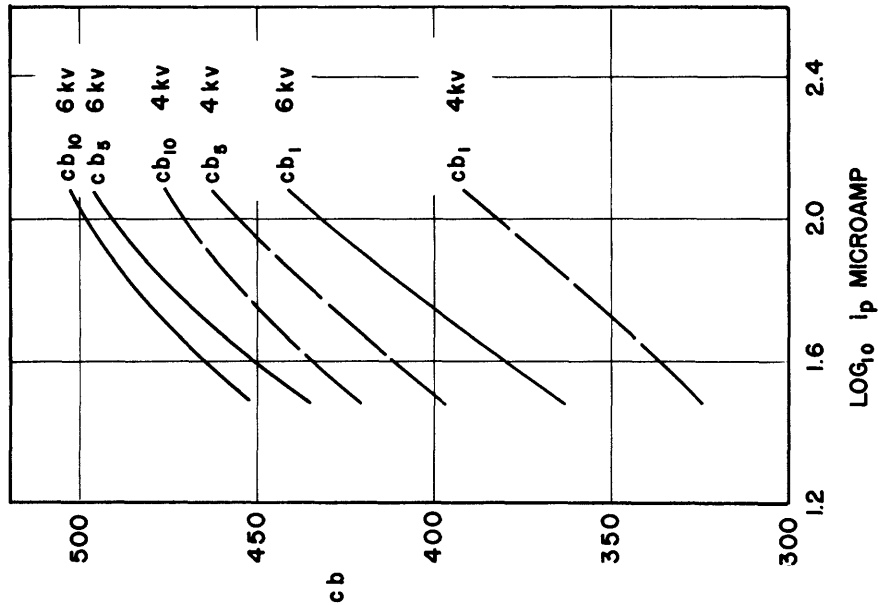
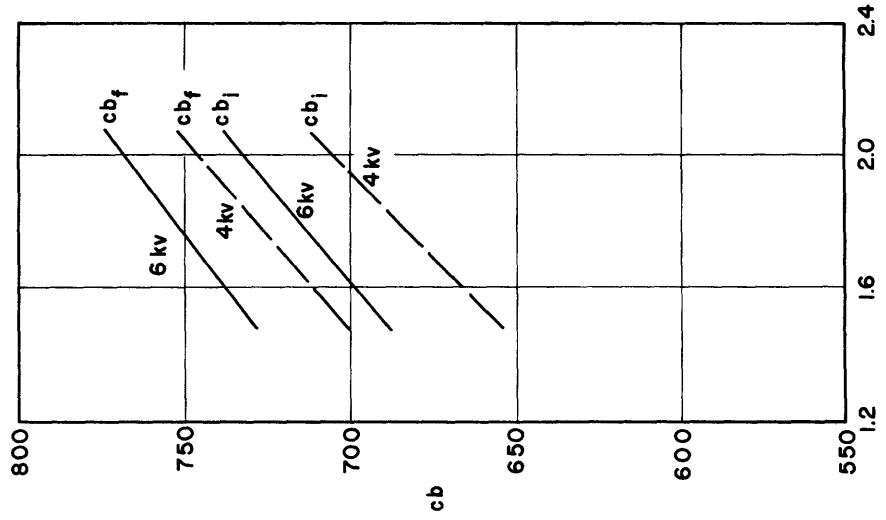


Figure 46

FLUORESCENCE AND INTEGRATED FLASH  
GE 4665

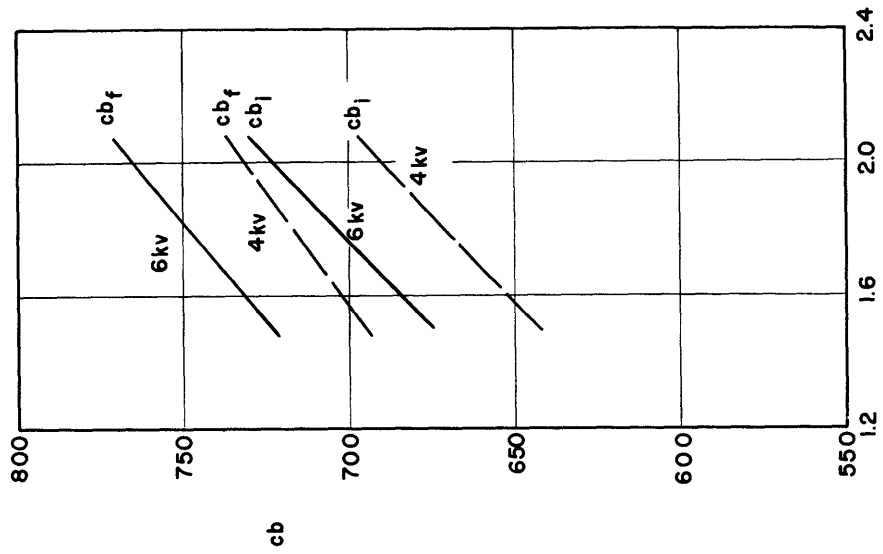
$V_0 = 6 \text{ kv}$   
 $= 4 \text{ kv}$



LOG<sub>10</sub> i<sub>p</sub> MICROAMP  
Figure 48

FLUORESCENCE AND INTEGRATED FLASH  
GE 4633

$V_0 = 6 \text{ kv}$   
 $= 4 \text{ kv}$



LOG<sub>10</sub> i<sub>p</sub> MICROAMP  
Figure 47

FLUORESCENCE AND INTEGRATED FLASH

GE 4609

$V_a = 6\text{ kv}$   
 $= 4\text{ kv}$

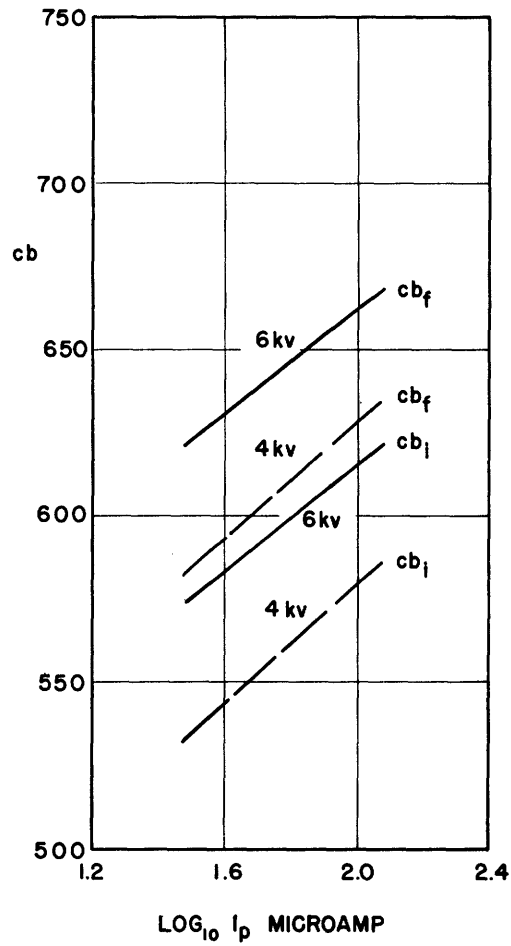


Figure 49

FLUORESCENCE AND INTEGRATED FLASH

RCA 5FP4A I

$V_a = 6\text{ kv}$   
 $= 4\text{ kv}$

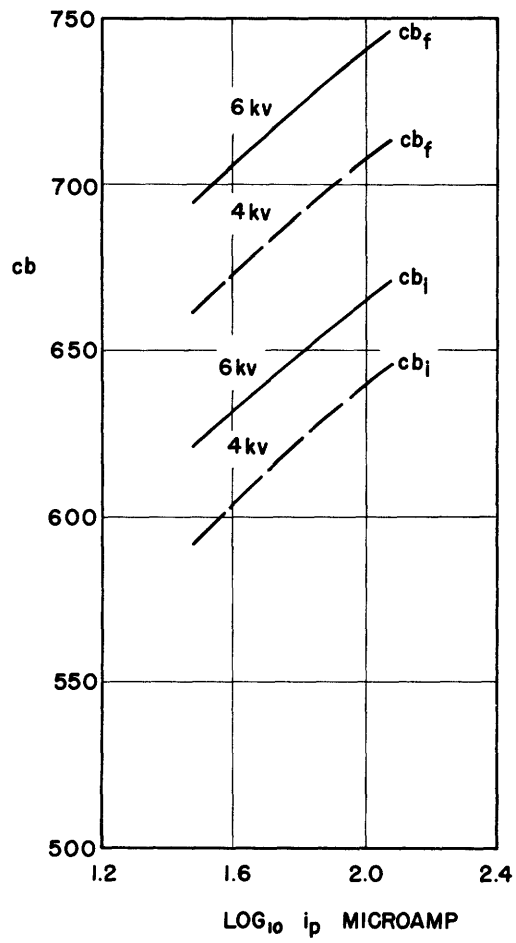


Figure 50

FLUORESCENCE AND INTEGRATED FLASH

RCA 5FPI4 C7570N 3940-18

$V_d = 6 \text{ kv}$   
 $= 4 \text{ kv}$

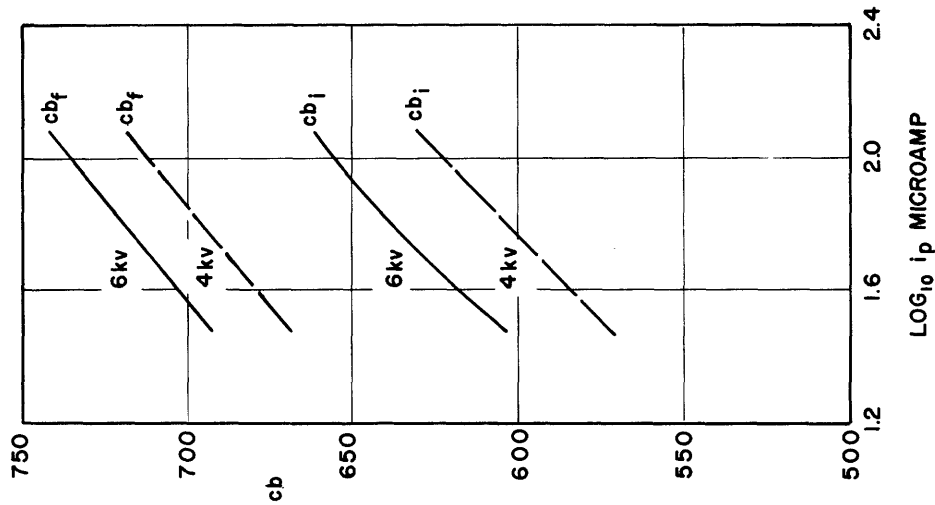


Figure 52

FLUORESCENCE AND INTEGRATED FLASH

RCA 5FPI4A 6331

$V_d = 6 \text{ kv}$   
 $= 4 \text{ kv}$

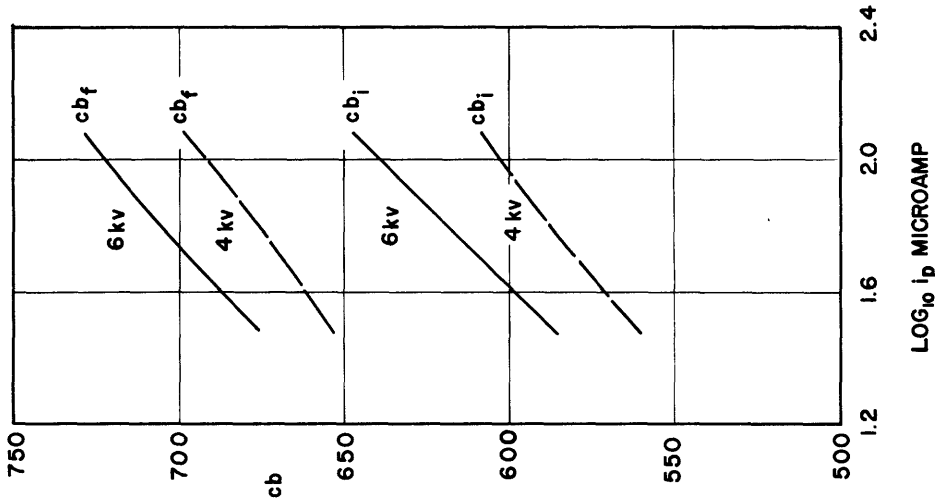


Figure 51

FLUORESCENCE AND INTEGRATED FLASH

GE 5FP14 C72745

$V_0 = 6 \text{ kv}$   
 $= 4 \text{ kv}$

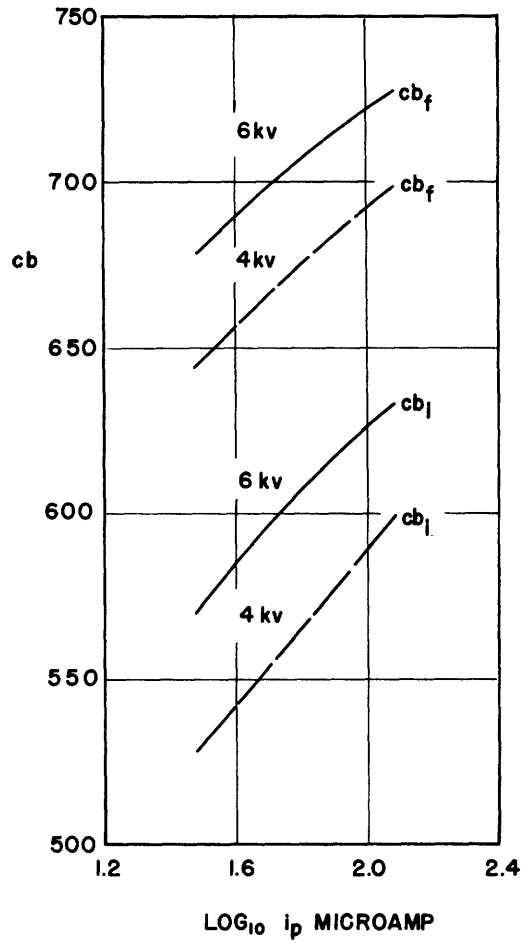


Figure 53

FLUORESCENCE AND INTEGRATED FLASH  
RCA 5FP7 A 2

$V_G = 6kv$   
 $= 4kv$

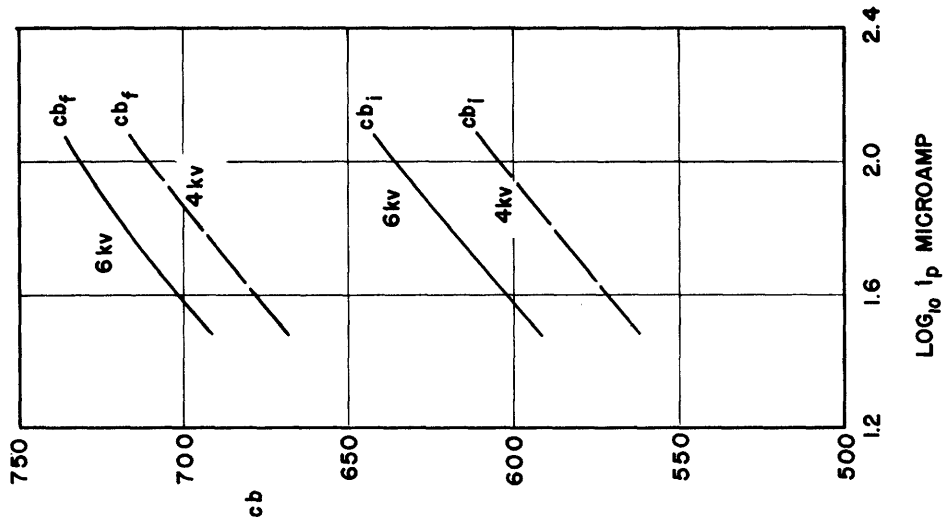


Figure 55

FLUORESCENCE AND INTEGRATED FLASH  
RCA 5FP7A 1

$V_G = 6kv$   
 $= 4kv$

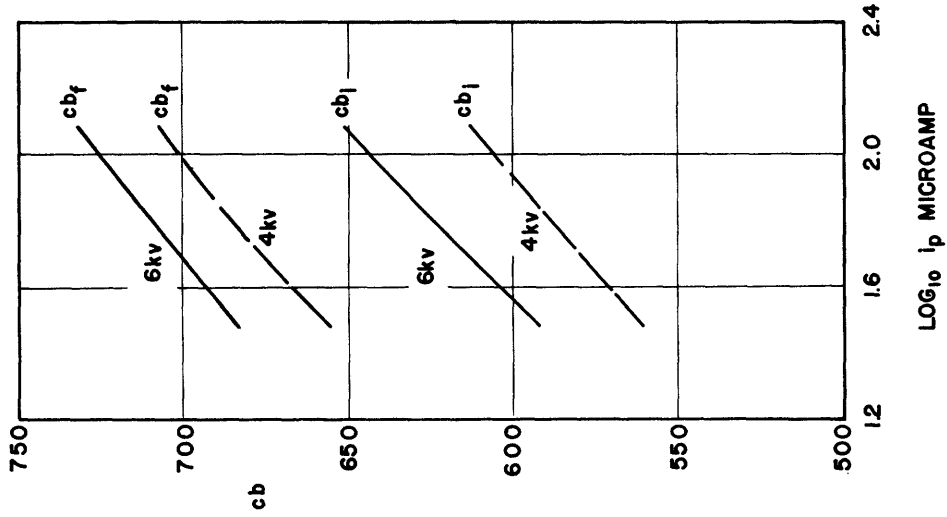


Figure 54

BIBLIOGRAPHY

Previous Research at the M.I.T. Radiation Laboratory:

1. Nottingham, W. B. "Excitation and Decay of Luminescence Under Electron Bombardment". R. L. Report 6-4S. Jan. 22, 1942.
2. Nottingham, W. B. "Proposed Performance Specifications for the P7 Long-Persistence Cascade Screen". R. L. Report. Aug. 12, 1942.
3. Nottingham, W. B. "Measurements of British CRT's with Long Persistence Screens". R. L. Report. Oct. 7, 1942.
4. Nottingham, W. B. "Graphical and Tabular Presentation of Results of Recent Tests on P7 Screens Prepared for P7 Conference". R. L. Report. April 5 and 6, 1943.
5. Nottingham, W. B. "Conference on P7 Cathode Ray Tubes Held April 5 and 6, 1943, Rad. Lab.". R. L. Report. May 14, 1943.
6. Nottingham, W. B. "Studies of British Phosphors of the Types 'C', 'H', 'K', and 'M'". R. L. Report 405. Aug. 2, 1943.
7. Nottingham, W. B. "Comparison of P-7 Screen Test Methods". R. L. Report S-9. Mar. 14, 1944.
8. Nottingham, W. B. "Notes on Photometry, Colorimetry and an Explanation of the Centibel Scale". R. L. Report 804. Dec. 17, 1945.
9. White, A. B. "Intermediate Persistence CRT Screens". R. L. Report VI-2/20/45. Feb. 20, 1945.
10. White, A. B. "Tabulation of CRT Screen Properties". R. L. Report S-48. May 1, 1945.
11. White, A. B. "Evaluation of Specifications for P14 CRT Screens". R. L. Report S-71. Jan. 14, 1946.

Previous Research not at the Radiation Laboratory:

12. Bradfield, G. and Garlick, G. F. J. "Comparison of Afterglow Characteristics of Cathode Ray Tube Screens with and without Cyclic Excitation". T.R.E. Laboratory Report T-1550.
13. Dushman, S. "Slow Phosphors for Radar Indicator Screens". NDRC Report D1-104. May 18, 1942.



14. Dushman, S. "Progress Report of Work on Duplex-Screen Tubes During 1941". NDRC Report. Oct. 14, 1942.
15. Hopkinson, R. G. "Factors Influencing the Decay Characteristics of Phosphorescent Screens for Cathode Ray Tubes". Research Laboratories of the General Electric Company, Ltd., Report 8261.
16. Jacob, J. E. B. "Build-up and Decay Characteristics of VCR35 and VCR517 Screens". Research Laboratories of the General Electric Company, Ltd., Report 8260.
17. Jesty, L. C. "Cathode Ray Tubes. Examination of Build-up and Decay Characteristics of Fluorescent Screens. Part I". Research Laboratories of the General Electric Company, Ltd., Report 8262.
18. Leverenz, H. W. "Summary of the RCA Research on Radar Indicator Screens". RCA Report. April 11, 1942.
19. Leverenz, H. W. "Final Report on Research and Development Leading to New and Improved Radar Indicators". NDRC Report 498. June 30, 1945.
20. Nottingham, W. B. "Electrical and Luminescent Properties of Willemite under Electron Bombardment". Journal of Applied Physics, vol. 8, no. 11, pp. 762-778. 1937.
21. Nottingham, W. B. "Electrical and Luminescent Properties of Phosphors under Electron Bombardment". Journal of Applied Physics, vol. 10, no. 1, pp. 73-83. 1939.

On the Description of the Nottingham Cathode Ray Tube Screen Test Equipment:

22. General Electric Bulletin. GEA 2394 A.
23. Nottingham, W. B. "Memorandum for Use in Conference on Test Equipment for Persistence Measurements". R. L. Report VI-12/10/41. Dec. 10, 1941.
24. Nottingham, W. B. "Report on Preliminary Trial of Test Equipment for Persistence Measurements". R. L. Report VI-1/17/42. Jan. 17, 1942.
25. Nottingham, W. B. "Memorandum Reporting Conference on CRT Screen Test Equipments March 26, 1942". R. L. Report VI-4/11/42. April 11, 1942.

26. Nottingham, W. B. "Memorandum Describing Circuits for the Measurement of Radiation Using the 931 Multiplier Phototube". R. L. Report VI-4/18/42. April 18, 1942.
27. Nottingham, W. B. "Memorandum for Use in Conference on CRT Test Equipment". R. L. Report 62-5/8/42. May 8, 1942.

Miscellaneous References:

28. Johnson, R. P. "Luminescence of Sulphide and Silicate Phosphors". Journal of the Optical Society of America, vol. 29, p. 387. 1939.
29. Nottingham, W. B. "Screens for Cathode Ray Tubes". Cathode Ray Tube Displays. Radiation Laboratory Series, vol. 22. Edited by Soller, T., Starr, M., and Valley, G. E. McGraw Hill Book Co. Unpublished.
30. RCA Tube Handbook. Aug. 1, 1944.
31. Wratten Filter Handbook.